YEAST OIL PRODUCTION BY HIGH CELL-DENSITY CULTIVATION
FROM RICE STRAW HYDROLYSATE
FOR BIO-POLYURETHANE FOAM MAKING

THIDARAT SAMRANRIT

A THESIS SUBMITTED IN PARTIAL FULLFILLMENT OF THE
REQUIREMENT FOR THE DEGREE OF MASTER OF SCIENCE
PROGRAM IN APPLIED BIOLOGY
FACULTY OF SCIENCE AND TECHNOLOGY
RAJAMANGALA UNIVERSITY OF TECHNOLOGY THANYABURI
ACADEMIC YEAR 2023

YEAST OIL PRODUCTION BY HIGH CELL-DENSITY CULTIVATION
FROM RICE STRAW HYDROLYSATE
FOR BIO-POLYURETHANE FOAM MAKING

THIDARAT SAMRANRIT

A THESIS SUBMITTED IN PARTIAL FULLFILLMENT OF THE
REQUIREMENT FOR THE DEGREE OF MASTER OF SCIENCE
PROGRAM IN APPLIED BIOLOGY
FACULTY OF SCIENCE AND TECHNOLOGY
RAJAMANGALA UNIVERSITY OF TECHNOLOGY THANYABURI
ACADEMIC YEAR 2023

Thesis Title   Yeast Oil Production by High Cell-Density Cultivation from Rice Straw Hydrolysate for Bio-Polyurethane Foam Making

Name – Surname   Miss Thidarat Samranrit

Program   Applied Biology

Thesis Advisor   Assistant Professor Atsadawut Areesirisuk, Ph.D.

Academic Year   2023

THESIS COMMITTEE

.... Kamonchai Cha-aim ....Chairman

(Assistant Professor Kamonchai Cha-aim, Ph.D.)

.... Thanasak Lomthong ....Committee

(Associate Professor Thanasak Lomthong, Ph.D.)

.... Jantima Teeka ....Committee

(Assistant Professor Jantima Teeka, Ph.D.)

.... Atsadawut Areesirisuk ....Committee

(Assistant Professor Atsadawut Areesirisuk, Ph.D.)

Approved by the Faculty of Science and Technology, Rajamangala University of Technology Thanyaburi in Partial Fulfillment of the Requirements for the Master's Degree

.... Nipat Jongsawat ....Dean of Faculty of Science and Technology

(Assistant Professor Nipat Jongsawat, Ph.D.)

29 August 2023

Thesis Title	Yeast Oil Production by High Cell-Density Cultivation from Rice Straw Hydrolysate for Bio-Polyurethane Foam Making
Name – Surname	Miss Thidarat Samranrit
Program	Applied Biology
Thesis Advisor	Assistant Professor Atsadawut Areesirisuk, Ph.D.
Academic Year	2023

ABSTRACT

The objectives of this research were to: 1) select the highest-performance yeast for yeast oil (YO) production using xylose as a carbon source, 2) study the influence of carbon source utilization and organic acid supplementation on YO production, 3) optimize the YO production from rice straw hydrolysate (RSH), 4) improve the YO production performance from RSH by fed-batch process, 5) estimate the kinetic of the YO production under various cultural conditions using mathematical models, and 6) examine the feasibility of bio-polyurethane (BPU) foam production using crude YO as a feedstock.

Firstly, the five yeast strains were cultured in a xylose-based oil production medium (X-OPM) to determine the YO production efficiency and fatty acid (FA) profile using GC-MS analysis. Then, the selected yeast strain was cultured in X-OPM at various initial xylose concentrations between 10 and 130 g/L. The effect of co-carbon source and acid supplementation on YO production was explored. Subsequently, the Box-Behnken Design (BBD) was conducted to investigate the optimum condition of YO production from RSH by varying concentrations of RSH, $(NH_4)_2SO_4$, and KH_2PO_4. Fed-batch processes were performed in feeding modes of RSH-based medium and RSH. Afterward, mathematical modeling was employed to simulate the YO production profile for estimating the kinetic parameters of yeast growth, substrate consumption, YO production, and acid consumption. Finally, the YO was converted to rigid and semi-rigid BPU foams. The BPU chemical

structures and properties were investigated by SEM, FTIR, density (ASTM D729), and water absorption (ASTM D570).

The study found that *Pseudozyma parantarctica* CHC28 was the most effective yeast among other strains by producing 3.36 ± 0.01 g/L of YO (oil content of $28.4 \pm 0.5\%$) at 144 h using 40 g/L of xylose as a carbon source. Additionally, the YO-producing parameters (YO concentration, $Y_{P/S}$, and oil content) obtained under various glucose-xylose mixing ratios were not significantly different (*p*-value > .05). Adding 1 g/L of acetic acid enhanced YO and oil content to 4.39 ± 0.30 g/L and $42.1 \pm 2.82\%$, respectively. The FA composition of *P. parantarctica* YO exhibited slight variations due to different cultural conditions, with C:16 and C:18 FAs as the main components. The optimum conditions of YO production from RSH were 10 g/L of RSH, 0.5 g/L of $(NH_4)_2SO_4$, and 9 g/L of KH_2PO_4, resulting in biomass and YO production of 4.67 ± 0.09 g/L and 1.02 ± 0.05 g/L, respectively. Moreover, the fed-batch process operated by RSH-based medium and RSH feeding could increase the YO to 3.76 ± 0.24 and 3.98 ± 0.16 g/L, respectively. In addition, fed-batch cultivation by both feeding modes could promote the $Y_{P/S}$ of 0.13 and oil contents exceeding 51%. The main FAs of RSH-based YO were C:16 and C:18, greater than 88.2%. Furthermore, the unconstructed mathematical models provided goodness-of-fit adequately to describe the oleaginous cultivation profiles. The YOs could be converted into BPU foam in rigid and semi-rigid forms. The SEM image of BPU foam revealed that the surface of rigid BPU was smooth with a few pores. In contrast, the semi-rigid BPU presented a rough surface with many non-uniform pores. The FTIR analysis demonstrated that the YO was successfully transformed into BPU. The density and water absorption were higher than 0.86 g/cm^3 and 23.3%. These results summarized that converting YO to BPU provided an alternative way for biopolymer production using xylose and RSH as primary carbon sources.

Keywords: yeast oil, *Pseudozyma parantarctica*, unconstructed mathematical modeling, rice straw hydrolysate, bio-polyurethane foam

Acknowledgments

Secondly, I would like to express sincere gratitude to my advisor, Assistant Professor Dr. Atsadawut Areesirisuk, for the superb tutorial, the valuable guidance, encouragement, help, and all support throughout this thesis.

Thirdly, I acknowledge my co-advisor, Assistant Professor Dr. Jantima Teeka, for also making suggestions and supporting my thesis.

Fourth, I would like to thank the thesis committee, Assistant Professor Dr. Kamonchai Cha-aim and Associate Professor Dr. Thanasak Lomthong for valuable comments and helpful suggestions.

Subsequently, I would especially like to thank my friends, sister, Bioengineering lab members, and the Division of Biology, Faculty of Science and Technology, RMUTT, for their help and support throughout this research.

Finally, I am especially thankful to my parents and family for their major encouragement, sincere love, and support of everything.

Thidarat Samranrit

Table of Contents

Table of Contents (Continued)

List of Tables

List of Figures

List of Figures (Continued)

List of Figures (Continued)

List of Abbreviations

BPU	Bio-polyurethane
YO	Yeast oil
YM	Yeast malt medium
X-YM	Xylose containing yeast malt medium
X-OPM	Xylose-based oil production medium
G-OPM	Glucose-based oil production medium
GX-OPM	Glucose and xylose mixing-based oil production medium
Glu:Xyl ratio	Glucose and xylose mixing ratio
EYO	Epoxidized yeast oils
YOP	Yeast oil-polyol
RSH	Rice straw hydrolysate
RSH-OPM	RSH-based oil production medium
HCD	High cell-density
a	Mass of BPU sample in air (g)
b	Mass of BPU sample and sinker in 2-propanol (g)
w	Mass of totally immersed sinker and partially immersed wire (g)
W_w	Wet weight of BPU (g)
D_w	Dry weight of BPU (g)
$\mu_{max,glu}$	Maximum specific growth rate on glucose (h^{-1})
$\mu_{max,xyl}$	Maximum specific growth rate on xylose (h^{-1})
$\mu_{max,10}$	Maximum specific growth rate at xylose 10 g/L (h^{-1})
X	Biomass concentration (g/L)
X_{max}	Maximum biomass concentration (g/L)
$X_{max,10}$	Maximum biomass concentration at xylose 10 g/L (g/L)
r	Biomass production ratio from consumed glucose
S_{glu}	Glucose concentration (g/L)
S_{xyl}	Xylose concentration (g/L)
$k_{i,glu}$	Substrate inhibition coefficient on glucose (g/L)
$k_{i,xyl}$	Substrate inhibition coefficient on xylose (g/L)

List of Abbreviations (Continued)

$Y_{x/s,glu}$	Biomass yield on glucose (g/g)
$Y_{x/s,xyl}$	Biomass yield on xylose (g/g)
ΔS	Substrate consumption (g/L)
P	Yeast oil (g/L)
α	Growth-associated product formation coefficient (g/g)
β	Non-growth associated product formation coefficient (g/(g h))
ms_{glu}	Cell maintenance coefficient on glucose (g/(g h))
ms_{xyl}	Cell maintenance coefficient on xylose (g/(g h))
$Y_{p/s,glu}$	Oil yield on the utilized glucose (g/g)
$Y_{p/s,xyl}$	Oil yield on the utilized xylose (g/g)
A	Acid concentration (g/L)
q_{Amax}	Maximum specific rate of acid consumption (g/(g h))
k_A	Saturated constant of acid (g/L)
n	Order of reaction
R^2	Coefficient of determination
$NRMS$	Non-normalized root mean square
$NRMS_{glu}$	Non-normalized root mean square of a model from glucose consumption
$NRMS_{xyl}$	Non-normalized root mean square of a model from xylose consumption
q_{cal}	Calculated data of a variable from the kinetic model
q_{exp}	Experimental data
$\bar{q}_{exp}$	Average of all the experimental data
N	Number of paired data

CHAPTER 1
INTRODUCTION

1.1 Background and Statement of Problems

Industrial polymers and plastics are made using fossil fuels, which has led to several socioeconomic and environmental issues. These include the buildup of polymers and non-biodegradable plastics and global warming brought on by excessive carbon dioxide emissions from burning fossil fuels [1-3]. Using bio-based plastics and polymers reduced the impact of fossil-based chemicals on the environment. Production of bioplastics is expected to rise annually, from 2.11 million tons in 2019 to 2.43 million tons in 2024. The bio-based chemical industry is based on renewable feedstocks [4, 5]; however, in 2019, the production of renewable bioplastic materials occupies less than 0.02 % of the global agricultural land [6]. To avoid further environmental issues, alternative renewable resources must be found to manufacture bioplastic and biopolymers.

An important class of thermoplastic and thermoset polymers called polyurethanes (PUs) are synthesized by combining polyols with poly-isocyanates [7]. Rigid foams are utilized in domestic applications and insulation boards to give durability and cushioning for related solutions, flexible PU foams are employed in healthcare and automotive applications [8].

The bio-polyurethane (BPU) form of PU foam can be made from vegetable oils such palm, soybean, canola, and sunflower oils [9-11]. However, the production of vegetable oil for BPU necessitates a huge amount of land and compost for oil-plant development, is climate-dependent, and affects food security through resource competition [12, 13]. Microbial oils have so garnered interest as a potential replacement for vegetable oils [13]. The oleaginous microorganisms (yeast, filamentous fungus, bacteria, and microalgae) generated and stored intracellular oil at up to 20% dry weight, according to earlier studies [14-16]. A wider range of tolerance to pH culture conditions, inhibitors, and ionic strength, as well as a rapid growth rate and high oil accumulation, oleaginous yeast has various benefits over other oleaginous microorganisms [16-18]. In

comparison to filamentous fungi, oleaginous yeast is easier to grow in large fermenters, has greater tolerance to metal ions, and uses less oxygen during metabolism of a range of substrates [19]. Bacterial cells are smaller and more difficult to collect than yeast cells. As opposed to microalgae, yeast can use a wider range of sugars and other basic carbon sources, and it doesn't require sunlight for photosynthesis, which turns carbon dioxide into oils [14]. *Pseudozyma parantarctica* CHC28 oleaginous yeast has primary intracellular oils as C:16 and C:18 fatty acids, similar to vegetable oils, and can collect oil within cells at up to 50% dry weight [20]. These characteristics indicate that *P. parantarctica* has the potential for yeast oil (YO) production.

Lignocellulosic biomass is a common renewable resource, comprising an organized entanglement of cellulose, hemicellulose, and lignin as the main structural components in plant cell walls [21, 22]. After pretreatment, cellulose and hemicellulose can be broken down into glucose and xylose units ideal for growing yeast [23-25]. Glucose is a general carbon source for oleaginous microorganisms [17]. Many yeast strains have shown efficient xylose metabolism including *Lipomyces starkeyi*, *Cryptococcus albidus*, *Rhodosporidium toruloides*, *Rhodutorula toroluides*, *Rhodotorula babjevae*, *Rhodotorula glutinis*, *Lipomyces tetrasporus*, and *Trichosporon oleaginosus* [23, 26-29]. Our preliminary study found that *P. parantarctica* CHC28 produced YO from xylose.

This research aims to select the oleaginous yeast that can consume xylose and rice straw hydrolysate (RSH) as the substrate for YO production, develop the high cell-density cultivation to enhance the YO production efficiency and investigate the feasibility of bio-polyurethane (BPU) foam production from crude YO on the laboratory scale.

1.2 Purpose of the Study

1.2.1 To select the highest-performance yeast for yeast oil production using xylose as a carbon source.

1.2.2 To study the effect of carbon sources and organic acids on yeast oil production.

1.2.3 To optimize the yeast oil production from rice straw hydrolysate.

1.2.4 To develop yeast oil production by high cell-density cultivation using rice straw hydrolysate as a carbon source.

1.2.5 To estimate the kinetic of the yeast oil production under various cultural conditions using mathematical models.

1.2.6 To study the feasibility of bio-polyurethane foam production using crude yeast oil as a feedstock in laboratory scale.

1.3 Scope of thesis

The scope of this research is the selection of the highest-performance yeast for yeast oil (YO) production using xylose as a carbon source. Five yeast strains which use in this study are *Cryptococcus albidus* TISTR 5103, *Pseudozyma parantarctica* CHC28, *Rhodotorula glutinis* TISTR 5159, *Rhodosporidium toruloides* TISTR 5186, and *Yarrowia lipolytica* TISTR 5212. The effect of xylose and xylose-glucose mixture on YO production and fatty acid profiles are studied in batch fermentation. Furthermore, the effect of organic acids supplement is investigated for enhancing YO production. Subsequently, the rice straw hydrolysate (RSH) is applied as the main carbon source for YO production. The optimum condition of YO production is studied by Box-Behnken experimental design and response surface methodology. Afterwards, the high-cell density cultivation is operated to enhance YO production using xylose, glucose, and RSH as the main carbon sources. Finally, the feasibility of bio-polyurethane foam production from crude YO is investigated on the laboratory scale.

1.4 Expectations of thesis

This thesis, I have the scope and limitations of studying which are concerned to the previous works which are:

1.4.1 Obtained the highest-performance yeast for yeast oil production using xylose as a carbon source.

1.4.2 Known the effect of carbon sources and organic acids on yeast oil production.

1.4.3 Obtained the optimum condition of yeast oil production from rice straw hydrolysate.

1.4.4 Received the process of yeast oil production by high cell-density cultivation using rice straw hydrolysate as a carbon source.

1.4.5 Known the kinetic of the yeast oil production under various cultural conditions using mathematical models.

1.4.6 Known the feasibility of bio-polyurethane foam production using crude yeast oil as a feedstock on the laboratory scale.

CHAPTER 2
LITERATURE REVIEWS

2.1 Fossil resources

The energy crisis is caused by the limited energy supply from existing fossil sources. Resources that will be used for energy are rapidly declining. In contrast, fossil resource demand is continuously increasing. This is a critical problem [30, 31]. The disadvantage of those fossil resources is that they cannot be reconstructed, affecting the economy and environment in all regions, increasing the carbon dioxide content, and causing global warming. Therefore, renewable resource production is essential in this situation [32]. The fossil-based resources have been used to synthesize polymeric materials. However, the dependencies on their derivative resources for these productions have several social, economic, and environmental issues. Critical problems are caused by the long-term degradation of chemical-based materials, tarnished green resources, and international disputes [2, 3]. Therefore, the plastics industry requires alternate green resources as raw materials. The bio-based polymers, i.e., polymers produced from renewable feedstock, might replace fossil sources and have environmental benefits such as decreasing carbon dioxide emission and plastics waste [33].

2.2 Polyurethane foam

Polyurethanes (PUs) represent a significant class of thermoplastic and thermoset polymers, as the reactions of various polyols and polyisocyanates can be tailored to provide a variety of mechanical, thermal, and chemical properties. The PUs include those polymers that contain many urethane groups (–HN–COO–) [34]. Polyurethane foams (PU foams) have a cellular structure and is used in various applications such as medical, automotive, household applications, and insulation boards. For associated solutions, PU foams provide better flexibility, toughness, and cushioning [8], and can be produced from plant oils reported by many authors [9, 10, 35-37]. Moreover, 50% of polymer foam production is made up of polyurethane foam, and the global polyurethane market has approximately 67% utilization [34].

2.2.1 Properties and chemical structure of PU foam

Polyurethane foam (PU foam) is a type of polymeric foam widely used due to its advantageous properties, such as low density, thermal conductivity, mechanical properties, and sound insulation capabilities. PU foam is commonly utilized as comfort, structural, and noise-insulating materials. It is produced through polymerization between the hydroxyl groups of a polyol and the isocyanate functional group associated with the urethane linkage. This is the exothermic reaction for producing urethane groups [38, 39], as presented in Figure 2.1.

$$R_{iso}\!-\!N\!=\!C\!=\!O \;+\; R_{polyol}\!-\!OH \longrightarrow R_{iso}\!-\!\!\left[\!N\!-\!C\!-\!O\right]\!\!-\!R_{polyol} \;+\; \Delta H$$

Isocyanate   Polyol   Urethane   Heat
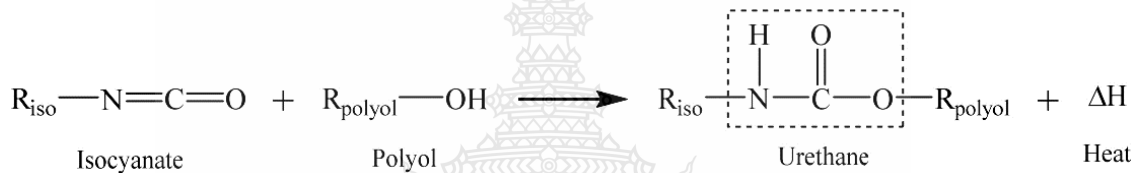
Figure 2.1 Interaction of urethane production.
Source: Ionescu, 2005 [39]

The interaction of isocyanate (-NCO) and water (H_2O) is important in producing polyurethane foams (PUFs). This interaction occurs almost simultaneously with the polymerization of isocyanate and polyol. The interaction of -NCO with H_2O leads to the expansion of PUFs, contributing to their unique structure (flexible, rigid, and semi-rigid PU foams). The resulting urethane groups are formed through this exothermic reaction [40], as demonstrated in Figure 2.2

$$R_{iso}-N=C=O \ + \ H_2O \longrightarrow R_{iso}-\overset{H}{\underset{|}{N}}-\overset{O}{\underset{||}{C}}-OH \ + \ CO_2$$

Isocyanate   Water   Unstable carbamic acid   Carbon dioxide

$$R_{iso}-\overset{H}{\underset{|}{N}}-\overset{O}{\underset{||}{C}}-OH \ + \ R_{iso}-N=C=O \longrightarrow R_{iso}-\overset{H}{\underset{|}{N}}-\overset{O}{\underset{||}{C}}-\overset{H}{\underset{|}{N}}-R_{iso}$$

Unstable carbamic acid   Isocyanate   Disubstituted urea
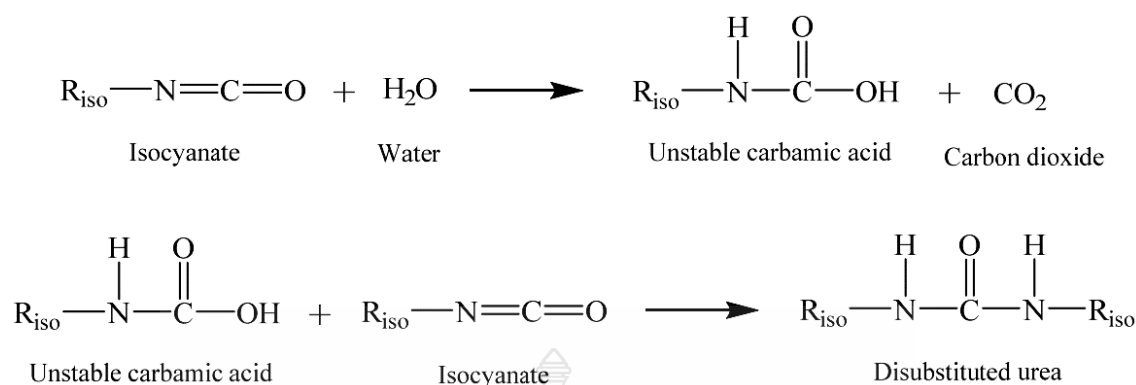
Figure 2.2 Interaction of the isocyanate and water.

Source: Ionescu, 2005 [39]

2.2.2 Application of PU foam on different properties

       1) Flexible polyurethane foam (FPUF) is a versatile material used in soft furnishings known for its flexibility and comfort. FPUF has good thermal insulation properties, making it suitable for applications where temperature regulation is important. It has excellent softening and shock-absorbing properties, providing comfort and support in mattresses, cushions, and furniture. FPUF is lightweight and has a high load-bearing capacity, making it durable and long-lasting. It is resistant to moisture and mold growth, contributing to its longevity and hygiene. However, FPUF is highly flammable and can release toxic gases when exposed to fire. Flame retardant additives, such as aluminum diethylphosphinate (ADP), can be incorporated to improve their fire safety properties [41].

       2) Rigid polyurethane foam (RPUF) is commonly applied for thermal insulation relevant in various fields, especially construction. It offers excellent thermal insulation performance and good mechanical properties. RPUF is used as an elastomer, foam, coating, fiber, and plastic in many applications. Its high performance and versatility make it suitable for construction, automotive, aerospace, and appliances. In the construction industry, RPUF is used for insulation in walls, roofs, and floors to improve energy efficiency and reduce heat transfer. RPUF is also used in the automotive

industry for insulation in vehicle interiors and refrigeration and air conditioning systems. Additionally, RPUF finds applications in furniture production, packaging materials, and various consumer goods [42].

3) Semi-rigid polyurethane foam (SRPUF) has good mechanical properties, making it suitable for various applications. SRPUF exhibits lower thermal conductivities than flexible polyurethane foam (FPUF) and higher flexibility than rigid polyurethane foam (RPUF). Due to their low thermal conductivity, SRPUF is used as thermal insulation in constructions, ships, automotives, and tubulars. SRPUF is utilized to absorb energy and lessen noise and vibration. Because of their open cells and elasticity structures, SRPUF has sound-absorbing qualities. Overall, semi-rigid PU foam has good mechanical properties, lower thermal conductivity than FPUF, and higher flexibility than RPUF. It is a thermal insulator for various applications, including sound absorption and vibration reduction [43].

2.3 Alternative oil resources

Various plant oils and animal fats including soybean, rapeseed, palm, and waste cooking oils are frequently used as feedstocks to produce biodiesel and bioplastic [44, 45]. Vegetable oils are used as a replacer for fossil resources. However, the cultivation of oil plants still has limitations, such as huge lands for cultivation, high production costs, and uncontrolled climatic conditions. Therefore, microbial oils are interested in replacing vegetable oils without those limitations [13].

Triglycerides, also known as fatty esters of glycerol, are the main component of vegetable oils, which are water-insoluble compounds of both plant and animal. Figure. 2.3 depicts the general chemical composition of vegetable oils which R_1, R_2, and R_3 are the fatty acid hydrocarbon chains. Depending on the specific oil structure, the R_1, R_2, and R_3 may have the same structure, but often have varied chain lengths and numbers of double bonds [46].
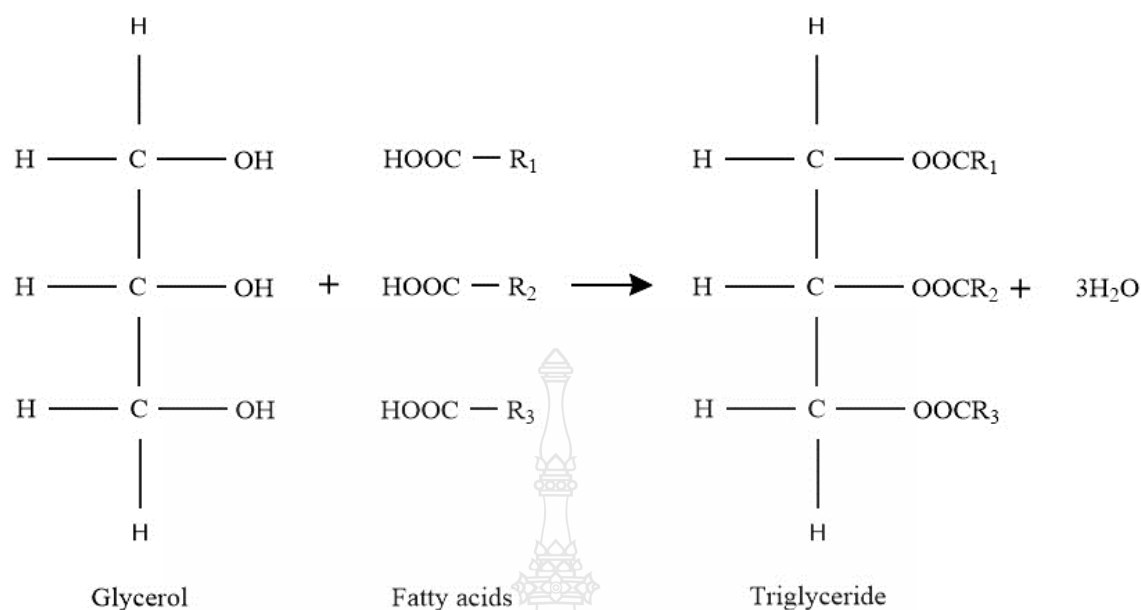
Figure 2.3 Chemical structure of triglyceride fatty acids in vegetable oil.
Source: modified from Sahoo and Das, 2009 [46]

Vegetable and waste cooking oils contain various fatty acids [47, 48]. The most general fatty acids are stearic, palmitic, oleic, linoleic, and linolenic acids. Triglycerides in vegetable oils comprise these fatty acids: stearic acid (C18) and palmitic acid (C16) are saturated fatty acids, while oleic acid (C18:1), linoleic acid (C18:2), and linolenic acid (C18:3) are unsaturated fatty acids. Ricinoleic acid, a bifunctional fatty acid with a hydroxyl group on the fatty acid chain, is also present in some vegetable oils, such as castor oil. Most triglyceride fatty acids are contained in vegetable oils [48], as shown in Figure 2.4.
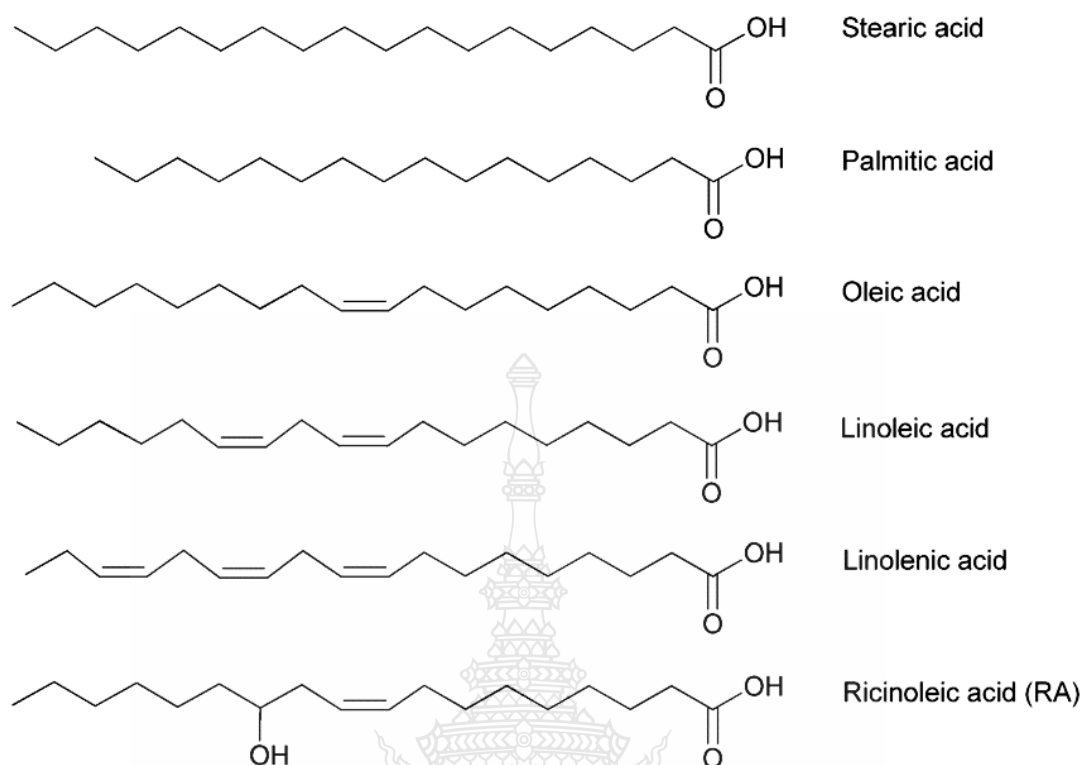
Figure 2.4 Main fatty acid profiles of vegetable and castor oils.

Source: Tschan *et al.*, 2012 [48]

2.4 Oleaginous yeast

Oleaginous microorganisms include microalgae, bacteria, mold, and yeast, which can accumulate oil in cells up to 20% of dry weight in the form of single-cell oil [14]. A previous study reported that some yeasts can accumulate oil droplets in cells ranging from 20% to 70%. However, the oil accumulation efficiency of each yeast species is different, and it has many advantages over general microorganisms, such as high growth rate and high oil accumulation [16]. The fatty acids (FAs) profiles of oleaginous yeast are similar to plant oils [49]. Several yeast strains, including *Rhodosporidium toruloides*, *Rhodotorula toroloides*, *Lipomyces tetrasporus*, *Yarrowia lipolytica*, *Trichosporon oleaginosus*, *Lipomyces starkeyi*, and *Cryptococcus albidus* can use the lignocellulosic hydrolysates as a carbon source for lipid production [23, 27]. *T. oleaginosus*, *L. starkeyi*, and *C. albidus* can metabolite the sorghum stalks and

switchgrass for lipid production. Moreover, the intracellular FAs of *Pseudozyma parantarctica* CHC28 have been reported. The FAs of *P. parantarctica* are similar to vegetable oils and can accumulate the oil within the cells up to 50% of dry weight [20]. Therefore, oleaginous yeast offers several benefits to overcome talents related to producing lignocellulose-based oil. [23].

       2.4.1 Mechanism of carbon source consumption

           Oleaginous yeast consumes different substrates using multi-metabolite pathways, as shown in Figure 2.5. For lignocellulose sugar consumption, which contains glucose and xylose, glucose is metabolized through glycolysis and converted into pyruvate to produce ATP and NADH as energy carriers. The normal mechanism occurs when cells need ATP for various cellular activities or biomass synthesis. Pyruvate can then be transformed by different metabolic pathways, such as the tricarboxylic acid (TCA) cycle to generate more ATP. In critical conditions, Yeast can perform the carbon degradation pathway, depending on the type of sugar and the energy requirement. In particular, cells require much NADPH during biosynthesis (essential for fatty acid synthesis). The NADPHs are highly produced using glucose through the pentose phosphate pathway (PPP) instead of the glycolysis pathway. In the PPP, glucose is converted into D-ribose 5-phosphate (R5P), and NADPH is generated for oil synthesis. Xylose can be metabolized by certain microorganisms, including oleaginous yeasts, through the xylose metabolism process. Xylose metabolism involves the conversion of xylose into xylulose, which can then enter the pentose phosphate pathway (PPP) for further metabolism. Xylose is first converted into xylulose by the enzyme xylose reductase (XYR), which requires NADPH as a cofactor. Xylulose is then phosphorylated by xylulokinase (XKS) to produce xylulose-5-phosphate, which can be further metabolized in the PPP to generate ATP and NADPH [17, 50, 51].
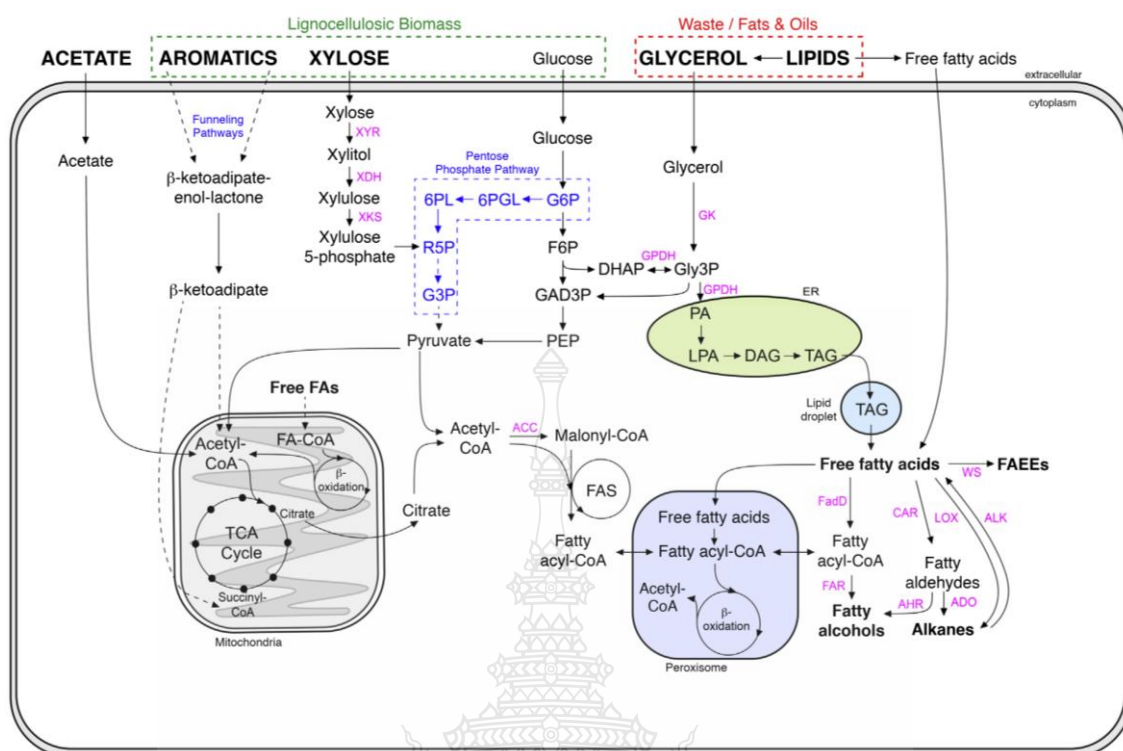
Figure 2.5 Pathways for assimilation of various substrates into fatty acid

Source: Spagnuolo *et al.*, 2019 [17]

2.4.2 Mechanism of microbial oil accumulation

Nitrogen depletion is crucial in initiating lipogenesis, inducing substrate-to-lipid conversion yields for storage as an energy reserve. Nitrogen starvation activates adenosine monophosphate (AMP) deaminase, which converts AMP to inosine monophosphate (IMP) and ammonia, increasing oil accumulation. The drop in AMP concentration negatively impacts the TCA cycle at the level of isocitrate dehydrogenase (IDH). Inhibition of isocitrate dehydrogenase in the mitochondria leads to citrate released into the cytoplasm that is broken down by the ATP-citrate lyase into oxaloacetate and acetyl-CoA, generating malonyl-CoA, which then reunifies with NADPH derived from sugar catabolism into acyl-CoA for fatty acid synthesis in endoplasmic reticulum to accumulate triacylglycerol (TAG) or triglyceride fatty acid droplet within cell [50, 52, 53]. The fatty acid synthesis of oleaginous yeast under nitrogen-limited conditions is illustrated in Figure 2.6.
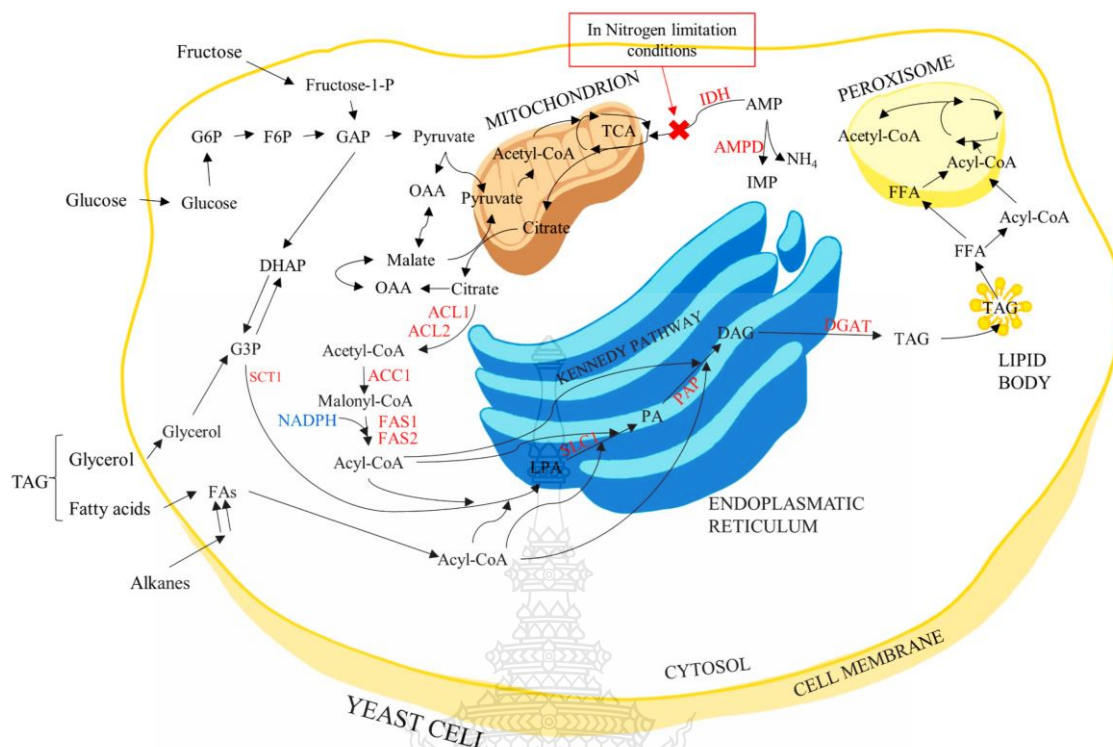
Figure 2.6 Synthesis TAGs in a yeast cell.

Source: Robles-Iglesias *et al*., 2023 [52]

2.4.3 Factors affecting microbial oil production

1) Physical factors: these refer to the tangible and measurable characteristics or conditions in the cultivation process that can affect the growth and oil production of oleaginous yeasts. Key physical factors are pH, temperature, and aeration/dissolved oxygen level. Besides, agitation speed, inoculum age and size, operation modes, feeding strategies, and fermentation period are important [52, 54, 55]. Liu *et al*. [56] found that *C. curvatus* ATCC 20509 is inhibited at pH below 4, and excessively high volatile fatty acids (VFAs) concentrations can suppress cell growth. While the initial pH level of the hydrolysate medium in a pH range between 5.5 and 7.5 is optimal for the growth and oil production of *Rhodotorula glutinis* [54]. Additionally, the temperature also plays a role, with most oleaginous yeasts growing best at around 30°C, although some can tolerate lower or higher temperatures [57]. Likewise, ample aeration during cultivation was crucial for successful microbial lipid production [54].

These physical factors need to be carefully considered and optimized to enhance microbial oil production and make it more cost-effective.

2) Chemical factors: oil synthesis by microorganisms requires a chemical compound in a medium with an excess of sugar compounds or related substrates (such as glycerol, polysaccharides, etc.) and a limited amount of other nutrients, normally nitrogen [58]. The imperfect nitrogen source in the medium-promoting yeast led to oil accumulation within cells, which replaced protein synthesis in the enriched-nitrogen medium [58]. The carbon and nitrogen ratio in medium culture and other parameters like aeration, inorganic salts, etc., impacting oleaginous potential include a high C/N ratio, which makes the sugar used for oil synthesis when nitrogen decreases [50, 58]. In addition, one of the necessary components for microorganism cultivation is phosphorous. It is combined into coenzymes, nucleic acids, proteins, and phospholipids [59, 60]. The varied ratios of carbon, nitrogen, and phosphorus are the main factors that impact the increase of sugar metabolite in the oil synthesis [61]. Therefore, finding the optimal substrate and essential nutrient conditions is critical for YO production.

2.5 Lignocellulosic biomass

2.5.1 Chemical structure of lignocellulose composition

Lignocellulosic materials are solids comprised of cellulose, hemicellulose, and lignin [62] (Figure 2.4) . Cellulose and hemicellulose are polysaccharides typically composed of glucose and xylose units. This compound is the main structural component in plant cell walls [63]. It is found in agricultural wastes such as RS, corncob, sugarcane bagasse, cassava pulp, woody, etc. [64-70]. Lignocellulosic biomass is an abundant renewable resource that is not edible. The hydrolysates of lignocellulose contain sugars, including glucose, xylose, and arabinose, which can be utilized by microbial fermentation.
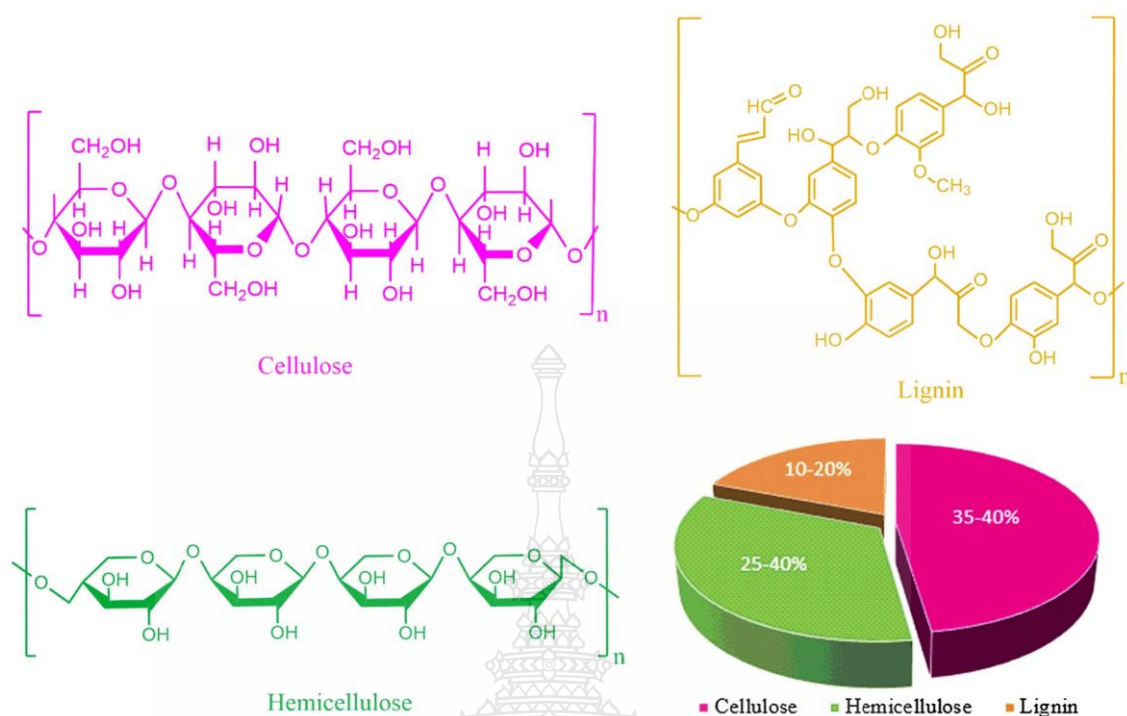
Figure 2.7 Compositions of lignocellulose.

Source: Amin *et al*, 2017 [62]

2.5.2 Hydrolysis of lignocellulosic biomass

Lignocellulose has the structure of solids containing cellulose, hemicellulose, and lignin; their utilization by microbes is naturally limited due to barriers from the compact structures of plant cell walls. Thus, the biomass pretreatment process was important in this case [23]. Hemicelluloses play a crucial role in binding cellulose microfibrils, creating physical barriers that restrict cellulose accessibility. It is widely recognized that hemicelluloses can have an adverse effect on cellulose hydrolysis [71]. Previous research has often employed methods such as dilute acid pretreatment at high temperatures (typically > 121 °C), alkaline hydrothermal pretreatment, or steam explosion to remove a substantial portion of the hemicelluloses before enzymatic hydrolysis for the digestion of monosaccharides like glucose, xylose, and arabinose [68-70]. Among these methods, alkaline pretreatment stands out as it operates at lower temperatures, resulting in less sugar degradation compared to acid pretreatment [72].

Notably, alkaline pretreatment using NaOH enhances the release of fermentable sugars from rice straw, leading to higher glucose yields [73]. These sugar-rich materials can serve as alternative resources for bio-based chemical production through microorganism fermentation [24]. However, lignocellulosic hydrolysates contain inhibitors such as furfural, 5-hydroxymethylfurfural (HMF), and acetic acid generated during hydrolysis. These byproducts can significantly impact the performance of microorganisms during fermentation, reducing microbial growth, metabolism, product yield, and overall productivity [74, 75]. Although lignocellulosic hydrolysis produces inhibitors that affect microbial activity, prior research has demonstrated successful oil production even in the presence of inhibitors, provided they are present in appropriate quantities as determined by the fatty acid profile. In such cases, these inhibitors had only a minor impact on oil synthesis [75]. However, to achieve the highest production yields, it may still be necessary to reduce the concentration of various inhibitors in lignocellulosic materials through detoxification methods.

2.5.3 Cultivation of oleaginous yeast by lignocellulosic hydrolysate

In many studies, the utilization of various lignocellulosic hydrolysates for yeast cultivation was successful for oil production as a carbon source. Previous research investigated the potential of rice straw hydrolysates for oil production by *Cryptococcus curvatus*, *Geotrichum candidum*, *Pichia kudriavzevii*, and *Lipomyces starkeyi* [76-78]. Moreover, *L. starkeyi* can use corn stover and sugarcane bagasse hydrolysate as substrates for oil production [79, 80]. In addition, *Rhodosporidium toruloides*-1588 can accumulate oil yield with cultivation in undetoxified wood hydrolysate [81, 82]. Yeast species *L. starkeyi*, *Rhodotorula glutinis*, *Rhodotorula babjevae*, and *Rhodotorula toruloides* present growth and oil accumulation differently on undiluted wheat straw hydrolysate [26]. Each yeast specie has specific metabolic characteristics and differences in oil accumulation performance under cultivation on various substrates [17]. Therefore, the selection of yeast strains is important for oil yield.

2.6 High cell-density cultivation

High cell-density refers to the concentration or abundance of cells in a culture or fermentation process. It measures how many cells are present per unit volume of the culture medium, often expressed as cells per milliliter or cells per liter. In the high cell-density cultivation of oleaginous yeast strains, a concentration of biomass dry cell weight (DCW) per unit volume is higher than a conventional batch process. This is achieved by optimizing growth conditions and high-concentrated carbon sources, such as using low-cost carbon sources like sugarcane molasses as a substrate. The aim is to enhance biomass and oil production, which is important for applications such as biodiesel production. High cell-density cultivation is achieved through batch and fed-batch fermentation modes, where a suitable feeding strategy is crucial to achieve high productivity and product yield [83, 84].

2.6.1 Batch fermentation

Batch mode is a fermentation process with a fixed volume of culture medium, substrate, and nutrients added only at the initial process. The culture can metabolize the nutrients and grow until the desired product is obtained or the nutrients are depleted. Batch fermentation has some disadvantages, including limitations in scalability and productivity, a limit on high osmotic pressure, variations in culture conditions over time, and a lack of continuous nutrient supply. It also requires longer fermentation times for high-efficiency product yield than continuous or fed-batch fermentation [58, 85]. Although batch fermentation is simple and widely used, however it has limitations that make it less suitable for large-scale and high-yield production processes.

2.6.2 Fed-batch fermentation

Fed-batch mode is a strategy used in fermentation processes to increase growth and production yields. It involves feeding mediums into the bioreactor at intervals during the fermentation process, such as sugars and essential nutrients. It can better control microbial growth conditions and nutrient availability, improving product yields and reducing by-product formation. This strategy is performed to avoid high concentrations of substrate affecting osmotic stress in the yeast cells [84, 86-88]. In addition, fed-batch mode has also increased the cell growth and improving the production of oils and carotenoids in various fermentation processes [89]. The advantages of fed-batch cultivation have been

illustrated in Figure 2.6, where S_0 represents the substrate concentration in the feed medium. X_i, S_i, and L_i represent the concentrations of cells, substrate, and oil in the broth, respectively. F_{in} represents the flow rate of nutrient feeding to the bioreactor [90].
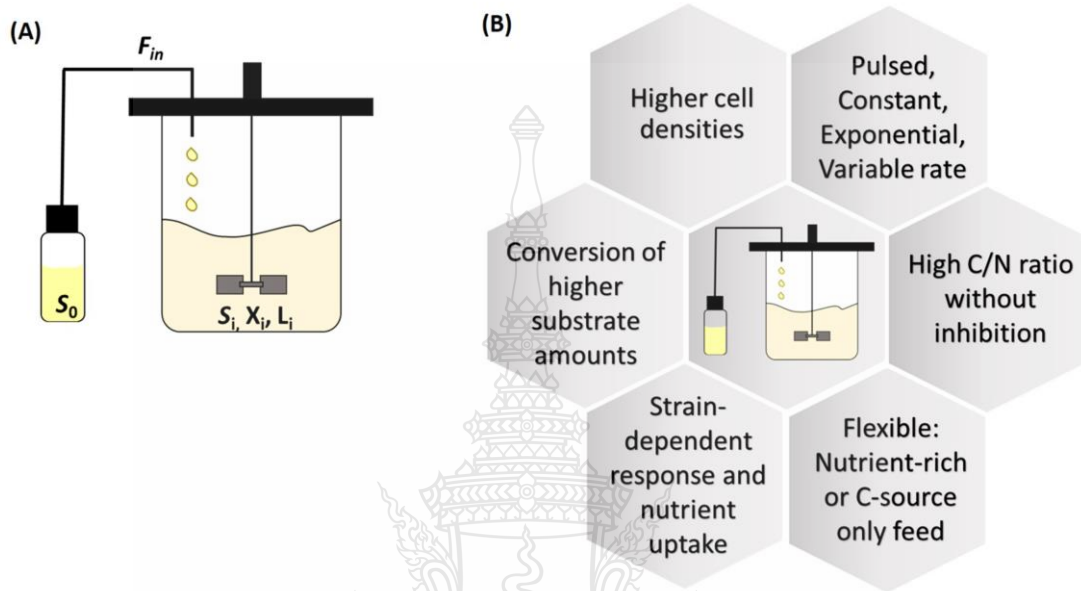
Figure 2.8 Advantages (B) of fed-batch cultivation (A) mode.

Source: Karamerou and Webb, 2019 [90]

2.6.3 Continuous fermentation

Continuous fermentation is a process in which fresh substrate is continuously added to the culture vessel, and the product is continuously removed, allowing for a steady-state operation. The substrate feeding and product removal are carried out continuously, resulting in higher productivity and shorter process time. While fed-batch fermentation implicates the periodic addition of substrate during the fermentation process without product removal. Continuous fermentation mode offers advantages such as higher productivity, efficient use of resources, and shorter process time compared to batch fermentation [85, 91]. It is particularly useful for industrial-scale production of biofuels, pharmaceuticals, and other bioproducts [92]. However, this process requires continuous supply and removal systems, which are more complex and costly than conventional batch

or fed-batch fermentation [85, 90]. Figure 2.7 presents the continuous mode operation, including the advantages and disadvantages of this process [90]. Overall, each fermentation mode provides advantages and disadvantages and depends on the specific requirements of the process and the desired outcomes.

Advantages	Disadvantages
Constant C/N ratio	Optimisation required for optimal N levels
Constant production yields at steady state	Potential degradation of strain's oil accumulating ability
Coupling with continuous processing	Potential risk of contamination and blockages
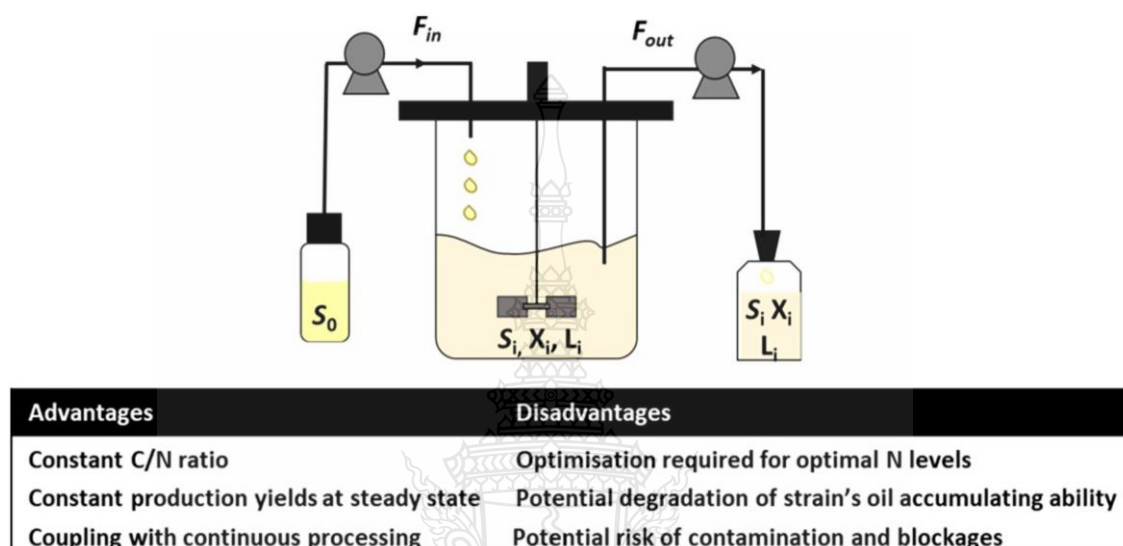
Figure 2.9 Continuous cultivation mode and its advantages and disadvantages.

Source: Karamerou and Webb, 2019 [90]

2.7 Reviews of the Literature

Lee *et al.* studied microbial oil production from sorghum stalks and switchgrass, which were the lignocellulose residues. Three oleaginous yeasts were cultured, including *Trichosporon oleaginosus* ATCC20509, *Lipomyces starkeyi* ATCC 56304, and *Cryptococcus albidus* ATCC10672, to investigate the efficiency. The results showed that *T. oleaginous* provided the highest performance for microbial oil production from sorghum stalk hydrolysate. The oil concentration, oil content, and oil yield were obtained at 13.1 g/L, 60, and 0.29 g/g, respectively [23].

Bonturi *et al.* investigated the adaptation of the yeast *Rhodosporidium toruloides* in undetoxified sugarcane bagasse hydrolysate in single-cell oil production. The hemicellulose hydrolysates were used instead of cellulosic. The result showed that the genes related to hydrolysate tolerance and oil accumulation were expressed differently

in parental and adapted strains. The adapted strain could produce more oils than the parental strain. The cultivation in a bioreactor scale could significantly improve the productivity and oil content to 54% and 33%, respectively [93].

Osorio-González *et al.* studied the utilization of woody biomass hydrolysate, which contained C5 and C6 sugars for oil production by yeasts. The result was reported that five different *R. toruloides* strains could utilize C5 and C6 sugars of hydrolysate. The result found that sugar consumption was similar between all strains and the maximum sugar consumption of C6 and C5 was 98 and 60%, respectively. The highest lipid production obtained from C6 and C5 was 23.33 and 14.67 g/L at 112 h and 120 h, respectively [29].

Chaiyaso and Manowattana studied the production of oil and carotenoid in yeast by the addition of organic acids in the optimized medium using formic acid, acetic acid, succinic acid, and citric acid at 0, 0.1, 0.5, and 1% (w/v), respectively. The result showed that adding some organic acids derived from the Krebs cycle supported the biosynthesis of the intracellular lipid. The highest oil and carotenoid production was increased to 5.39 g/L and 64.92 mg/L, respectively, by adding 0.5% (w/v) succinic acid [94].

Amza *et al.* studied the optimization of lipid production of *Lipomyces starkeyi* D35 using high cell-density cultivation under a low C/N ratio medium. The batch cultivation was performed using glucose and xylose as major carbon sources. The result showed that mixed glucose and xylose as substrates achieved the highest cell yield at 96 h. In contrast, single xylose feeding provided the highest lipid yield at 120 h. Moreover, the main FA contents were C18:1 and C16:0, likewise plant oils [95].

According to Uprety *et al.*, crude glycerol was converted into polyols utilizing a mix of biological and chemical methods. *R. toruloides* ATCC 10788, an oleaginous yeast, transformed crude glycerol into microbial oil. The results indicated that during 7 days in a batch-bioreactor, ATCC 10788 produced the maximum oil content of 18.69 g/L. A chemical process was used to further transform the acquired microbial oil into polyol molecules. The creation of rigid and semi-rigid polyurethane foams was used to test the compatibility of the polyol compound for the manufacturing of polyurethane (PU). FT-IR and 1H NMR were used to characterize the PU foams made from microbial, canola,

and palm oils. Canola, palm, and microbial oil polyols had hydroxyl values of 230.30, 266.86, and 222.32 mg KOH/g of a sample, respectively [96].

CHAPTER 3
MATERIALS AND METHODS

3.1 Chemicals, Apparatus and Equipments

	Company / Brand
3.1.1 Acetic acid (CH_3COOH)	QRëC
3.1.2 Acetonitrile (CH_3CN)	Macron Fine Chemicals™
3.1.3 Aluminium foil	Renolds metal
3.1.4 Ammonium sulfate ((NH_4)$_2SO_4$)	UNIVAR
3.1.5 Analytical balance	OHAUS
3.1.6 Autoclave	N-BIOTEC / NB-1080
3.1.7 Beaker	SCHOOT
3.1.8 Biosafety cabinet (BSC)	ESCO
3.1.9 Boron trifluoride-methanol (CH_4BF_3O)	SIGMA-ALDRICH
3.1.10 Burette, Size	QUALICOLOR
3.1.11 di-Butyltin dilaurate	
($(CH_3(CH_2)_3)_2Sn(O_2C(CH_2)_{10}CH_3)_2$)	Alfa Aesar
3.1.12 Calcium chloride dehydrate	
($CaCl_2 \cdot 2H_2O$)	UNIVAR
3.1.13 Centrifuge	SIGMA / 2-16PK
3.1.14 Centrifuge tube	Nalgene
3.1.15 Chloroform ($CHCl_3$)	RCI Labscan
3.1.16 Citric acid powder ($C_6H_{10}O_8 \cdot H_2O$)	KEMAUS
3.1.17 Duran bottle	SCHOOT
3.1.18 Ethyl acetate ($C_4H_8O_2$)	QRëC
3.1.19 Flask	PYREX
3.1.20 Formic acid (CH_2O_2)	QRëC
3.1.21 Glucose ($C_6H_{12}O_6$)	SRL
3.1.22 Hexane (C_6H_{14})	KEMAUS
3.1.23 Hot air oven	Binder

		Company / Brand
3.1.24	Hydrochloric acid (HCl)	QRёC
3.1.25	Hydrogen peroxide (H_2O_2)	UNIVAR
3.1.26	Incubator and shaker	N-BIOTEK / NB-205V
3.1.27	Iron (III) chloride RPE ($FeCl_3$)	CARLO ERBA Reagents
3.1.28	Magnesium sulfate heptahydrate ($MgSO_4 \cdot 7H_2O$)	UNIVAR
3.1.29	Malt extract powder	SRL
3.1.30	Methanol (CH_3OH) AR Grade	KEMAUS
3.1.31	Methanol (CH_3OH) HPLC grade	RCI Labscan
3.1.32	di-Methylethanolamine ((CH_3)$_2$$NCH_2CH_2OH$)	Alfa Aesar
3.1.33	di-Methypolysiloxane ($CH_3(Si(CH_3)_{20})n \cdot Si(CH_3)_3$)	SIGMA
3.1.34	Microtube	Nalgene
3.1.35	Peptone	SRL
3.1.36	Phosphoric acid (H_3PO_4)	QRёC
3.1.37	Plastic plate	Hycon
3.1.38	Potassium dihydrogen phosphate (KH_2PO_4)	SRL
3.1.39	Potassium hydroxide (KOH)	UNIVAR
3.1.40	Sodium acetate (CH_3COONa)	UNIVAR
3.1.41	di-Sodium hydrogen phosphate dodecahydrate ($Na_2HPO_4 \cdot 12H_2O$)	KEMAUS
3.1.42	Sodium hydroxide (NaOH)	UNIVAR
3.1.43	Spectrophotometer	SHIMADZU / UV-1800
3.1.44	Succinic acid ($C_4H_6O_4$)	KEMAUS
3.1.45	Test tube	PYREX
3.1.46	Toluene di-isocyanate ($C_9H_6N_2O_2$)	Alfa Aesar
3.1.47	Volumetric flask	PYREX
3.1.48	Vortex mixture	Scientific Industries / G560E

	Company / Brand
3.1.49 Xylose ($C_5H_{10}O_5$)	-
3.1.50 Yeast extract	IYEAST
3.1.51 Zinc sulphate heptahydrate	
($ZnSO_4 \cdot 7H_2O$)	Ajax Finechem

3.2 Microorganism

Four yeast strains were supplied from the Thailand Institute of Scientific and Technological Research (TISTR) , and one strain was in the stock culture of the Biotechnology Laboratory, Division of Biology, Faculty of Science and Technology, RMUTT, Pathum Thani, Thailand, as follows:

3.2.1 *Cryptococcus albidus* TISTR 5103

3.2.2 *Pseudozyma parantarctica* CHC28

3.2.3 *Rhodotorula glutinis* TISTR 5159

3.2.4 *Rhodosporidium toruloides* TISTR 5186

3.2.5 *Yarrowia lipolytica* TISTR 5212

3.3 Method

3.3.1 Stock culture preparation

The five yeast strains included *Cryptococcus albidus* TISTR 5103, *Pseudozyma parantarctica* CHC28, *Rhodotorula glutinis* TISTR 5159, *Rhodosporidium toruloides* TISTR 5186, *Yarrowia lipolytica* TISTR 5212 were cultured at 30 °C for 24 h in YM containing 10 g/L of xylose (X-YM) as the primary carbon source. A 250 mL flask containing one full loop of the yeast strain was inoculated with 30 mL of X-YM broth and then cultivated for 24 hours at 30 °C in an orbital shaking incubator (NB-205V, N-Biotek, South Korea) at 200 rpm. Then a 2 mL microtube was aseptically filled with 0.8 mL of cultivated yeast and 0.2 mL of 75% v/v glycerol. The culture was then used in this investigation as a stock culture and kept at -80 °C.

3.3.2 Starter preparation

The stock culture was inoculated into 30 mL of X-YM to create the yeast starter, which was then cultivated for 24 hours at 30 °C and 200 rpm. When transferring a 5 mL aliquot of active yeast to 50 mL of yeast potato dextrose (YPD) medium, dextrose

was replaced with xylose (20 g/L) as the primary carbon source [97] and cultured at the above-mentioned condition. Using a hemacytometer and a microscope to determine the viable cells in stater, containing about 8 log cells/mL.

3.3.3 Rice straw hydrolysis

The rice straw (RS, Pathum-KK01) was rinsed and cleaned of dust and dirt with deionized water. The cleaned RS was dried at 40 °C for 24 h. After drying, the RS was manually cut with scissors and ground by a grinder for a size of 1-2 cm RS. They were packaged in sealed plastic bags and kept at 4 °C until use in the following experiment [68]. The dried RS was hydrolyzed by alkaline hydrolysis [72]. Briefly, sieved dried RS was mixed with 2% (w/v) NaOH solution with a solid loading of 10% (w/v) and incubated at 80 °C for 24 h. The alkaline-hydrolyzed RS was filtered using white muslin fabric and washed with deionized water until the drained water was colorless. Then, it was hydrolyzed with enzymes by a modified method of Lugani *et al*. and Valles *et al*. [73, 98]. The enzymatic hydrolysis was performed at 50 °C, 72 h. with 50 mM acetate pH 5.5 as a buffer by adding the cellulase and xylanase (1:1 ratio) at 0.8% (v/w) to alkaline-hydrolyzed RS. The rice straw hydrolysate (RSH) was concentrated by evaporation at 60 °C and rotated 150 rpm under a carefully adjusted vacuum at 120 to 45 mbar. The residue of RS was separated from concentrated RSH by centrifugation (2-16PK, Sigma, Germany) at 15 °C, 7,500 rpm ($5,974 \times g$) for 10 min. The composition of RSH was determined by HPLC.

3.3.4 Selection of the highest-performance yeast for YO production using xylose-based medium

The 15 mL of each yeast starter were transferred to 135 mL of xylose-based oil production medium (X-OPM) composed of 50 g xylose, 0.5 g yeast extract, 1 g $(NH_4)_2SO_4$, 7 g KH_2PO_4, 6.3 g $Na_2HPO_4 \cdot 12H_2O$, 1.5 g $MgSO_4 \cdot 7H_2O$, 0.15 g $CaCl_2 \cdot 2H_2O$, 0.09 g $FeCl_3$, and 0.02 g $ZnSO_4 \cdot 7H_2O$ per liter. The cultures were incubated at 30 °C with 200 rpm shaking rate. A sample was withdrawn throughout cultivation to determine the concentration of biomass, YO, and xylose consumption. The experiments were performed in triplicates. Furthermore, the YO production efficiency was expressed as the yield of biomass and YO, oil content, and growth and oil

production rate. The yeast strain that provided the highest YO production efficiency was selected to use in the further experiment.

3.3.5 YO production by batch fermentation

3.3.5.1 Effect of initial xylose concentration on YO production

P. parantarctica CHC28 yeast starter in an aliquot of 15 mL was added to 135 mL of X-OPM, which had xylose concentrations ranging from 10 to 130 g/L. The culture was shaken at 200 rpm and incubated at 30 °C. Samples were taken at regular intervals to measure the concentration of biomass, YO, and xylose consumption. Three duplicates of each experiment were carried out. The biomass and YO yields, oil content, growth rate, and YO production rate were used to express the yeast growth and YO production efficiency. For the next trials, the ideal beginning xylose concentration was selected.

3.3.5.2 Effect of glucose and xylose mixing ratio on YO production

This experiment used combinations of glucose and xylose as co-carbon sources and was conducted in an oil production medium. The oil production medium's glu:xyl ratio (glu:xyl ratio) was adjusted to be 1:0, 0:1, 1:2, 1:1, and 2:1 [99]. A sample was taken during culture at regular intervals to determine the fermentation parameters. Measurements were taken in triplicate while the culture was incubated under the preceding conditions.

3.3.5.3 Enhancement of YO production by organic acid supplementation

In X-OPM, the effects of adding organic acids (acetic, citric, and succinic acid) at different concentrations (1 to 10 g/L) on the synthesis of yeast oil were studied [94]. Under the aforementioned conditions, each experiment was carried out three times. In accordance with the results of earlier tests, the sample was taken to assess the fermentation parameter.

3.3.6 YO production from RSH

3.3.6.1 Optimization of YO production from RSH by response surface methodology.

A 15 mL of *P. parantarctica* CHC28 inoculum was inoculated to 150 mL of RSH-based oil production medium (RSH-OPM). The concentrations of RSH (X_1) at 5 to 15 g/L, $(NH_4)_2SO_4$ (X_2) at 0.5 to 4.5 g/L, and KH_2PO_4 (X_3) at 0 to 14 g/L

were varied according to Table 3.1. The Box-Behnken design (BBD) was used to design the experimental plan for 15 runs (Table 3.1). The culture was incubated at 30 °C at 200 rpm shaking speed. The biomass and YO concentration of each treatment were measured as the response variable. The experimental data were calculated using Design Expert version 13.0 (Stat-Ease, USA). A second-order polynomial quadratic equation established the relationship between the independent and response variables (Eq. 1). The obtained equation was used to predict the optimum condition for YO production from RSH. After that, the optimum condition was validated in triplicates.

$$Y = \sum_{i=1}^{N} \beta_{ii} X_i^2 + \sum_{i=1}^{N} \sum_{j>1}^{N} \beta_{ij} X_i X_j \sum_{i=1}^{N} \beta_i X_i + \beta_0 \qquad (1)$$

Table 3.1 Box-Behnken experimental design

Run	RSH (A) (g/L)	$(NH_4)_2SO_4$ (B) (g/L)	KH_2PO_4 (C) (g/L)
1	5	0.5	7
2	15	0.5	7
3	5	4.5	7
4	15	4.5	7
5	5	2.5	0
6	15	2.5	0
7	5	2.5	14
8	15	2.5	14
9	10	0.5	0
10	10	4.5	0
11	10	0.5	14
12	10	4.5	14
13	10	2.5	7
14	10	2.5	7
15	10	2.5	7

3.3.6.2 YO production from RSH under high-cell density cultivation by fed-batch fermentation.

Fifteen milliliter of *P. parantarctica* CHC28 starter was transferred to 135 mL of optimized RSH-OPM following the previous study. The culture was incubated at 30 °C with 200 rpm shaking rate. The sample was collected to analyze the fermentation parameters. The feeding strategies were studied in fed-batch fermentation. The culture was supplied by RSH or RSH-OPM when the sugar concentration was almost consumed (every 72 h) and was incubated at the same condition at a time. The experiments were triplicates. Samples were periodically collected to determine the YO production efficiency following the previous experiment.

3.3.7 Feasibility of YO conversion into BPU foam

The process of conversion crudely extracted YO into BPU foam. The method of Uprety *et al.*, which was modified and used for the BPU preparation Three distinct chemical processes were coupled in the transformation: (i) oil epoxidation; (ii) oxirane ring opening to turn epoxidized yeast oils (EYO) into polyols; and (iii) BPU foam generation from polyols [96].

Chemical reactions were used to carry out oil epoxidation. A 250 mL glass screw-top container was filled with ten grams of YO. Before adding 11 mL of hydrogen peroxide gently using a glass dropper, ethyl acetate and formic acid were added at a rate of 11 and 0.9 g, respectively. After that, the mixture was heated for six hours at 60 °C using a hot plate magnetic stirrer with a 900 rpm stirring rate. After that, the YO phase and aqueous phase were separated, and a 1:1 ratio of deionized water was used twice throughout the washing process. Hot air drying at 140 °C for 3 h removed the remaining solvents and water from the cleaned YO phase to produce the EYO. Then, 10 g of EYO were heated on a heating plate to 85 °C. The yeast oil-polyol was produced by adding one gram of phosphoric acid to the warmed EYO and mixing it at 300 rpm for one hour (YOP). The YOP was combined with 5 g of toluene di-isocyanate to create stiff and semi-rigid BPU foams. Then, 1 g of dibutyltin dilaurate, 1 g of di-methylethanolamine, and 2 g of di-methypolysiloxane were added to the solution mixture as the primary catalyst, co-catalyst, and surfactant, respectively. When making rigid-BPU foam, water was not

added; however, when making semi-rigid BPU foam, 4 mL of water was added to 10 g of polyols as a blowing agent.

3.3.8. Summary of method

Figure 3.1 The flow chart of experiment in this research.

3.3.9 Mathematical modeling

The growth rate of oleaginous yeast in GX-OPM was investigated, with the yeast growth model expressed as a dynamic logistic equation. Yeast growth was represented by a sigmoid curve restricted by maximum biomass concentration (Eq. (2)) [100].

$$\frac{dX}{dt} = \mu_{max} X \left(1 - \frac{X}{X_{max}} \right) \tag{2}$$

Glucose and xylose inhibitory effects (Eqs. (3) and (4)) were associated with the model of specific growth rate [101], with glucose and xylose as co-carbon sources in GX-OPM. Yeast growth rates were described by combining the ratio of consumed glucose (r) and xylose ($1-r$), as defined by the modified logistic equations presented as Eqs. (5) and (6) [100]:

$$\text{Glucose inhibition} = \left(\frac{1}{1 + \frac{S_{glu}}{k_{i,glu}}} \right) \tag{3}$$

$$\text{Xylose inhibition} = \left(\frac{1}{1 + \frac{S_{xyl}}{k_{i,xyl}}} \right) \tag{4}$$

$$\frac{dX_{glu}}{dt} = \mu_{max,glu} Xr \left(1 - \frac{X}{X_{max}} \right) \left(\frac{1}{1 + \frac{S_{glu}}{k_{i,glu}}} \right) \tag{5}$$

$$\frac{dX_{xyl}}{dt} = \mu_{max,xyl} X(1\text{-}r) \left(1 - \frac{X}{X_{max}} \right) \left(\frac{1}{1 + \frac{S_{xyl}}{k_{i,xyl}}} \right) \tag{6}$$

where $\mu_{max,glu}$ and $\mu_{max,xyl}$ are the maximum specific growth rate (h^{-1}) on glucose and xylose, X is the biomass concentration (g/L), X_{max} is the maximum biomass concentration (g/L), r is the biomass production ratio from consumed glucose, S_{glu} and S_{xyl} are the glucose and xylose concentration (g/L), and $k_{i,glu}$ and $k_{i,xyl}$ are the substrate inhibition

coefficient (g/L) on glucose and xylose. Total growth rate of yeast in GX-OPM over the cultivation time was shown in Eq. (7).

$$\frac{dX}{dt} = \frac{dX_{\text{glu}}}{dt} + \frac{dX_{\text{xyl}}}{dt}$$ (7)

The glucose and xylose uptake were derived regarding utilization for biomass growth, oil production, and cell maintenance [102]. The models for glucose and xylose consumption rates depending on yeast growth rates (including the intracellular product, YO) and biomass concentration were shown as Eqs. (8) and (9), respectively. The yield of oleaginous biomass and cell maintenance coefficients were estimated in the mathematic models.

$$\frac{dS_{\text{glu}}}{dt} = -\left[\frac{dX_{\text{glu}}}{dt}\left(\frac{1}{Y_{\text{x/s,glu}}}\right) + ms_{\text{glu}}X\right]$$ (8)

$$\frac{dS_{\text{xyl}}}{dt} = -\left[\frac{dX_{\text{xyl}}}{dt}\left(\frac{1}{Y_{\text{x/s,xyl}}}\right) + ms_{\text{xyl}}X\right]$$ (9)

where $Y_{\text{x/s,glu}}$ and $Y_{\text{x/s,xyl}}$ are the biomass yields on glucose and xylose, ms_{glu} and ms_{xyl} are the cell maintenance coefficients (g/g h) on glucose and xylose, respectively.

The YO production rate related to biomass concentration, following the Luedeking-Piret equation as Eq. (10).

$$\frac{dP}{dt} = \alpha\frac{dX}{dt} + \beta X$$ (10)

In Eq. (10), α and β are the growth-associated and non-growth associated product formation coefficients, respectively [103], If $\alpha \neq 0$ and $\beta \neq 0$, the YO production is partially associated with yeast growth; if $\alpha \neq 0$ and $\beta = 0$, the YO production is exactly associated with yeast growth; and if $\alpha = 0$ and $\beta \neq 0$, the YO production is not associated with yeast growth. In addition, the correlations between biomass yields and oil yields on

45

the utilized glucose and xylose ($Y_{p/s,glu}$ and $Y_{p/s,xyl}$) are represented in Eqs. (11) and (12), respectively.

$$Y_{p/s,glu} = \alpha Y_{x/s,glu} \tag{11}$$

$$Y_{p/s,xyl} = \alpha Y_{x/s,xyl} \tag{12}$$

The Michaelis-Menten kinetics was used to describe the acid (acetic acid, citric acid, and succinic acid) consumption rate of *P. parantarctica* CHC28 following Eq. (13).

$$\frac{dA}{dt} = -\left(\frac{q_{Amax}A}{k_A + A}\right)^n X \tag{13}$$

where q_{Amax} is the maximum specific rate of acid consumption, k_A is the saturated constant of acid, and n is the order of the reaction [104].

In this study, the empirical coefficients (i.e., $\mu_{max,glu}$, $\mu_{max,xyl}$, X_{max}, $k_{i,glu}$, $k_{i,xyl}$, $Y_{x/s,glu}$, $Y_{x/s,xyl}$, $Y_{p/s,glu}$, $Y_{p/s,xyl}$, ms_{glu}, ms_{xyl}, α, β, q_{Amax}, and k_A) presented in Eqs. (2) to (13) were defined as fermentation kinetic parameters, which depend on cultural conditions. The fermentation kinetic parameters of the mathematical models were estimated as the values required for best model fit to the experimented data. Data fitting was conducted using the Berkeley Madonna™ program [105].

3.3.10 Statistical analysis of model fitting

The coefficient of determination (R^2) is typically used to determine the proportion of variance in the dependent variable predicted from the independent variable. In this study, R^2 was employed to investigate the best fit of a kinetic expression to the experimental data [106], and defined as Eq. (14):

$$R^2 = \frac{\sum_{i=1}^{N}(q_{cal} - \bar{q}_{exp})^2}{\sum_{i=1}^{N}(q_{cal} - \bar{q}_{exp})^2 + \sum_{i=1}^{N}(q_{cal} - q_{exp})^2} \tag{14}$$

In Eq. (14), q_{cal} represents the calculated data of a variable from the kinetic model, while q_{exp} and $\bar{q}_{exp}$ are the experimental data and average of all the experimental data, respectively. The non-normalized root mean square (*NRMS*) was used to investigate the actual error between the calculated experimental data at all points [107], and expressed as Eq. (15):

$$NRMS = \sqrt{\frac{\Sigma_{i=1}^{N}\left(q_{cal} - q_{exp}\right)^2}{N}} \qquad (15)$$

where N is the number of paired data.

    3.3.11 Calculation

        3.3.11.1 Biomass yield ($Y_{x/s}$)

           The yield efficiency of biomass was calculated as followed by the equation below:

$$Y_{x/s} = \frac{\Delta X}{\Delta S}$$

where ΔX and ΔS were produced biomass (g/L) and consumed substrate (g/L).

        3.3.11.2 Oil yield ($Y_{p/s}$)

$$Y_{p/s} = \frac{\Delta P}{\Delta S}$$

where ΔP was produced YO (g/L).

        3.3.11.3 Oil content (%)

$$Y_{p/x} = \frac{\Delta P}{\Delta X} \times 100$$

3.3.12 Analysis

3.3.12.1 glucose and xylose concentration

The glucose and xylose concentrations were quantified by high-performance liquid chromatography (HPLC) using an LC-20AD (Shimadzu, Japan) equipped with a refractive index detector (RID-20A, Shimadzu, Japan) and a Pinnacle II Amino analytical column (3μm, 150 × 4.6 mm size). The HPLC instrument was operated at 35 °C using 75% (v/v) acetonitrile as a mobile phase at 1 mL/min.

3.3.12.2 Organic acid concentration

Acetic, citric, and succinic acids were investigated using an Ultra Aqueous C18 column (5μm, 150 × 4.6 mm size) and a UV-Vis detector at 210 nm (SPD-20A, Shimadzu, Japan). The analyzed mobile phase was 50 mM potassium phosphate (pH 2.0) and acetonitrile mixed at a 99:1 ratio with flow rate of 1 mL/min.

3.3.12.3 Oil concentration

Three milliliter of the cell suspension was separated by centrifugation (2-16PK, Sigma, Germany) at 4 °C, 10,000 rpm (9,167 × g) for 10 min. Next, the cells were separated and washed with deionized water. Then, the sample was centrifuged to separate the cells pellet again. The washed cell was mixed with 1 mL of 4 N hydrochloric acid (HCl) and hydrolyzed at 60°C for 2 h. The hydrolyzed cell pellet was mixed with 2 mL of methanol and chloroform mixing solution (mixing ratio for 1:1). After 15-30 mins, it was layer-separated substances. The lowest layer of oil-riched chloroform was sucked and transferred to a new test tube. The residual cell pellet was added with 2 mL of chloroform and was gently mixed. The oil-riched chloroform layer was transferred and pooled with the previous chloroform layer. The oil-riched chloroform was evaporated to remove chloroform. The oil was dried at 80 °C for 24 h, placed in a desiccant chamber, and weighed. The oil concentration was expressed as grams of oil per liter of fermentation broth (g/L) [108].

3.3.12.4 Biomass concentration

A 2 mL of the cell suspension was separated by centrifugation (2-16PK, Sigma, Germany) at 4 °C, 10,000 rpm (9,167 × g) for 10 min. Next, the supernatant was collected for measuring the sugar and organic acid by HPLC. The cell pellets were harvested and cleaned twice with deionized water before drying at 80 °C for

24 h until constant weight. The dried cell pellets were weighed and expressed as a gram of biomass per liter of a sample [20].

3.3.12.5 Fatty acid composition

(1) The preparation of solution for analyzing the fatty acid form

The preparation of solution for analyzing the fatty acid form. The internal standard was prepared from heptadecanoic acid (C17:0) with a concentration of 20 mg/mL, conducted by 0.3 g heptadecanoic acid into 15 mL of chloroform. Then, the 20 µL of an internal standard solution was mixed with the volume of 1 mL solution of methanol and chloroform by 1:1 ratio. The potassium hydroxide (KOH) and hydrochloric (HCL) in methanol solutions were prepared with 0.5 N and 0.7 N concentrations, respectively, stored at 4 °C. After that, the saturated salt solution of sodium chloride (NaCl) was prepared by weighing sodium chloride dissolved in water until the salt solution was saturated [49].

(2) Preparation of fatty acid methyl ester

A 0.05 g of an oil sample was mixed with 4 mL chloroform ($CHCl_3$) and 0.5 mL internal standard (C17:0) solution, dried the solvent with nitrogen gas (N_2), then potassium hydroxide solution was added with the volume of 2 mL and cover the tube tightly, mixed the solution for 30 sec. The solution was immersed at 100 °C in a water bath for 10 min and chilled to stop the reaction. The solution of hydrochloric acid (HCl) and boron trifluoride (BF_3) was added for 2 mL and 3 mL, respectively. The tube was closed tightly and mixed for 30 sec. Then, it was soaked in a water bath again for 10 min and cooled in cold water. Then, the saturated salt solution and hexane (C_6H_{14}) were added with the volume of 3 mL and 2 mL, respectively. After that, it was separated into two layers. The top layer solution was sucked and mixed with hexane. The hexane layer containing fatty acid methyl esters was filtered via 0.2 µm polyvinylidene fluoride (PVDF) syringe filter. The composition of FAMEs was measured by gas chromatography-mass spectrometry (GC-MS) [49] using a GC system equipped with an MS-QP 2010 SE mass detector (Shimadzu, Japan). Aliquots of 10 µl were injected employing an InertCap Wax capillary column (0.25 mm I.D. × 30 m, GL Science Inc., Japan). Injector temperature was 250 °C with a split ratio of 1:80. The column temperature was operated by temperature program as follows: 50 °C for 3 min, increasing with a rate of 10 °C/ min

to 200 °C and increasing to 250 °C for 3 °C/min. Helium (constant flow, 1 mL/min) was used as a carrier gas [20].

3.3.12.6 Physical properties of BPU foam

BPU density was measured following the American Standard Test Method (ASTM) D792. The BPU sample was weighed in the air and while submerged in 2-propanol at 23 ± 1 °C. A sinker and wire were used to ensure that the sample was completely submerged. The density (g/cm^3) was expressed in Eq. (16):

$$\text{Density} = \left[\frac{a}{(a+w)-b}\right] \times 997.6 \times 10^{-3} \tag{16}$$

where a is the mass of BPU sample in air (g), b is the mass of BPU sample and sinker in 2-propanol (g), and w is the mass of totally immersed sinker and partially immersed wire (g).

Water absorption of BPU was measured following ASTM D570. BPU was dried in an oven, cooled in a desiccator, and weighed. The dried BPU was then soaked in water at 23 ± 1 °C for 24 h. The wet BPU was removed from the water, patted dry with a lint-free cloth, and weighed. Water absorption (%) was expressed following Eq. (17):

$$\text{Water absorption} = \left[\frac{(W_w - D_w)}{D_w}\right] \times 100 \tag{17}$$

where W_w and D_w are the wet weight (g) and dry weight (g) of BPU.

3.3.12.7 Chemical and surface structure of BPU foam

The chemical structure of YO and BPU foam were analyzed by Fourier transform Infrared (FT-IR) analysis [96]. The surface structure of BPU foam was studied by scanning electron microscope (SEM) [10].

3.3.12.8 Statistical analysis

All experimental data and the fermentation kinetic parameters were computed as mean values $\pm$ standard deviation (SD). Significant differences between values were determined by one-way ANOVA and Duncan's multiple range test (SPSS 15.0 software, SPSS Inc., USA) at p-value ≤ 0.05.

3.4 Experimental place

This study was performed at Biotechnology Laboratory, Division of Biology, Faculty of Science and Technology, and Department of Materials and Metallurgical Engineering, Faculty of Engineering, Rajamangala University of Technology Thanyaburi, Thanyaburi, Pathum Thani.

CHAPTER 4
RESULTS AND DISCUSSIONS

4.1 Selection of the highest-performance yeast for YO production using xylose-based medium

The different yeast strains were cultured in media containing xylose as the sole carbon source. The xylose consumption, growth, and YO production profiles of different yeasts were shown in Figure 4.1A to C. The result revealed that all yeast strains could assimilate the xylose for growth excellently excluding *Y. lipolytica* TISTR 5212. While *P. parantarctica* CHC28 and *R. toruloides* TISTR 5186 could produce the YO higher than other experimental strains.

The efficiency of biomass and oil production by yeast strains was presented in Table 4.1. The biomass was produced ranking as 12.01 ± 0.20 to 13.77 ± 0.09 g/L, only strain TISTR 5212 provided biomass at 2.94 ± 0.13 g/L. The strain CHC28 had the highest YO (3.20 ± 0.12 g/L), YO yield ($Y_{p/s}$) (0.07 ± 0.00), and oil content (24.78 ± 0.75 %). These results indicated that CHC28 was an oleaginous yeast strain that could efficiently transform the xylose into YO.

In previous research, oil production by different yeast strains and main carbon sources has been studied. The main carbon sources of oil production were generally divided into two main groups, including pure (glucose, xylose, glycerol, etc.) [109-112] and complex carbon source (lignocellulosic and starch-based material, agro-industrial by-product, etc.) [28, 80, 113-116].

The oil production from biodiesel-derived crude glycerol by *Rhodosporidium fluviale* DMKU-RK253 was optimized. The oil content was increased to 63.8% of dry biomass. The crude glycerol obtained from biodiesel production was also purified and used as the sole carbon source for oil production by *P. parantarctica* CHC28. The result demonstrated that the oil was produced and accumulated within the cells up to 50% of the dry weight [20].

The yeast strains, including *Lipomyces tetrasporus*, *Rhodotorula toroloides*, and *Yarrowia lipolytica* can utilize lignocellulose-derived sugars as carbon sources for oil production with oil accumulations different of 62.87, 63.23, and 34.90 %, respectively [27]. Likewise, *Trichosporon oleaginosus*, *Lipomyces starkeyi*, and *Cryptococcus albidus* can metabolite the sorghum stalks for oil production with oil accumulations of 60, 44, and 42 %, respectively [23]. In addition, Osorio-González *et al*. [29] reported that five strains of *R. toruloides* utilized glucose and xylose sugars in wood hydrolysate similarly. However, the oil production was different and depended on the experimental strains. Thereby, it could be summarized that the species and main carbon source affect the oil production of the oleaginous strain. The CHC28 was chosen to study the enhancement of oil production efficiency in the xylose-based medium for the next experiments.
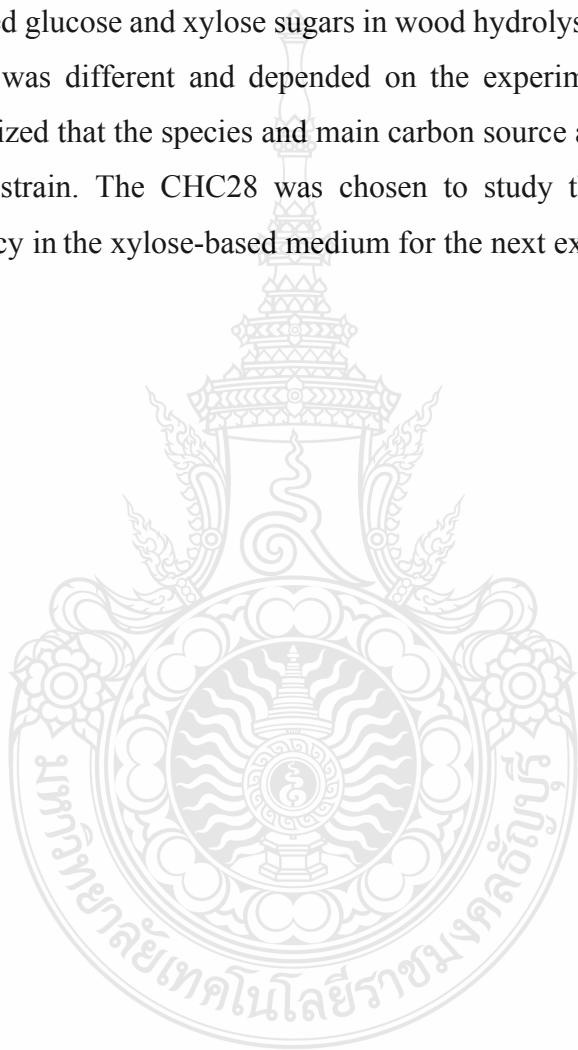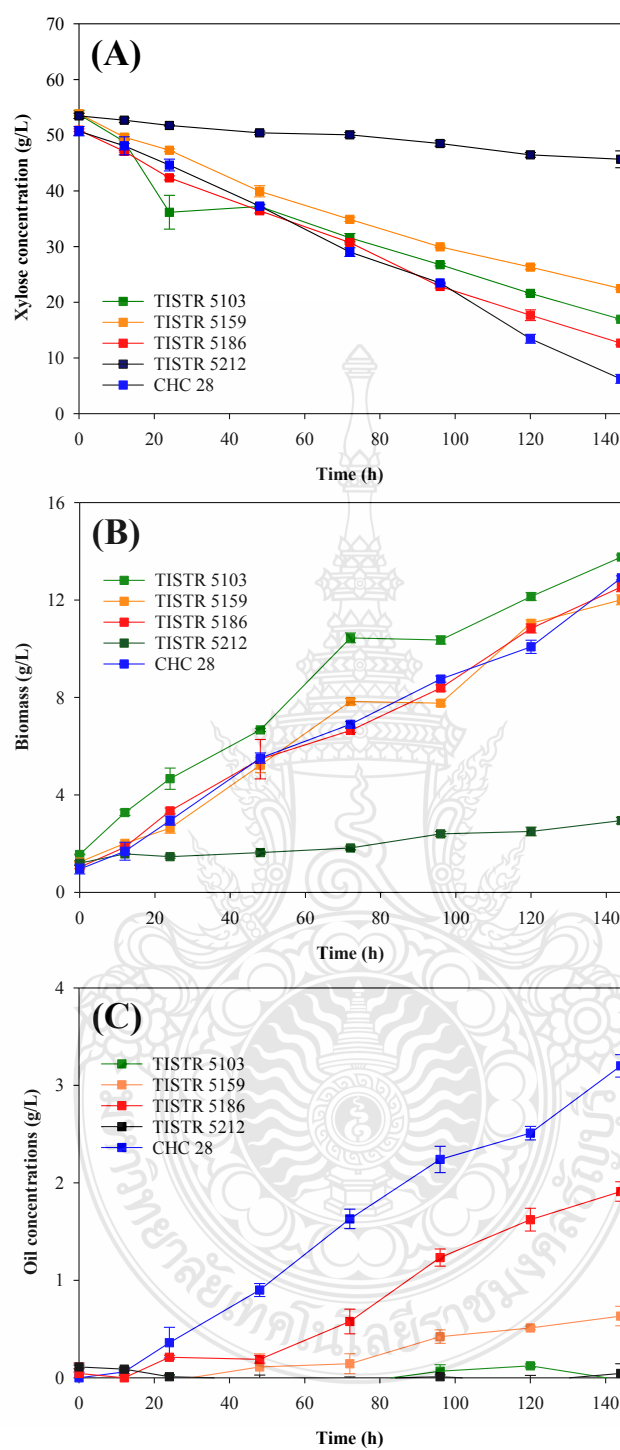
Figure 4.1 Time profiles of (A) xylose consumption and the production of (B) biomass and (C) YO of various oleaginous yeasts cultured in X-OPM at 144 h. Data are represented as mean ± SD bar.

Table 4.1 Parameter of biomass and YO production by various oleaginous yeasts with xylose as the main carbon source at 50 g/L.

Yeast strains	X (g/L)	P (g/L)	ΔS (g/L)	$Y_{x/s}$	$Y_{p/s}$	Oil content (%)
P. parantarctica CHC28	12.91 ± 0.08[b]	3.20 ± 0.12[a]	44.48 ± 0.12[a]	0.29 ± 0.00[b]	0.07 ± 0.00[a]	24.78 ± 0.75[a]
C. albidus TISTR 5103	13.77 ± 0.09[a]	0.02 ± 0.02[d]	36.77 ± 0.84[b]	0.37 ± 0.01[ab]	0.00 ± 0.00[d]	0.16 ± 0.14[d]
R. glutinis TISTR 5159	12.01 ± 0.20[d]	0.63 ± 0.06[c]	31.36 ± 0.40[c]	0.38 ± 0.01[ab]	0.02 ± 0.00[c]	5.27 ± 0.47[c]
R. toruloides TISTR 5186	12.54 ± 0.23[c]	1.91 ± 0.10[b]	38.24 ± 0.26[b]	0.33 ± 0.01[ab]	0.05 ± 0.00[b]	15.24 ± 0.97[b]
Y. lipolytica TISTR 5212	2.94 ± 0.13[e]	0.04 ± 0.07[d]	7.78 ± 1.95[d]	0.40 ± 0.12[a]	0.01 ± 0.01[d]	1.44 ± 0.72[d]

[*]Data are mean ± SD; different superscripts in the same column indicate significant differences at p-value ≤ .05.
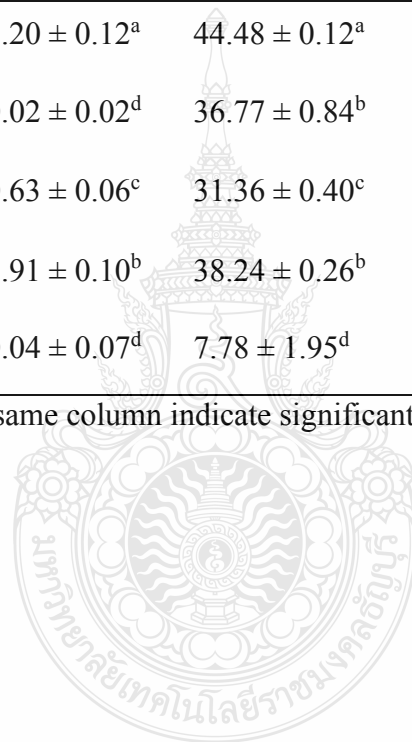
4.2 Effect of initial xylose concentration on yeast growth and YO production

The effect of *P. parantarctica* CHC28 cultivation in X-OPM containing different initial xylose concentrations was investigated, with results shown in Figure 4.2A to C. The results showed that yeast could completely uptake xylose in X-OPM containing xylose lower than 40 g/L (Figure 4.2A). When the yeast was cultured in X-OPM containing a carbon source ranging from 50 to 130 g/L, the xylose consumption ranged from 28.63 ± 0.52 to 44.48 ± 0.12 g/L at 144 h of cultivation. Yeast biomass increased consistently as the carbon source increased and reached the highest level (12.91 ± 0.08 g/L) at xylose content of 50 g/L.

The biomass then gradually decreased at xylose content over 60 g/L (Figure 4.2B). At the xylose concentration increased from 10 to 40 g/L, YO was continuously enhanced (Figure 4.2C). By contrast, at higher xylose levels, YO was dramatically reduced. It was demonstrated that the growth and YO production of *P. parantarctica* influenced by substrate inhibition of high xylose concentration. Substrate consumption, yield of biomass and YO, and oil content at the end of cultivation are summarized in Table 4.2.

The highest $Y_{x/s}$ and $Y_{p/s}$ were 0.43 ± 0.01 and 0.10 ± 0.01 at 10 and 80 g/L, respectively. Xylose concentration of 40 g/L gave the highest YO and oil content at 3.36 ± 0.01 g/L and $28.4 \pm 0.5\%$, respectively, with xylose thoroughly utilized. Results suggested that increase in carbon source concentration increased the osmotic pressure of the cultivation medium, which impacted the growth and product development of microorganisms [27, 84, 85].

In a previous study, the effect of glucose concentration on growth and oil production of *Rhodotorula toruloides* ATCC 204091 was explored. It was found that *R. toruloides* ATCC 204091 had higher growth and oil production when glucose increased from low to moderate levels (5 to 90 g/L), causing biomass and oil production increased from 16.0 to 23.2 g/L and 10.5 to 17.8 g/L, respectively. However, growth and oil production decreased at glucose concentration above 120 g/L [84].

In addition, *Cutaneotrichosporon oleaginosus* and *Yarrowia lipolytica* were cultured in the medium under various glycerol concentrations in terms of C/N ratios (30:1 to 300:1). Highest oil contents of *C. oleaginosus* and *Y. lipolytica* were obtained at 71%, and 66% under C/N ratios 175 and 140, respectively [117]. Consequently, the influence

of xylose on oil formation of the yeast strain *Papiliotrema laurentii* UFV-1 was also studied at different C/N ratios. The results indicated that the highest oil content in a cell was 63.5% (5.9 g/L of oil) at C/N ratio of 100:1 [118].

These results suggested that the concentration and type of carbon source are crucial factors affecting the efficiency of oil production for microbes. Furthermore, oil can be produced using several carbon sources at different concentrations. Especially, *P. parantarctica* CHC28 is an oleaginous yeast that could consume diverse carbon sources to form YO [18, 105].

Table 4.2 Fermentation parameters in X-OPM at different initial xylose concentrations at 144 h.

Xylose (g/L)	ΔS (g/L)	$Y_{x/s}$	$Y_{p/s}$	Oil content (%)
10	10.0 ± 0.17^a	0.43 ± 0.01^a	0.04 ± 0.0^f	8.6 ± 1.2^d
20	20.12 ± 0.33^b	0.35 ± 0.01^c	0.04 ± 0.0^e	12.7 ± 0.0^c
40	41.95 ± 0.17^b	0.28 ± 0.0^d	0.08 ± 0.0^c	28.4 ± 0.5^a
50	44.48 ± 0.12^b	0.29 ± 0.0^d	0.07 ± 0.0^d	24.8 ± 0.8^b
60	33.19 ± 1.32^d	0.35 ± 0.0^c	0.09 ± 0.0^{ab}	26.7 ± 1.5^{ab}
80	29.42 ± 1.23^d	0.35 ± 0.01^c	0.10 ± 0.01^a	28.4 ± 1.0^a
110	33.16 ± 1.43^c	0.35 ± 0.01^c	0.09 ± 0.0^b	26.1 ± 0.7^{ab}
130	28.63 ± 0.52^d	0.37 ± 0.01^b	0.10 ± 0.01^a	26.5 ± 1.6^a

*Data are presented as mean ± SD; different superscripts in the same column indicate significant differences at *p*-value ≤ .05.
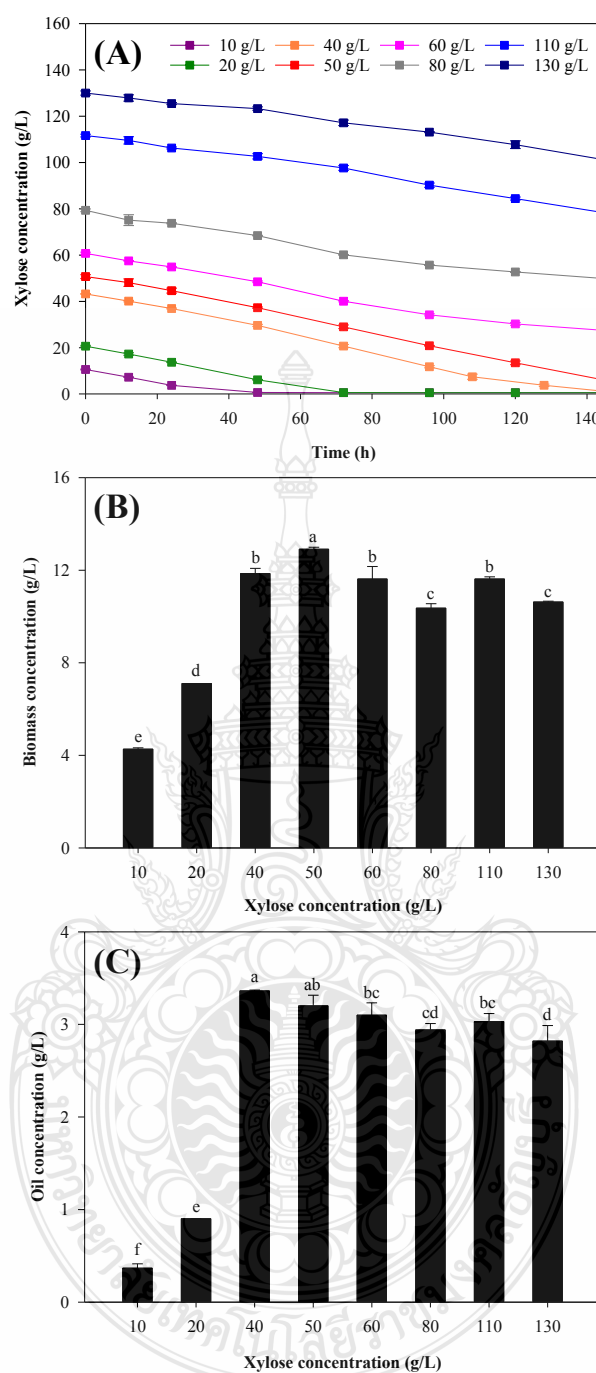
Figure 4.2 Time profiles of (A) xylose consumption and the production of (B) biomass and (C) YO of *P. parantarctica* CHC28 in X-OPM containing different initial xylose concentrations at 144 h. Data are represented as mean ± SD bar. The different superscripts indicate significant differences at *p*-value ≤ .05.

4.3 Effect of glucose and xylose mixtures as co-carbon sources on growth and YO production

The effect of co-carbon sources in GX-OPM on yeast growth and YO production was investigated under different glu:xyl ratios and presented in Figure 4.3, 4.4 and Table 4.3. Single and co-carbon sources were wholly utilized for growth and YO production of *P. parantarctica* CHC28 in all experiments (Figure 4.3 and 4.4), with biomass and YO concentration ranging from 10.92 ± 0.08 to 11.86 ± 0.23 g/L and 2.68 ± 0.15 to 3.36 ± 0.01 g/L, respectively. Comparing G-OPM and X-OPM, *P. parantarctica* CHC28 cultured in X-OPM could produce more biomass and YO than G-OPM (Table 4.3).

The $Y_{x/s}$, $Y_{p/s}$, and oil content obtained from X-OPM were 0.28, 0.08, and $28.4 \pm 0.5\%$, respectively. Results in Table 4.3 demonstrated that yeast CHC28 synthesized YO from xylose (3.36 ± 0.01 g/L) more than glucose (2.70 ± 0.07 g/L) by 24%. YO yield ($Y_{p/s} = 0.08$) was greatly increased using xylose as the main carbon source. Likewise, mycelia cells of *Cunninghamella echinulate* and *Mortierella isabellina* showed higher oil content derived from xylose than glucose as a carbon source [119]. Previous research showed that pentose sugar metabolism typically occurs through the pentose phosphate pathway (PPP) and phosphoketolase (PPK) [51]. The PPP catabolizes hexose into pentose sugar, producing D-ribose-5-phosphate and erythrose-4-phosphate that are used to synthesize nucleic acids and amino acids, respectively. The PPP releases NADPH which is utilized for oil synthesis. The PPP comprises two main stages. First, hexose sugar is oxidized and transformed to pentose sugar (D-ribulose 5-phosphate), releasing CO_2 and NADPH, while in the second stage, D-ribulose 5-phosphate is transformed into D-ribose-5-phosphate, followed by xylulose-5-phosphate, D-glyceraldehyde-3-phosphate, and erythrose-4-phosphate. The xylulose-5-phosphate is then transformed into acetyl-CoA, while erythrose-4-phosphate is used as a substrate in the glycolysis pathway (GLP) to generate ATP [51].

On the other hand, xylose is metabolized by the phosphorolytic reaction to produce acetyl-CoA from xylulose-5-phosphate using PPK as the critical enzyme [120-123]. The xylose metabolism pathway initiates from xylose, xylitol, and xylulose with enzymes xylose reductase (XR), xylitol dehydrogenase (XDH), and xylulokinase (XLK), respectively, according to xylulose-5-phosphate, with NADPH provided in this route

[120, 124]. Conversion of xylose into acetyl-CoA by the PPK system yielded 2 mol of acetyl-CoA from 1 mol of xylose, which is higher than glucose metabolism via the GLP and PPP (1.67 mol) pathways [120]. Therefore, using xylose as the primary carbon source during the development of oleaginous yeast resulted in high oil yield [125, 126].

A mixture of glucose and xylose could stimulate growth and YO production of *P. parantarctica* CHC28 (Table 4.3). Comparing co-carbon sources, maximum biomass concentration was recorded at a 2:1 glu:xyl ratio, with no significant difference when xylose was mainly used (glu:xyl ratio at 0:1). The YO concentration, substrate consumption, $Y_{x/s}$, $Y_{p/s}$, and oil content were not significantly different when cultivating *P. parantarctica* CHC28 in a co-carbon source-based medium. Furthermore, the YO production efficiency significantly reduced when a glucose and xylose mixture was employed as the co-carbon sources compared with xylose (Table 4.3). This result suggested that the mechanism of sugar utilization proceeded sequentially under mixed glucose and xylose cultivation.

Glucose was consumed first, while consumption of the other sugars was inhibited by catabolic repression or allosteric competition of sugar-transporting enzymes [109], thereby affecting the efficiency of utilizing xylose for oil production in GX-OPM.

Oil yields at 32 and 34% of consumed glucose and xylose, respectively were reported, according to the stoichiometry theory of oil production obtained from a substrate [119, 125, 127]. In this study, oil yield was closely expressed according to the stoichiometry theory as 33.34, 33.0, and 32.66% for glu:xyl ratios of 1:2, 1:1, and 2:1, respectively. Adopting xylose as the primary carbon source rather than glucose and other co-carbon sources greatly improved the efficiency of YO synthesis. This result concurred with the YO production of *R. toruloides* BOT-A2, *R. toruloides* CBS 14, *R. glutinis* CBS 3044, *L. starkeyi* InaCC Y604, *Cryptococcus* sp. MTCC 5455, and *Pseudozyma hubeiensis* BOT-O utilizing xylose as the major carbon source [28, 111, 128, 129].

Previous research demonstrated the YO production from lignocellulosic biomass such as wheat and rice straw, sugarcane bagasse, and corncob composed of glucose and xylose as the primary sugar following arabinose at lower concentrations [78, 79, 97, 130]. The glu:xyl ratios of those hydrolysates were different and depended on their original compositions and hydrolysis process. Suggestion, *P. parantarctica* CHC28 might produce

YO using the hydrolysate of cellulosic and hemicellulosic materials containing combined glucose and xylose as main carbon sources. *P. parantarctica* CHC28 was also a potentially suitable oleaginous yeast strain to investigate YO synthesis from lignocellulosic materials comprising various ratios of glucose and xylose.
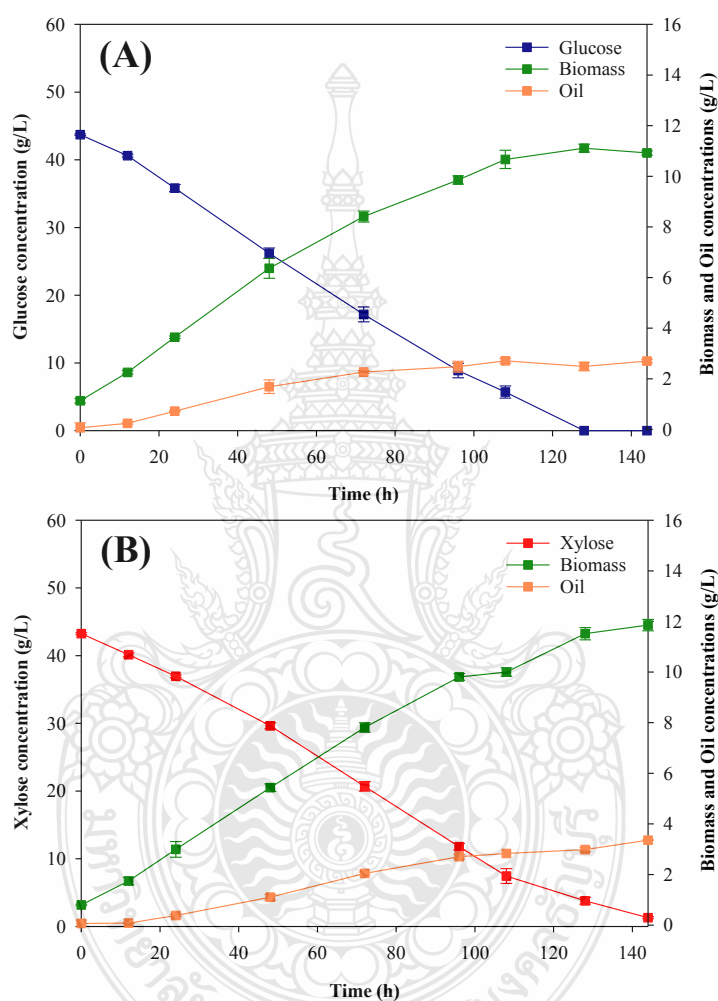
Figure 4.3 Time profiles of growth and YO production under glu:xyl ratios of (A) 1:0 and (B) 0:1 in the oil production medium. Data are represented as mean ± SD bar.
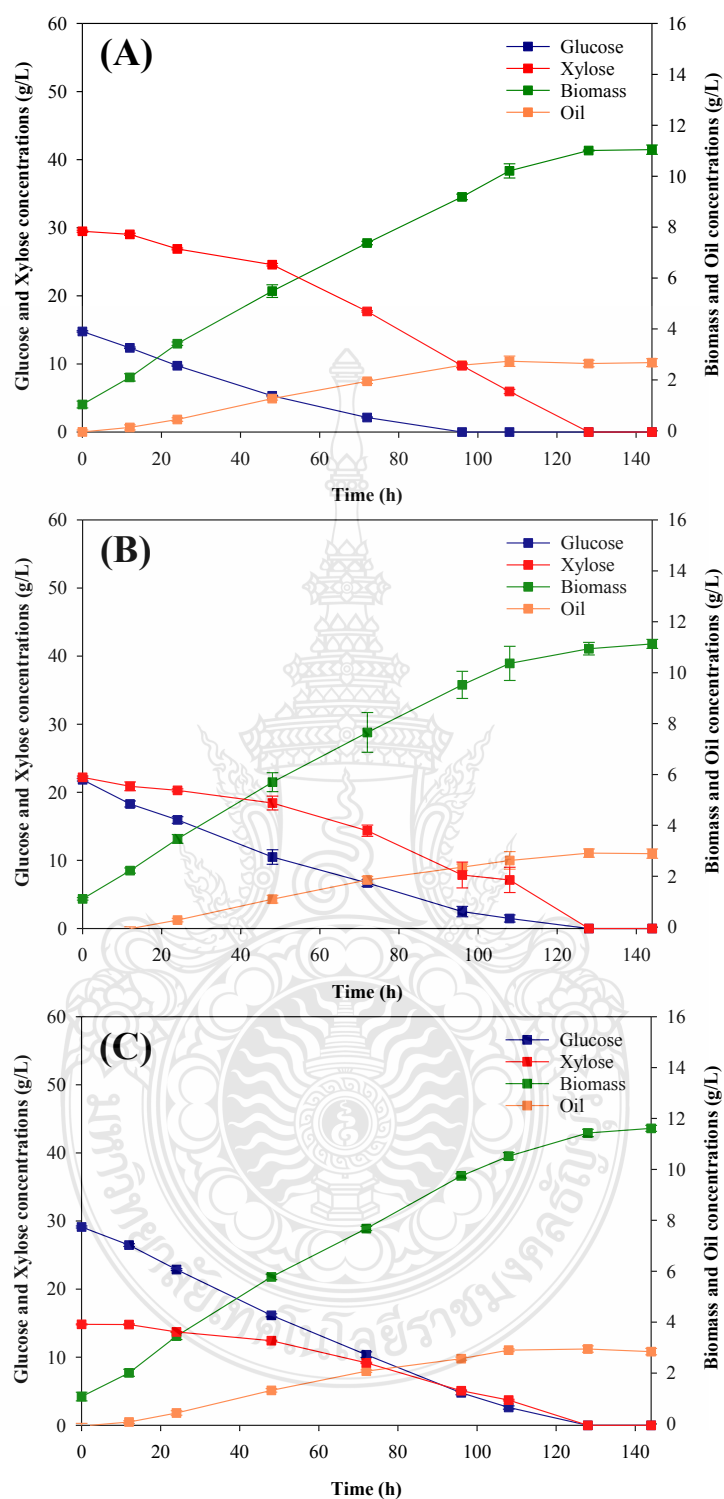
Figure 4.4 Time profiles of growth and YO production under glu:xyl ratios of (A) 1:2, (B) 1:1, and (C) 2:1 in the oil production medium. Data are represented as mean ± SD bar.

Table 4.3 Fermentation parameters in glucose and xylose mixtures as co-carbon sources at 144 h.

Glu:Xyl ratio	X (g/L)	P (g/L)	ΔS (g/L)	$Y_{x/s}$	$Y_{p/s}$	Oil content (%)
1:0	10.92 ± 0.08^b	2.70 ± 0.07^b	43.72 ± 0.12^b	0.25 ± 0.0^c	0.06 ± 0.0^b	24.7 ± 0.7^b
0:1	11.86 ± 0.23^a	3.36 ± 0.01^a	43.09 ± 0.17^c	0.28 ± 0.0^a	0.08 ± 0.0^a	28.4 ± 0.5^a
1:2	11.04 ± 0.18^b	2.68 ± 0.15^b	44.27 ± 0.27^a	0.25 ± 0.0^c	0.06 ± 0.0^b	24.2 ± 1.1^b
1:1	11.13 ± 0.18^b	2.89 ± 0.18^b	44.07 ± 1.20^{ab}	0.25 ± 0.0^c	0.07 ± 0.0^{ab}	26.0 ± 1.6^b
2:1	11.61 ± 0.12^a	2.84 ± 0.13^b	43.94 ± 0.22^{ab}	0.26 ± 0.0^b	0.06 ± 0.0^b	24.5 ± 1.1^b

[*]Data are presented as mean $\pm$ SD; different superscripts in the same column indicate significant differences at p-value $\leq .05$.

4.4 Enhancement of YO production by organic acid supplementation

The influence of organic acid supplementation was investigated and shown in Figure 4.5 and Table 4.4. Adding acetic acid significantly influenced yeast growth, resulting in reduced oleaginous biomass with increasing acetic acid concentration. Maximum biomass was obtained at 10.3 ± 0.05 g/L ($Y_{x/s} = 0.24$) at 1 g/L of acetic acid (Figure 4.5A and Table 4.4). Maximum YO concentration of 4.39 ± 0.30 g/L ($Y_{p/s} = 0.10$) was achieved at 1 g/L of acetic acid, and 31.5% higher than the unsupplemented condition (Figure 4.5B and Table 4.4). Furthermore, 1 g/L of acetic acid gave the highest oil content at $42.1 \pm 2.8\%$, higher than the unsupplemented condition by 1.4 times. This result demonstrated that acetic acid (1 g/L) accelerated YO production and substrate assimilation of CHC28 by triggering intracellular oil production, thereby providing a slightly shorter conversion pathway to acetyl-CoA, a crucial precursor in oil formation [131-133].

However, excessive concentration of acetic acid (> 5 g/L) ruptured the cell membrane, causing leakage of intracellular oil [132]. The influences of citric and succinic acids on biomass and YO formation were also investigated and presented in Figure 4.5 and Table 4.4. Citric and succinic acids exhibited slightly different yeast growths, the biomass ranged from 11.17 ± 0.23 to 11.32 ± 0.04 g/L and 9.63 ± 0.09 to 10.18 ± 0.16 g/L, respectively. While YO spanned from 3.12 ± 0.02 to 3.65 ± 0.16 g/L for citric acid and succinic acid supplementation, respectively.

These results suggested that citric and succinic acids were intermediate substances in the TCA cycle that had minimal effects on enhancing intracellular oil. These intermediate substances were re-generated to constantly compensate and adjust the balance of the TCA cycle [134]. Therefore, adding citric acid and succinic acid did not affect the oil production of CHC28.
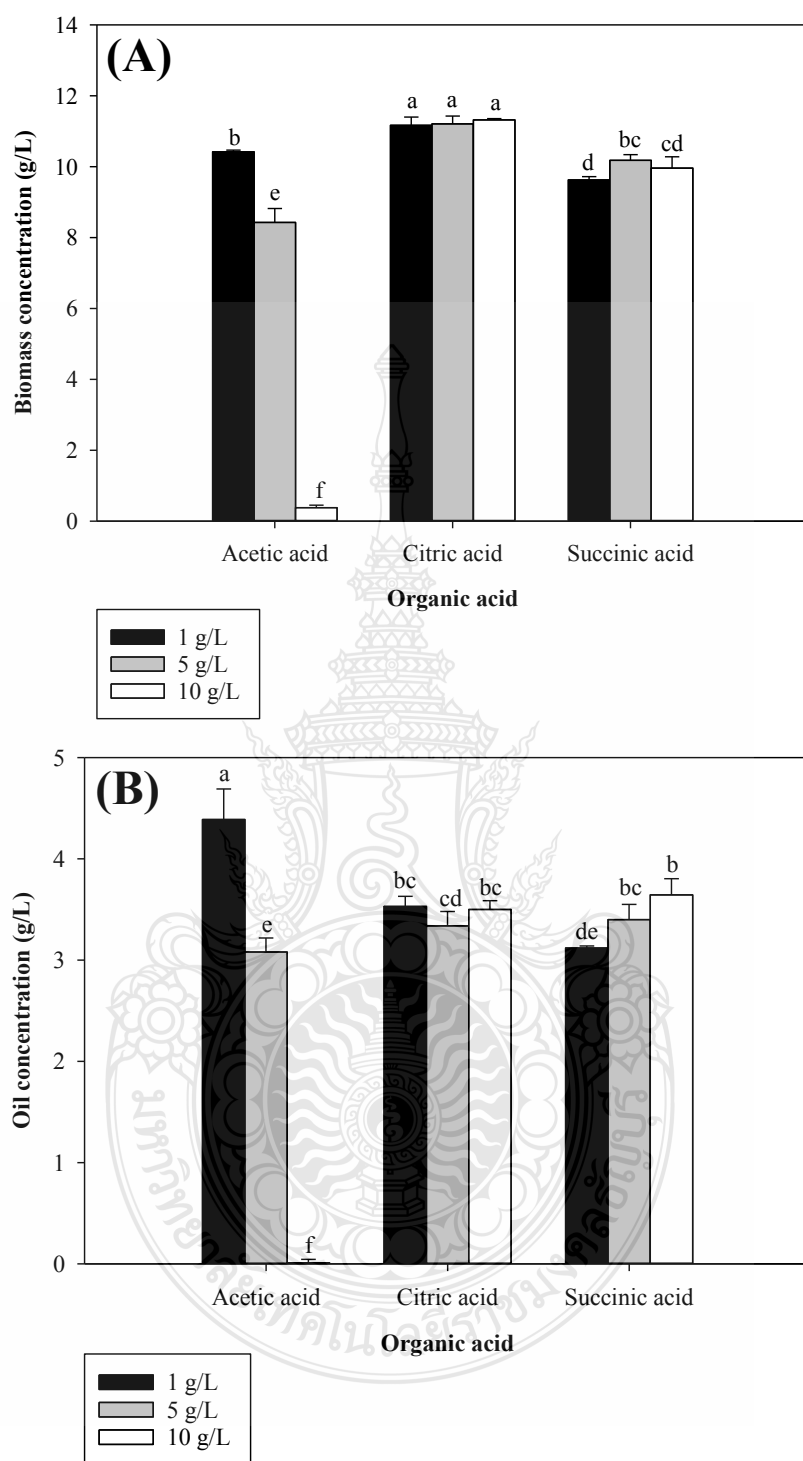
Figure 4.5 (A) Biomass and (B) YO production of *P. parantarctica* CHC28 cultivation in organic acids containing X-OPM at 144 h. Data are represented as mean ± SD bar.

Table 4.4 Influence of organic acid supplementation on growth and oil production in X-OPM at 144 h.

Conditions	ΔS (g/L)	$Y_{x/s}$	$Y_{p/s}$	Oil content (%)
Control	41.95 ± 0.17^c	0.28 ± 0.0^a	0.08 ± 0.0^b	28.4 ± 0.5^d
Acetic acid (g/L)				
1	43.70 ± 0.54^a	0.24 ± 0.0^{ab}	0.10 ± 0.01^a	42.1 ± 2.8^a
5	38.07 ± 0.64^e	0.22 ± 0.01^b	0.08 ± 0.0^b	36.5 ± 1.6^b
10	1.99 ± 0.28^f	0.19 ± 0.06^c	0.02 ± 0.0^c	8.3 ± 0.0^e
Citric acid (g/L)				
1	42.63 ± 0.24^b	0.26 ± 0.01^a	0.08 ± 0.0^b	31.7 ± 1.1^{cd}
5	42.36 ± 0.08^{bc}	0.27 ± 0.01^a	0.08 ± 0.0^b	29.9 ± 1.6^d
10	42.76 ± 0.68^{ab}	0.27 ± 0.0^a	0.08 ± 0.0^b	30.9 ± 0.7^{cd}
Succinic acid (g/L)				
1	41.23 ± 1.23^d	0.23 ± 0.0^a	0.08 ± 0.0^b	32.4 ± 0.5^{cd}
5	41.55 ± 0.31^{cd}	0.25 ± 0.01^{ab}	0.08 ± 0.0^b	33.4 ± 0.9^c
10	41.39 ± 0.16^{cd}	0.24 ± 0.01^{ab}	0.08 ± 0.0^b	36.6 ± 2.0^b

*Data are mean $\pm$ SD; different superscripts in the same column indicate significant differences at p-value $\leq .05$.

4.5 Compositions of rice straw hydrolysate

The rice straw was prepared and hydrolyzed by chemical and enzymatic hydrolysis. The compositions of rice straw hydrolysate (RSH) are shown in Table 4.5. The hydrolysis of RS released glucose, which was the major lignocellulosic sugar reached at a concentration of 24.7 ± 1.7 g/L ($70.3 \pm 0.3\%$), as well as xylose and arabinose, produced at 9.2 ± 0.7 ($26.1 \pm 0.2\%$) and 1.3 ± 0.2 g/L ($3.6 \pm 0.1\%$), respectively. Similarly, a study by Chen *et al*. reported that the alkaline-pretreated process and cellulase hydrolysis resulted in a higher glucose content compared to the acid-pretreated treatment [135]. The glucose content from the hydrolysis of RS strains RPY GENG and RIL272 increased to 72.95 and 71.37%, respectively. In contrast, the acid-pretreated (H_2SO_4) and cellulase hydrolysis of RS strains RPY GENG and RIL272 yielded the highest glucose

content at 70.2 and 69.0%, respectively [135]. However, Rashid *et al.* demonstrated a different result, showing that NaOH-pretreated RS (from Perlis, Malaysia) followed by cellulase hydrolysis resulted in a glucose content of 66.9% [72]. It was suggested that alkaline pre-hydrolysis successfully removed the lignin, increasing the surface area for more enzymatic hydrolysis accessibility [135, 136]. In contrast, high acid concentration pretreatment was found to negatively impact glucose yield, particularly in RS with a low lignin composition [135]. Glucose derived from cellulose hydrolysis through enzymatic processes, constitutes the primary structure within lignocellulosic plant cell walls. The lignocellulose structure consists of cellulose (35 to 40 %), hemicellulose (25 to 40 %), and lignin (10 to 20 %) [62]. However, the sugar composition in various plants was different. The RS species of *japonica* and *indica* given different ratios of the cell wall composition by cellulose, hemicellulose, and lignin ranging from 30 to 50%, 10 to 20%, and 10 to 30%, respectively [135]. Besides, the RS PR121 contained 25.94, 17.64, and 15.82% of cellulose, hemicellulose, and lignin, respectively [137]. In addition, furfural was not detected, while the 5-hydroxymethylfurfural (5-HMF) was generated during the hydrolysis of RS for 0.005 ± 0.001 g/L. The 5-HMF and furfural were generated when lignocellulosic material was degraded [138]. Likewise, the acid hydrolysis of exhausted olive pomace generated 5-HMF and furfural at 0.11 and 1.89 g/L, respectively, yielding glucose and xylose at 4.89 and 23.72 g/L, respectively [139]. Moreover, the diluted acid hydrolysis of sugarcane bagasse provided 11.8 g/L glucose and 125.3 g/L xylose and released 5-HMF and furfural at 0.07 and 0.45 g/L, respectively [140]. The 5-HMF and furfural released by acid-hydrolyzed corn stove ranged from 1.35 to 2.97 g/L and 1.46 to 2.98 g/L, respectively, including glucose (1.13 to 8.30 g/L) and xylose (8.44 to 45.22 g/L) [141]. In contrast, the hydrolysis of brewers' spent grain did not yield detectable levels of 5-HMF and furfural under slightly releasing glucose (26.4 g/L) and xylose (6.2 g/L). While higher glucose and xylose releasing at 50.6 to 69.1 g/L and 12.6 to 18.2 g/L, respectively, showed 5-HMF and furfural ranged from 0.006 to 0.009 and 0.009 to 0.014 g/L, respectively, for dilute acid-pretreated and enzyme hydrolysis [142]. The furfural and 5-HMF released during the degradation of cellulose fractions of lignocellulosic biomass were denoted as the crucial inhibitors of microbial metabolism, influencing the bioconversion of sugars into target product [79, 143]. Our preparation provides RSH with

high levels of glucose and xylose as the main components, along with low furfural and 5-HMF content. The RSH was used as the primary carbon source for YO production in this study.

Table 4.5 The compositions of RSH.

Compositions	Concentrations (g/L)
Glucose	24.7 ± 1.7
Xylose	9.2 ± 0.7
Arabinose	1.3 ± 0.2
Furfural	Not detected
5-HMF	0.005±0.001

4.6 Optimization of yeast oil production from RSH by response surface methodology

The optimum condition of yeast growth and YO production from *P. parantarctica* CHC28 using RSH-based oil production medium (RSH-OPM) was arranged as 15 runs of Box-Behnken design (Table 4.6). The influence of three independent variables, including total sugar of RSH (A), $(NH_4)_2SO_4$ (B), and KH_2PO_4 (C) on biomass (Y_1) and YO production (Y_2) were investigated. The experimental results of biomass and YO ranged at 0.23 to 5.93 g/L and 0.19 to 1.72 g/L, respectively, at 144 h of cultivation. The biomass and YO were maximized through BBD, accorded by second-order quadratic model. The high biomass (4.28 to 5.93 g/L) was obtained from the experimental results which used 10 g/L of total sugar of RSH (run 9–15). The almost biomass was decreased when 5 and 15 g/L total sugar of RSH was used. The excess of $(NH_4)_2SO_4$ (runs 3 and 4) and KH_2PO_4 (runs 7 and 8) provided a negative impact on YO production. The highest YO was achieved at 1.72 g/L (run 2) when $(NH_4)_2SO_4$ and KH_2PO_4 were added for 0.5 and 7 g/L, respectively. Previous research has reported that the nitrogen limitation affected the oil accumulation of oleaginous yeast. A high C/N ratio of the medium could catabolite the sugar for oil synthesis when the nitrogen was depleted [50]. The

incompleteness of nitrogen source in the medium promoting yeast generated oil and accumulated within cells, replacing protein synthesis in the enriched-nitrogen medium [58]. Amount limited-nitrogen sources impact the biosynthesis perturbation of the citric acid cycle because of isocitrate dehydrogenase inhibition in the mitochondrial made to citrate released into the cytoplasm, which is caused by decreasing adenosine monophosphate (AMP) level [60] that broke down by the ATP-citrate lyase into oxaloacetate and acetyl-CoA then reunifies with NADPH derived from the sugar catabolism for the fatty acid synthesis [50, 51]. Phosphorus is an essential component incorporating nucleic acids, phosphorylated proteins, phospholipids, and coenzymes [59, 60]. Previous research reported that the limitation of nitrogen and phosphorus sources resulted in a slight decrease in biomass, while oil content increased and continually enhanced by carbon sources metabolized [60, 61]. Therefore, the nitrogen and phosphorus limitations and excess carbon sources are the key factors of YO production efficiency. Our finding indicated that the RS hydrolysis process provided a lack of inhibiting by-products (furfural and 5-HMF) from lignocellulosic biomass. It also demonstrated that the RSH was the effective substrate as a carbon source for biomass and YO production.

The analysis of variance (ANOVA) and code regression coefficients of the quadratic model for find the influencing factors to biomass and YO production were shown in Table 4.6. The statistical analysis results of biomass showed that p-value of biomass and YO production models were 0.0759 and 0.0192, respectively. It was indicated that the biomass model was not significant at the confidence level of 95% (p-value $> .05$), whereas the YO model was significantly different (p-value $\leq .05$). In addition, the lack of fit of both models was not significant (p-values $= 0.1175$ and 0.2934), indicating that the regression models had suitability for experimental data. The value of the coefficient of determination (R^2) of biomass and YO models were 0.8739 and 0.9314, respectively, indicating that the experimental findings and predicted data were well correlated (Table 4.6). It also revealed that particular 12.61 and 6.86% of the overall changes could not be accounted for by the biomass and YO fitted models, respectively. For biomass generation, the total sugar of RSH had a much higher impact than $(NH_4)_2SO_4$ and KH_2PO_4. The quadratic coefficient of RSH based-total sugar (A^2) was significant with the p-value at .0042. Furthermore, the total sugar of RSH likewise had the most impact

69

on YO synthesis (p-value = .0257), similar to biomass production. The results also found that the quadratic coefficients of RSH based-total sugar (A^2) and $(NH_4)_2SO_4$ (B^2) had significant p-values of .0495 and .0464, respectively. Additionally, the interaction effect of biomass and YO models between the two variables (AB, AC, and BC) was also found to be insignificant (p-value > .05). Consequently, the second order quadratic equation for biomass (Y_1) and YO production (Y_2) was described by Eqs. (18) and (19).

$$Y_1 = -4.70 + 1.91A + 0.11B + 0.15C - 0.06AB + 0.02AC + 0.02BC - 0.09A^2 + 0.05B^2 - 0.02C^2 \tag{18}$$

$$Y_2 = -0.35 + 0.30A - 0.35B - 0.02C - 0.03AB + 0.01AC + 0.01BC - 0.01A^2 + 0.07B^2 - 0.002C^2 \tag{19}$$

Table 4.6 ANOVA results of BBD for biomass and YO production from RSH.

Source	Biomass					YO				
	Sum of squares	df	Mean square	F-value	p-value	Sum of squares	df	Mean square	F-value	p-value
Model	28.31	9	3.15	3.85	0.0759	3.03	9	0.3365	7.55	0.0192*
A–RSH	17.88	1	17.88	21.89	0.0054**	0.4396	1	0.4396	9.86	0.0257*
B–$(NH_4)_2SO_4$	0.0156	1	0.0156	0.0191	0.8955	0.1554	1	0.1554	3.49	0.1209
C–KH_2PO_4	0.4276	1	0.4276	0.5234	0.5018	0.0060	1	0.0060	0.1340	0.7293
AB	1.42	1	1.42	1.74	0.2445	0.2500	1	0.2500	5.61	0.0641
AC	1.19	1	1.19	1.46	0.2811	0.1640	1	0.1640	3.68	0.1132
BC	0.2669	1	0.2669	0.3268	0.5923	0.0441	1	0.0441	0.9893	0.3656
A^2	20.32	1	20.32	24.87	0.0042**	0.2964	1	0.2964	6.65	0.0495*
B^2	0.1603	1	0.1603	0.1962	0.6763	0.3087	1	0.3087	6.93	0.0464*
C^2	3.88	1	3.88	4.75	0.0812	0.0433	1	0.0433	0.9721	0.3694
Residual	4.08	5	0.8169			0.2229	5	0.0446		
Lack of Fit	3.76	3	1.25	7.67	0.1175	0.1768	3	0.0589	2.56	0.2934
Pure Error	0.3267	2	0.1633			0.0461	2	0.0230		
Cor Total	32.40	14				3.25	14			
	$R^2 = 0.8739$					$R^2 = 0.9314$				

*p-value $\leq$ .05 and **p-value $\leq$ .01.
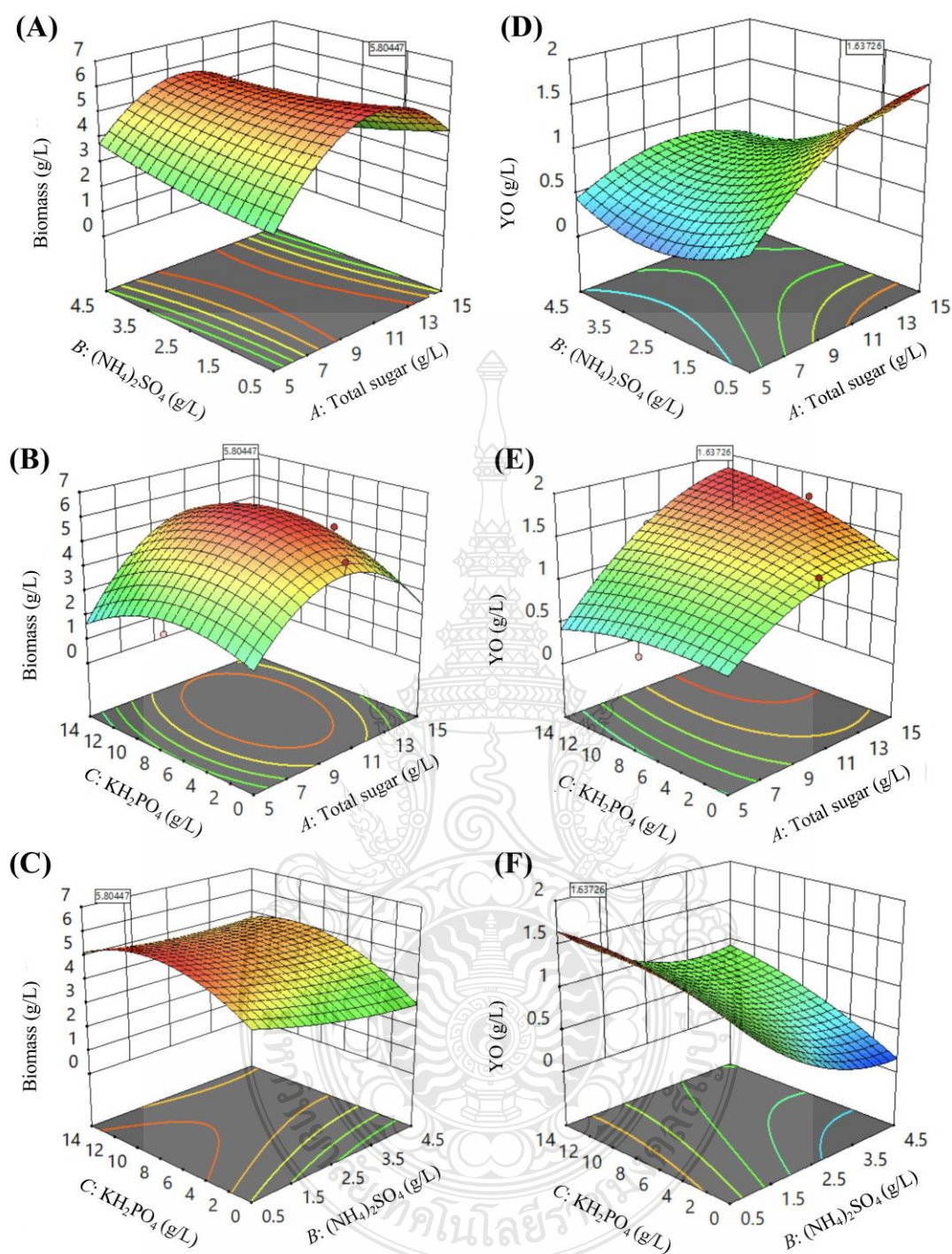
Figure 4.6 3D surface and 2D contour graph of biomass (A), total sugar of RSH and $(NH_4)_2SO_4$; (B), total sugar of RSH and KH_2PO_4; and (C), $(NH_4)_2SO_4$ and KH_2PO_4 and YO production (D), total sugar of RSH and $(NH_4)_2SO_4$; (E), total sugar of RSH and KH_2PO_4; and (F), $(NH_4)_2SO_4$ and KH_2PO_4 from RSH-medium analyzed by RSM.

The Eqs. (18) and (19) were employed to create the three-dimensional (3D) response surface graph and the related two-dimensional (2D) contour to determine the optimum combination of the assessed variables (Figure 4.6A to F). The biomass increase as total sugar of RSH rised from 5 to 10 g/L, until it entered to a saddle-shaped region (Figure 4.6A). The biomass response decreased as total sugar of RSH increased. The contour map presented the sligh interaction between $(NH_4)_2SO_4$ and total sugar of RSH. The interaction effect of KH_2PO_4 and total sugar of RSH (Figure 4.6B), increase of KH_2PO_4 and total sugar of RSH from 0 to 7 g/L and 5 to 10 g/L enhance the biomass to highest contour area. The biomass also dropped as both variables increased. The biomass slightly increased with increasing of KH_2PO_4 and lowering of $(NH_4)_2SO_4$ (Figure 4.6C).

The combined effect of total sugar of RSH and $(NH_4)_2SO_4$ on YO production presented the weak interaction, YO rised as total sugar of RSH rised from 5 to 15 g/L (Figure 4.6D). In addition, YO gradually reached to the highest contour area as increase of KH_2PO_4 and total sugar of RSH (Figure 4.6E). Consequently, YO increased as KH_2PO_4 raised and $(NH_4)_2SO_4$ dropped (Figure 4.6F). The optimum condition which achieved from second-order quadratic model was at 10 g/L RSH, 0.5 g/L $(NH_4)_2SO_4$, and 9 g/L KH_2PO_4. Subsequently, CHC28 was cultured under the optimum condition by batch mode (Figure 4.7). The result found that the biomass and YO concentration were achieved at 4.67 ± 0.09 g/L and 1.02 ± 0.05 g/L at 144 h. Furthermore, it was observed that xylose was completely consumed, and glucose remained at only approximately 6.9% of the initial concentration after 72 h of yeast cultivation (Figure 4.7). This finding highlights the suitability of the RSH, prepared in this study, as a favorable substrate for YO production by *P. parantarctica* CHC28.

Our research reveals a variable response during yeast cultivation for YO production. The total sugar content of RSH showed a positive correlation with both the maximum biomass and YO production. However, to enhance YO production efficiency from RSH, it is essential to consider all three studied variables and other control factors concurrently to optimize the YO production process. This approach can lead to further improvements in YO production by *P. parantarctica* CHC28 using the low 5-HMF containing RSH as a substrate.
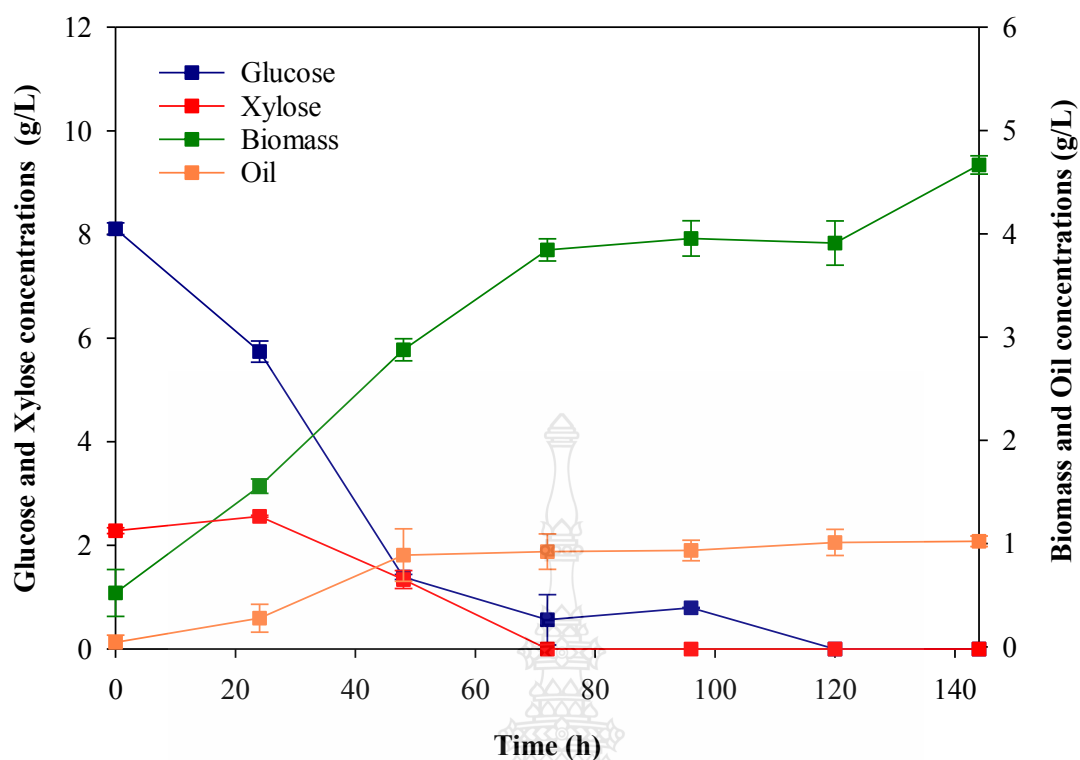
Figure 4.7 Schematic of oleaginous yeast cultivation for YO production from RSH-medium under optimum condition by batch fermentation.

4.7 High cell-density cultivation by fed-batch mode for YO production from RSH

The high cell-density (HCD) cultivation has been performed to enhance biomass and YO production and reduce the inoculum propagating time. The inoculum has only been prepared for the initial batch mode. To completely utilize total fermentable sugars on RSH (glucose and xylose), RSH was used to prepare the cultivation medium (RSH-OPM) and feeding medium. RSH-based medium and RSH have been added as the main carbon sources during shaking flask culture to improve biomass and YO production efficiency for fed-batch mode. When the total sugar was fully consumed (every 72 h), The feeding was aseptically transferred into culture for an increment of the total sugar at approximately 10 g/L total sugar. The fed-batch mode was compared for biomass and YO production by feeding with RSH-based medium and RSH. The schematic of volumetric biomass and YO production were depicted in Figure 4.8.

As illustrated in Figure 4.8A and B, *P. parantarctica* continually exhibited a sequential consumption of glucose and xylose in RSH in the 1st to 3rd feeding batch when both RSH-based medium and RSH were fed. In contrast, the glucose in RSH was partially consumed in the 4th batch. A repeating sequential utilization pattern was observed in the 1st to 3rd batches of fed-batch culture process, indicating continuous catabolic repression activity [144]. As an example, in the 1st batch of both feedings, glucose was rapidly and completely consumed within 72 h after feeding, similar to the trend of xylose utilization (Figure 4.8A and B). The results clearly demonstrated that the glucose uptake rate was higher than that of xylose. Interestingly, xylose consumption was initiated only when the glucose levels were nearly depleted.

This result is comparable to the utilization of corn stover for microbial lipogenesis [144]. It was proposed that when glucose was maintained at a low concentration, xylose and glucose may be assimilated concurrently. In contrast, glucose was only partially used, and xylose was entirely metabolized at 288 h of feeding in the 4th batch of RSH feeding (Figure 4.8B). As shown in Figure 4.8B, the quantity of carbon source consumption was obviously declined at the last feeding of process. It was suggested that RSH feeding might not be enough essential nutrients for the growing and metabolic activities of yeast cells, impacting the cell viability and substrate consumption of carbon sources and product formation. RSH feeding only contained carbon sources without other essential nutrients for yeast, causing shorter cell viability than RSH-based medium feeding. Also, *Rhodosporidium toruloides* 32489 cultivation by impurified crude glycerol contained various mineral salt as carbon source. It presents the benefits for yeast growth with osmoregulation and a healthy physiological for growth and reproduction to improve biomass and oil synthesis. It demonstrated that oil production in crude glycerol is higher than in glucose and pure glycerol [145]. Similarly, *Rhodotorula mucilaginosa* G43 and *Candida tropicalis* X37 synthesize YO from crude glycerol higher than pure glycerol [146].

In addition, the result presented that the volumetric biomass and YO were consistently enhanced throughout the fed-batch culture (Figure 4.8A and B, and Table 4.7). These values levels reached their highest at the end of the 3rd cycle. Specifically, when fed with RSH-based medium and RSH, the volumetric biomass attained the maximum levels at 7.36 ± 0.18 and 6.61 ± 0.08 g/L, while the YO production achieved its highest levels at 3.77 ± 0.09 and 3.98 ± 0.16 g/L, respectively (Table 4.7).

Compared to batch mode, the $Y_{x/s}$ achieved in fed-batch mode was lower (Table 4.7). However, the fed-batch mode provided a higher $Y_{p/s}$ than the batch mode. This result demonstrated that the repeated feeding of the carbon source could increase the C/N ratio of cultivation. Thereby the lipogenesis of the oleaginous yeast is highly induced. Moreover, yeast demonstrates the ability to utilize the substrate efficiently and continuously in fed-batch cultivation, which is the limitation of the batch cultivation [27, 84, 85].

The oil content of both feeding conditions increased to over 50% since the end of the 2nd batch (Table 4.7). This value was even higher than that observed in batch mode, indicating that RSH sugar uptake significantly contributed to YO synthesis through the fed-batch method. The accumulated quantity of YO achieved in this study is comparable to several other research findings that used agro-waste hydrolysate as a substrate. For instance, the oil content of oleaginous yeast *Lipomyces tetrasporus* cultured in switchgrass hydrolysate was reported to be 53.4% w/w [147]. Additionally, the culture of *Cryptococcus* sp. using corncob hydrolysate provided oil content of 63.5% and 59% w/w, respectively [148]. Similarly, *R. toruloides* DSMZ 4444 and *Cutaneotrichosporon oleaginosum* grown in corn stover hydrolysate delivered oil content of 59% and 61.7% w/w, respectively [149, 150]. Moreover, using pasta processing waste hydrolyzed by an enzymatic process as the sole substrate, *Sporobolomyces roseus* CFGU-S00 achieved an oil content of 40% w/w [151]. These findings collectively highlight the potential of using different agro-waste hydrolysates to produce high oil content in various oleaginous yeast species. In conclusion, this study demonstrated that the fed-batch mode could effectively enhance the oil content of *P. parantarctica* when cultured using RSH as the primary carbon source.
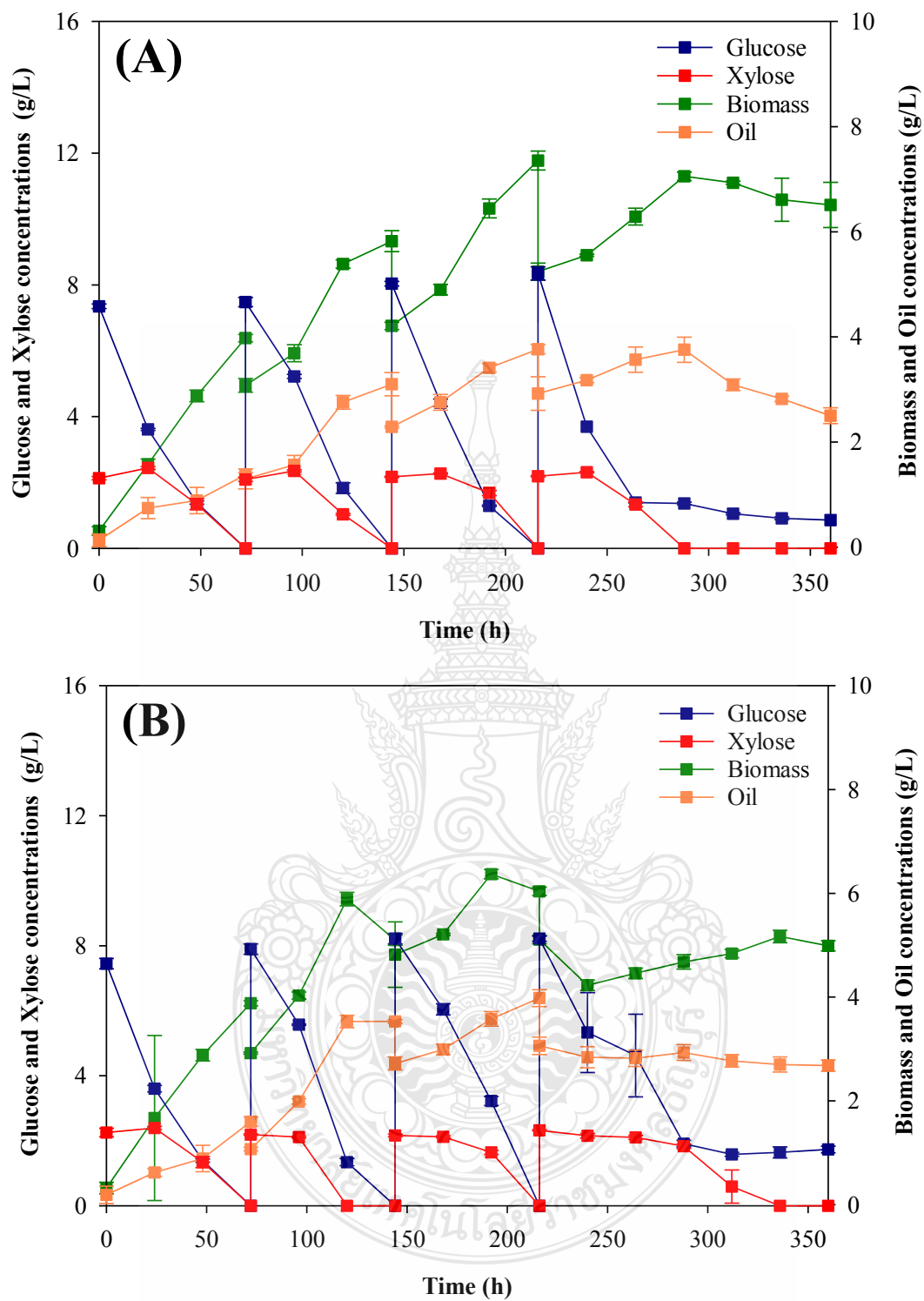
Figure 4.8 Volumetric YO production profile under high cell-density cultivation by fed-batch fermentation feeding with (A) RSH-based medium and (B) RSH.

Table 4.7 Parameters of volumetric yeast oil production under RSH-based medium by different cultivation modes.

Cultivation modes	X (g/L)	P (g/L)	ΔS (g/L)	$Y_{x/s}$	$Y_{p/s}$	Oil content (%)
Batch mode	4.67 ± 0.09^f	1.02 ± 0.05^e	10.39 ± 0.17^a	0.45 ± 0.01^g	0.10 ± 0.01^f	21.90 ± 0.69^f
Fed-batch mode with RSH based-medium feeding						
1st Batch	3.98 ± 0.07^g	1.38 ± 0.04^d	9.48 ± 0.04^f	0.42 ± 0.01^a	0.15 ± 0.0^c	34.65 ± 1.28^e
2nd Batch	5.82 ± 0.20^d	3.10 ± 0.22^c	19.05 ± 0.20^e	0.31 ± 0.01^c	0.16 ± 0.01^b	53.34 ± 5.22^c
3rd Batch	7.36 ± 0.18^a	3.77 ± 0.09^{ab}	29.26 ± 0.25^d	0.25 ± 0.0^d	0.13 ± 0.0^d	51.21 ± 0.15^c
4th Batch	7.06 ± 0.08^b	3.76 ± 0.24^{ab}	38.44 ± 0.48^a	0.18 ± 0.0^f	0.10 ± 0.01^e	53.21 ± 2.73^c
Fed-batch with RSH feeding						
1st Batch	3.88 ± 0.05^g	1.60 ± 0.09^d	9.69 ± 0.28^f	0.40 ± 0.02^b	0.17 ± 0.01^b	41.28 ± 2.76^d
2nd Batch	5.09 ± 0.10^e	3.53 ± 0.03^b	19.78 ± 0.45^e	0.26 ± 0.0^d	0.18 ± 0.01^a	69.46 ± 2.03^a
3rd Batch	6.61 ± 0.08^c	3.98 ± 0.16^a	30.17 ± 0.63^c	0.22 ± 0.0^e	0.13 ± 0.0^d	60.16 ± 1.76^b
4th Batch	4.68 ± 0.14^f	2.93 ± 0.15^c	36.97 ± 0.80^b	0.13 ± 0.0^g	0.08 ± 0.01^f	62.71 ± 2.70^b

X, P, and ΔS were the accumulated values. Different superscripts presented a significant difference in the same column at p-value $\leq .05$.

The total production of biomass and YO by fed-batch mode were depicted in Figure 4.9A and B. At the 4th batch of RSH-based medium feeding, these values were achieved at the significant highest of 1.30 ± 0.04 and 0.62 ± 0.07 g/L, respectively. In contrast, the RSH feeding of fed-batch mode provided the maximum total biomass and YO at 0.91 ± 0.02 and 0.54 ± 0.01 g/L, respectively. This result showed that the fed-batch mode with RSH-based medium feeding provided a significantly effective strategy feeding better than RSH feeding.

The total production of biomass and YO through the fed-batch mode is illustrated in Figure 4.9A and B, respectively. Notably, during the 4th batch cycle with RSH-based medium feeding, these values reached the highest significant levels at 1.30 ± 0.04 and 0.62 ± 0.07 g, respectively (Figure 4.9A and B). In contrast, employing RSH feeding in the fed-batch mode resulted in a maximum total biomass and YO of 0.91 ± 0.02 and 0.54 ± 0.01 g, respectively, at the 3rd batch cycle. the total production of RSH feeding subsequently declined during the 4th batch cycle (Figure 4.9A and B). The result suggested that the 3rd batch presented that glucose and xylose were thoroughly consumed. While the 4th batch showed a declining carbon consumption capacity, as illustrated in Figure 4.9B, biomass and YO production decreased together after feeding the 4th batch RSH. Moreover, the yeast might reuse the intracellular YO instead of other carbon sources, affecting its accumulated YO and oleaginous biomass. Therefore, the product decrease after the 3rd batch might be caused by other essential nutrients that originated as insufficient for cultivation in the 4th batch of RSH feeding. This discovery is significant, as it emphasizes the superior effectiveness of the fed-batch mode with RSH-based medium feeding, leading to higher total biomass and YO production than RSH feeding alone (Table 4.8). The RSH-based medium feeding strategy proved more effective in promoting the growth and YO production of *P. parantarctica* CHC28 during fed-batch mode. This approach involved the supplementation of essential nutrients to the medium during each feeding cycle, enabling the yeast to efficiently utilize carbon sources for sustained growth and YO production over extended cultivation periods. Similarly, applying a nitrogen source in every feeding cycle during the fed-batch cultivation of *Sporobolomyces roseus* CFGU-S005 was investigated. The results demonstrated a twofold increase in production efficiency compared to batch mode, yielding 6.6 g/L of

lipids and 3.4 mg/L of carotenoids at the culmination of the cultivation process [89]. Furthermore, prior research explored the utilization of double-fold essential nutrients, including nitrogen and phosphate sources, in a fed-batch fermentation setup for *Trichosporon oleaginosus*. This approach resulted in sustained growth and enhanced oil production, with the organism exhibiting robust performance until nearly all substrate was consumed [152]. These findings collectively underscore the significance of the RSH-based medium feeding strategy in facilitating high-cell density cultivation.
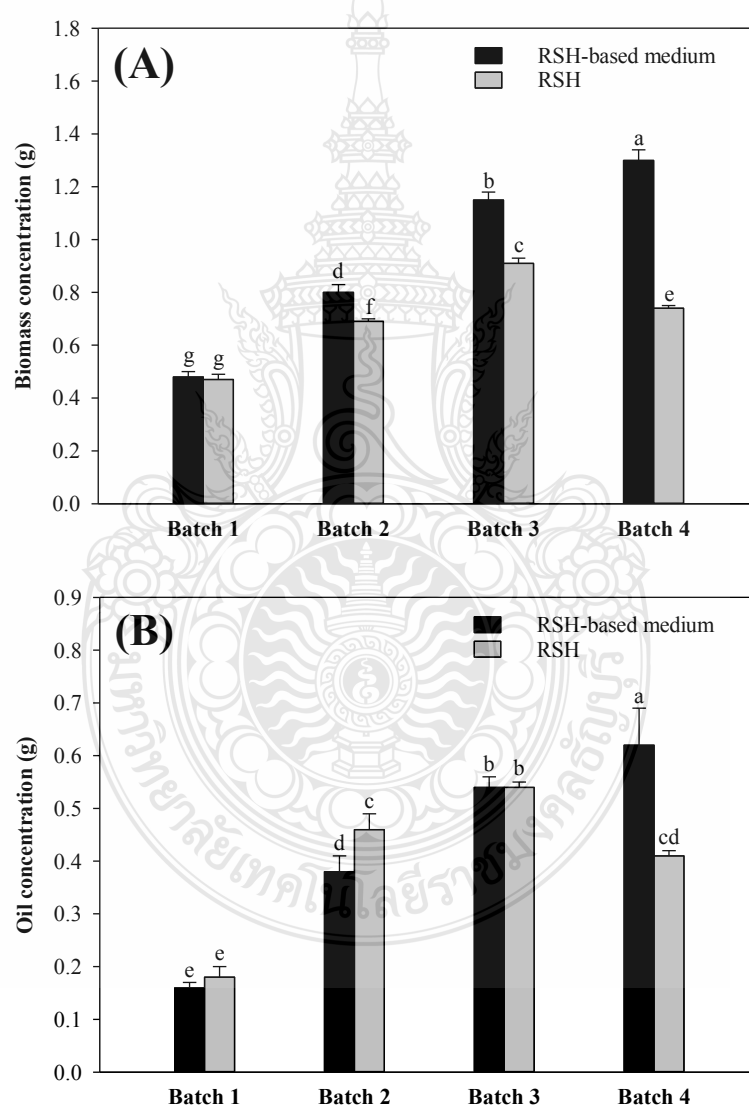
Figure 4.9 Total production of biomass and YO under high cell-density cultivation by fed-batch fermentation feeding with (A) RSH-based medium and (B) RSH.

Table 4.8 Summary parameters of yeast oil production under different optimum cultivations.

Cultivations	X (g/L)	P (g/L)	ΔS (g/L)	$Y_{x/s}$	$Y_{p/s}$	Oil content (%)
Batch						
Xylose (40 g/L)	11.86 ± 0.23	3.36 ± 0.01	41.95 ± 0.17	0.28 ± 0.0	0.08 ± 0.0	28.4 ± 0.5
Xylose (40 g/L) and acetic acid (1 g/L)	10.3 ± 0.05	4.39 ± 0.30	43.70 ± 0.54	0.24 ± 0.0	0.10 ± 0.01	42.1 ± 2.8
RSH (10 g/L)	4.67 ± 0.09	1.02 ± 0.05	10.39 ± 0.17	0.45 ± 0.01	0.10 ± 0.01	21.90 ± 0.69
Fed-batch						
RSH based-medium feeding	7.36 ± 0.18	3.77 ± 0.09	29.26 ± 0.25	0.25 ± 0.0	0.13 ± 0.0	51.21 ± 0.15
RSH feeding	6.61 ± 0.08	3.98 ± 0.16	30.17 ± 0.63	0.22 ± 0.0	0.13 ± 0.0	60.16 ± 1.76

*Data are mean ± SD.

4.8 Mathematical modeling

4.8.1 Kinetics of YO production under various initial xylose concentrations

The kinetic parameters of non-linear mathematic models were estimated by curve fitting. The experimental value was fitted with the model value by minimizing the differences using the curve fit function of Berkeley Madonna^{TM} (www.berkeleymadonna.com). Under different initial xylose concentrations, X_{max} and μ_{max} were estimated according to Eq. (2). The influences of initial xylose concentration on the relative maximum biomass (X_{max}/X_{max10}) and relative maximum specific growth rate (μ_{max}/μ_{max10}) are illustrated in Figure 4.10. These parameters were expressed by comparing the modeled X_{max} and μ_{max} for each initial xylose concentration with 10 g/L xylose. Results showed that enhancement of xylose concentration dramatically increased the modeled X_{max} and relative maximum biomass (Figure 4.10). By contrast, increase in xylose concentration decreased the modeled μ_{max}, while the relative maximum specific growth rate also decreased (Figure 4.10). This result indicated that high initial xylose concentration in X-OPM depressed μ_{max} but promoted X_{max} of *P. parantarctica* CHC28. Previous research reported that increased initial xylose concentration impacted yeast cell growth [92, 153, 154]. High sugar concentration reduced cell membrane liquidity, with longer time required to transport biomolecules via the transmembrane layer of yeast cells [155]. Thus, increasing xylose concentration decreased the growth rate of yeast CHC28.

Simulation of the YO production profile was conducted at various initial xylose concentrations, ranging from 10 to 130 g/L, using mathematical models for yeast growth, YO production, and substrate consumption (Eqs. (2) to (12)). The resulting R^2 values ranged from 0.913 to 1, as shown in Figures 4.11 to 4.14. Furthermore, the *NRMS* was calculated for all conditions, which ranged between 0.061 and 4.067, as indicated in Table 4.9. These values demonstrate that the model accurately and consistently explained the measurements, providing reliable and precise insights into YO production under different initial xylose concentrations.

The kinetic parameters obtained from the mathematical equations are presented in Table 4.9. The highest μ_{max} value was observed at 0.103 h^{-1} with an initial xylose concentration of 10 g/L, followed by a declining trend as the xylose concentration increased. For xylose concentrations of 20 and 40 g/L, μ_{max} remained relatively high at

0.080 h^{-1}. However, when the initial xylose concentration exceeded 60 g/L, μ_{max} dropped to under 0.053 h^{-1}. Conversely, X_{max} increased from 4.31 to 14.63 g/L with increasing xylose concentration (Table 4.9). The k_i value decreased as the xylose concentration rose, indicating an increased substrate inhibition effect under high substrate concentrations. The $Y_{x/s}$ values showed slight differences and ranged from 0.30 to 0.37. The highest $Y_{p/s}$ value was 0.12 at an initial xylose concentration of 40 g/L (Table 4.9), and it gradually decreased with higher xylose concentrations. The m_s values were constrained to very low across all xylose concentrations, suggesting that most xylose was minimally utilized for cell maintenance (Table 4.9). Additionally, the α value was greater than the β value in all experiments (Table 4.9), indicating that the entire YO product was generated together with the yeast growth as a growth-associated product. These results provide valuable insights into the relationship between kinetic parameters and xylose concentration, clarifying the YO production behavior during the experiments.
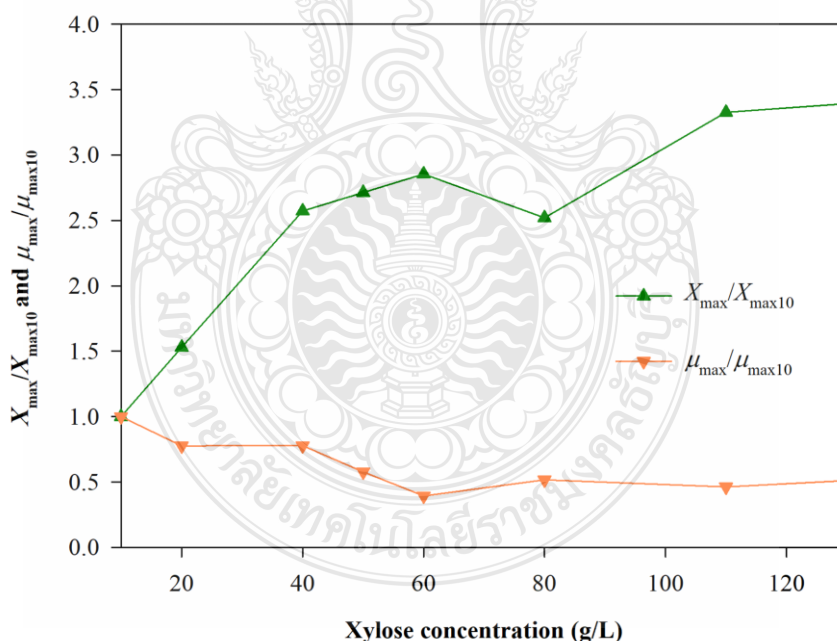
Figure 4.10 Relative maximum biomass (X_{max}/X_{max10}) and relative maximum specific
growth rate (μ_{max}/μ_{max10}) of *P. parantarctica* CHC28 cultivation in different
xylose concentrations.
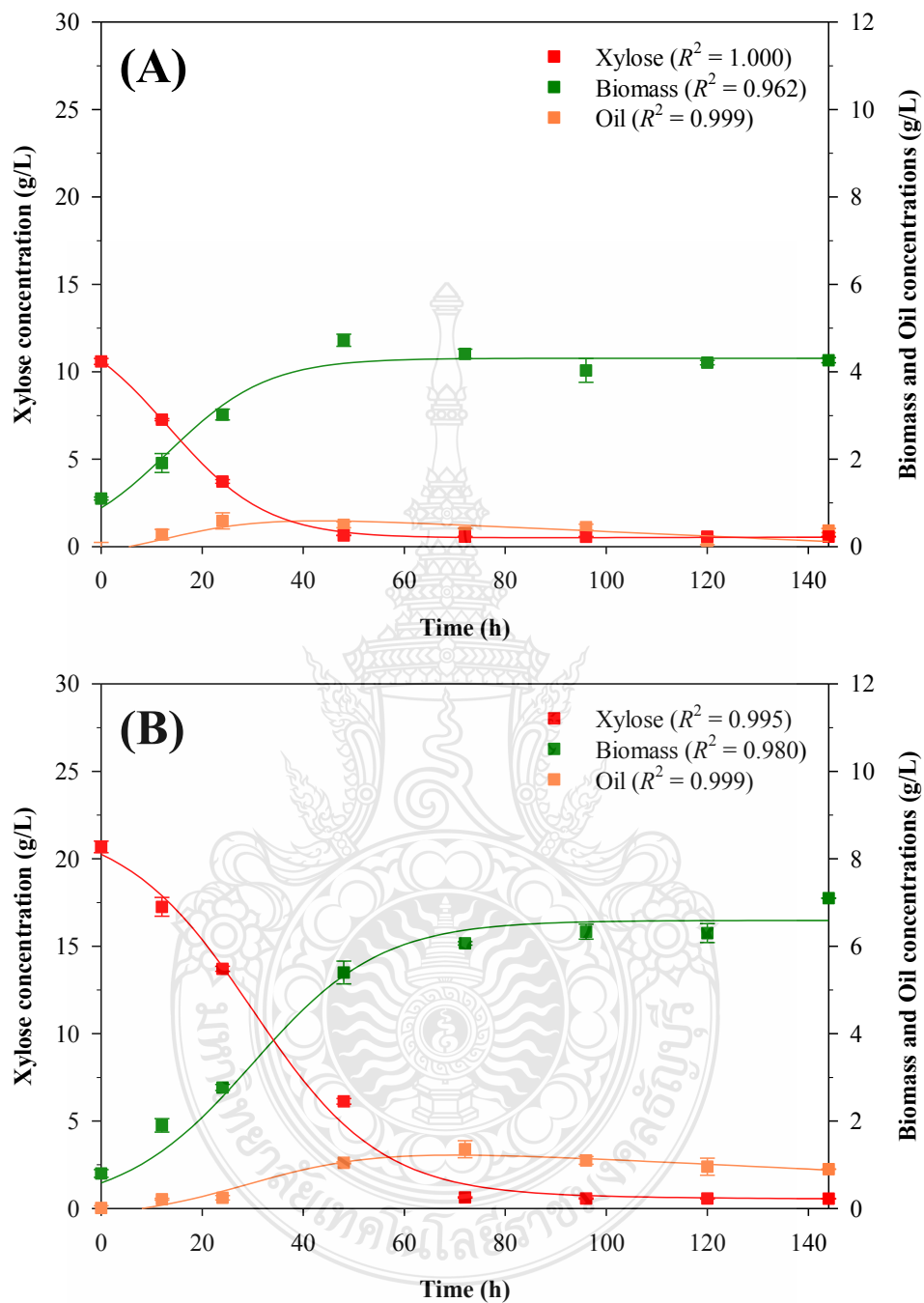
Figure 4.11 Experimental results (symbols) and model predictions (lines) of substrate consumption, cell growth, and YO production profiles of *P. parantarctica* CHC28 cultured at 10 and 20 g/L xylose concentrations.
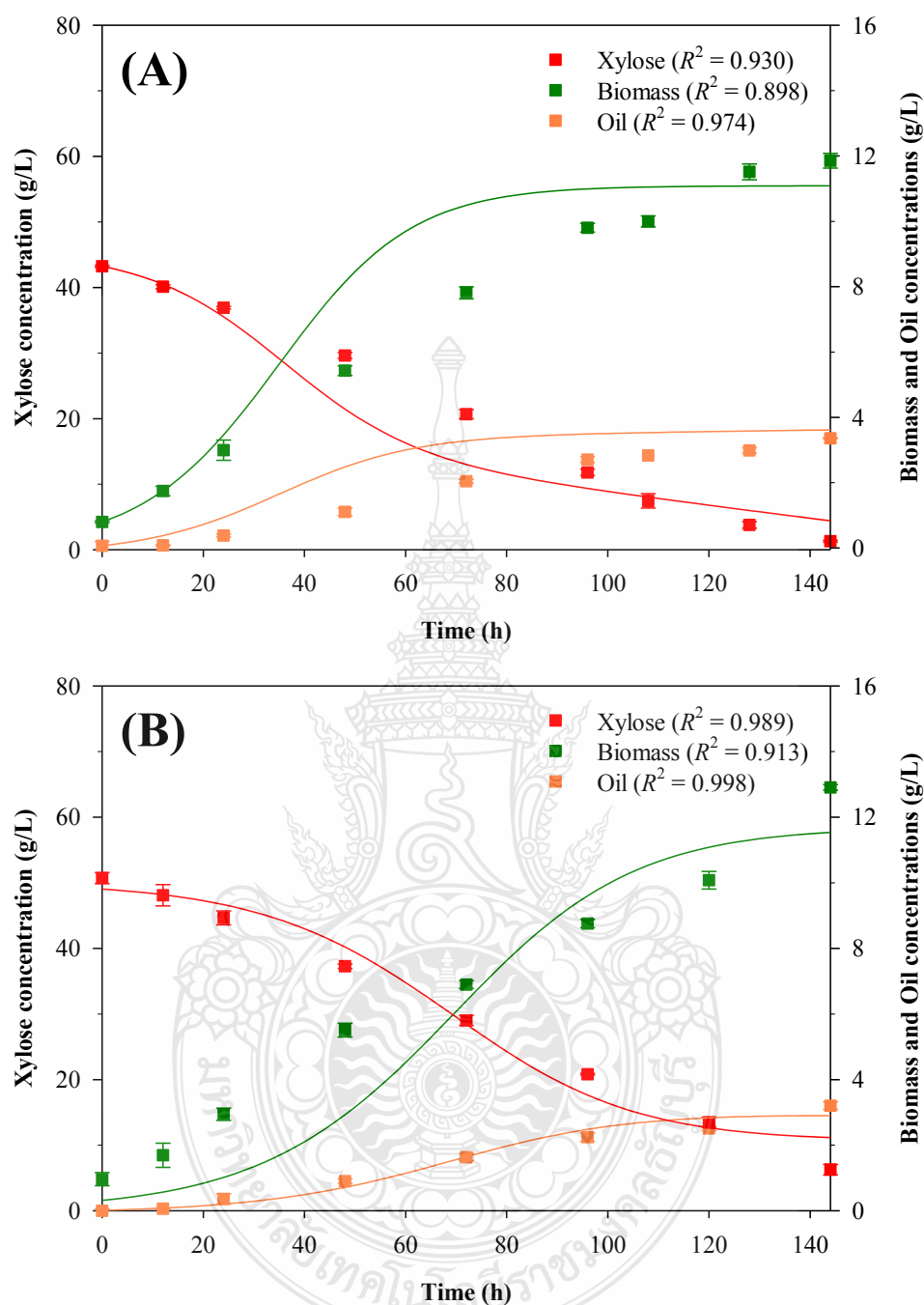
Figure 4.12 Experimental results (symbols) and model predictions (lines) of substrate consumption, cell growth, and YO production profiles of *P. parantarctica* CHC28 cultured at 40 and 50 g/L xylose concentrations.
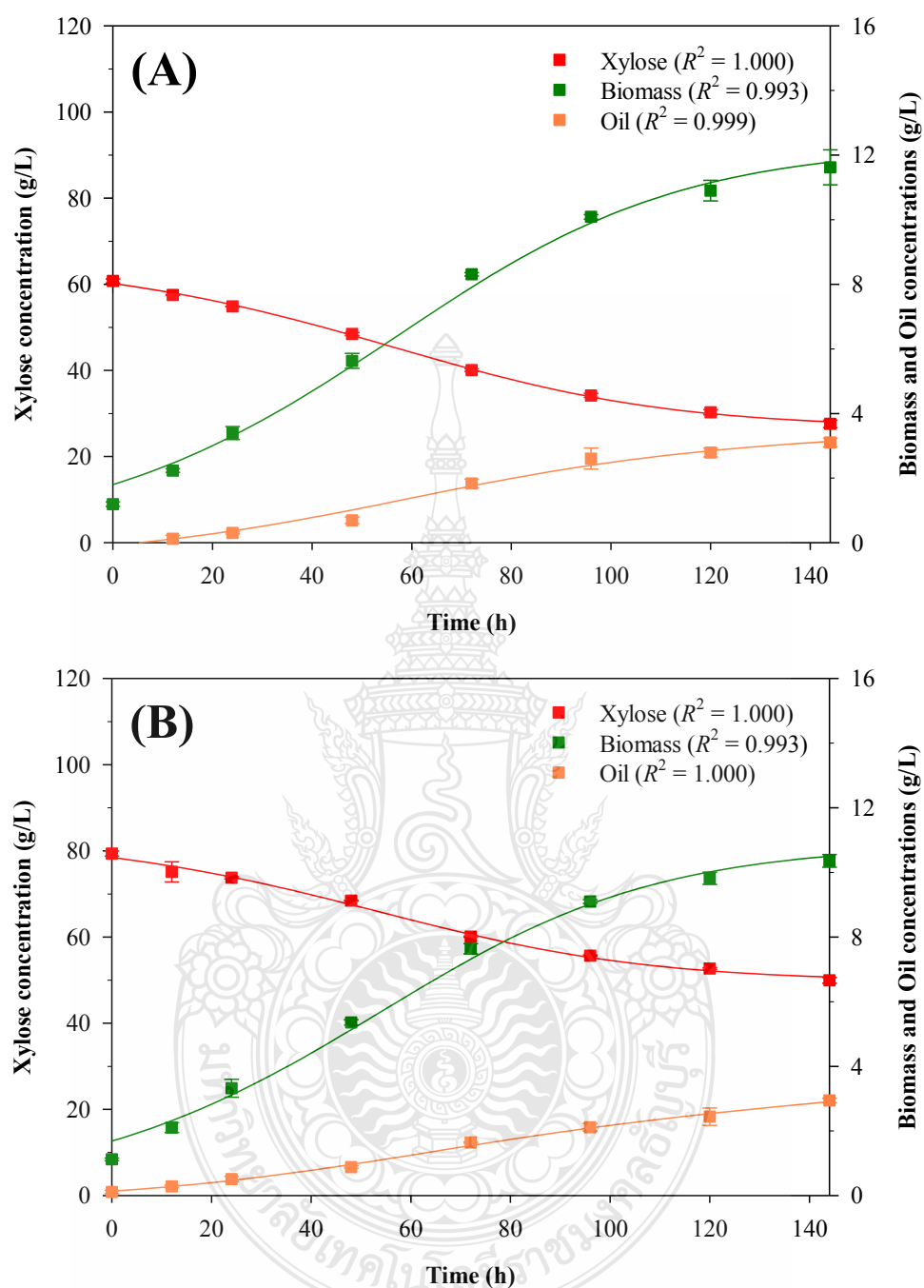
Figure 4.13 Experimental results (symbols) and model predictions (lines) of substrate consumption, cell growth, and YO production profiles of *P. parantarctica* CHC28 cultured at 60 and 80 g/L xylose concentrations.

Figure 4.14 Experimental results (symbols) and model predictions (lines) of substrate consumption, cell growth, and YO production profiles of *P. parantarctica* CHC28 cultured at 110 and 130 g/L xylose concentrations.

Table 4.9 The parameter-estimated by the kinetic model of different xylose concentrations.

Xylose concentration (g/L)	Cell growth				Substrate consumption			YO production			
	μ_{max}	X_{max}	k_i	NRMS	$Y_{x/s}$	m_s	NRMS	α	β	$Y_{p/s}$	NRMS
10	0.103	4.31	857	0.246	0.34	0	0.078	0.262	0.001	0.09	0.119
20	0.080	6.59	717	0.341	0.31	0	0.609	0.270	0.001	0.08	0.100
40	0.080	11.09	445	1.418	0.37	0.009	4.067	0.324	0	0.12	0.769
50	0.060	11.70	311	1.413	0.30	0	3.109	0.274	0	0.08	0.197
60	0.041	12.31	212	0.303	0.30	0.001	0.404	0.278	0	0.08	0.142
80	0.053	10.86	120	0.280	0.31	0	0.777	0.190	0.001	0.06	0.061
110	0.048	14.34	99	0.257	0.31	0	0.669	0.139	0.002	0.04	0.153
130	0.053	14.63	74	0.280	0.32	0.001	0.707	0.105	0.003	0.03	0.133

4.8.2 Kinetics of YO production under mixture glucose and xylose

The simulation profile of YO production by *P. parantarctica* CHC28 in G-OPM and X-OPM was illustrated in Figure 4.15A and B, respectively. The R^2 values of yeast growth profiles in G-OPM and X-OPM ranged from 0.949 to 0.999 and from 0.898 to 0.974, respectively. While under GX-OPM, the R^2 values of different glu:xyl ratios at 1:2, 1:1, and 2:1 ranged from 0.850 to 0.968, 0.837 to 0.948, and 0.883 to 0.915, respectively (Figure 4.16A to C). The *NRMS* was obtained at 0.148 to 4.067 for the above condition (Table 4.10). The $\mu_{max,xyl}$ of yeast cultured in X-OPM (0.080 h^{-1}) was higher than $\mu_{max,glu}$ in G-OPM (0.071 h^{-1}), while yeast cultivation in GX-OPM revealed that the estimated $\mu_{max,glu}$ was higher than $\mu_{max,xyl}$ in all glu:xyl ratios. Yeast growth was promoted by glucose greater than xylose in co-carbon source cultivation. Furthermore, variation of the glu:xyl ratio in GX-OPM influenced both $\mu_{max,glu}$ and $\mu_{max,xyl}$. The $\mu_{max,xyl}$ accelerated when $\mu_{max,glu}$ dropped (Table 4.10). The yeast modulated glucose as the carbon source supply to maintain its growth, while utilization of the other sugars was inhibited by catabolic repression or allosteric competition of the sugar-transporting enzymes after consuming glucose [109].

The $Y_{x/s,glu}$ and $Y_{x/s,xyl}$ values were estimated by using the substrate consumption model (Eqs. (8) and (9)). Under a single carbon source, $Y_{x/s,glu}$ (0.30) was lower than $Y_{x/s,xyl}$ (0.37) (Table 4.10). Furthermore, when yeast was cultured in GX-OPM, glucose repression occurred at increasing glucose levels, resulting in $Y_{x/s,glu}$ decrease from 0.60 to 0.30. By contrast, $Y_{x/s,xyl}$ was increased to 0.88 with increasing glucose levels (Table 4.10). A previous study reported that 1 mol of xylose was converted to 2 mol of acetyl-CoA by the PPK system, while 1 mol of glucose yielded 1.67 mol of acetyl-CoA via the GLP and PPP pathways [120]. This study showed that acetyl-CoA was obtained from xylose utilization rather than glucose. Therefore, xylose provided biomass yield greater than glucose [125, 126].

The $m_{s,glu}$ and $m_{s,xyl}$ values were also relatively low (Table 4.10), suggesting that both substrates were mainly used for growth and YO production. The α value was higher than the β value in all experiments, indicating that YO of *P. parantarctica* CHC28 was the growth-associated product. It was suggested that increased oleaginous yeast growth also enhanced YO formation.
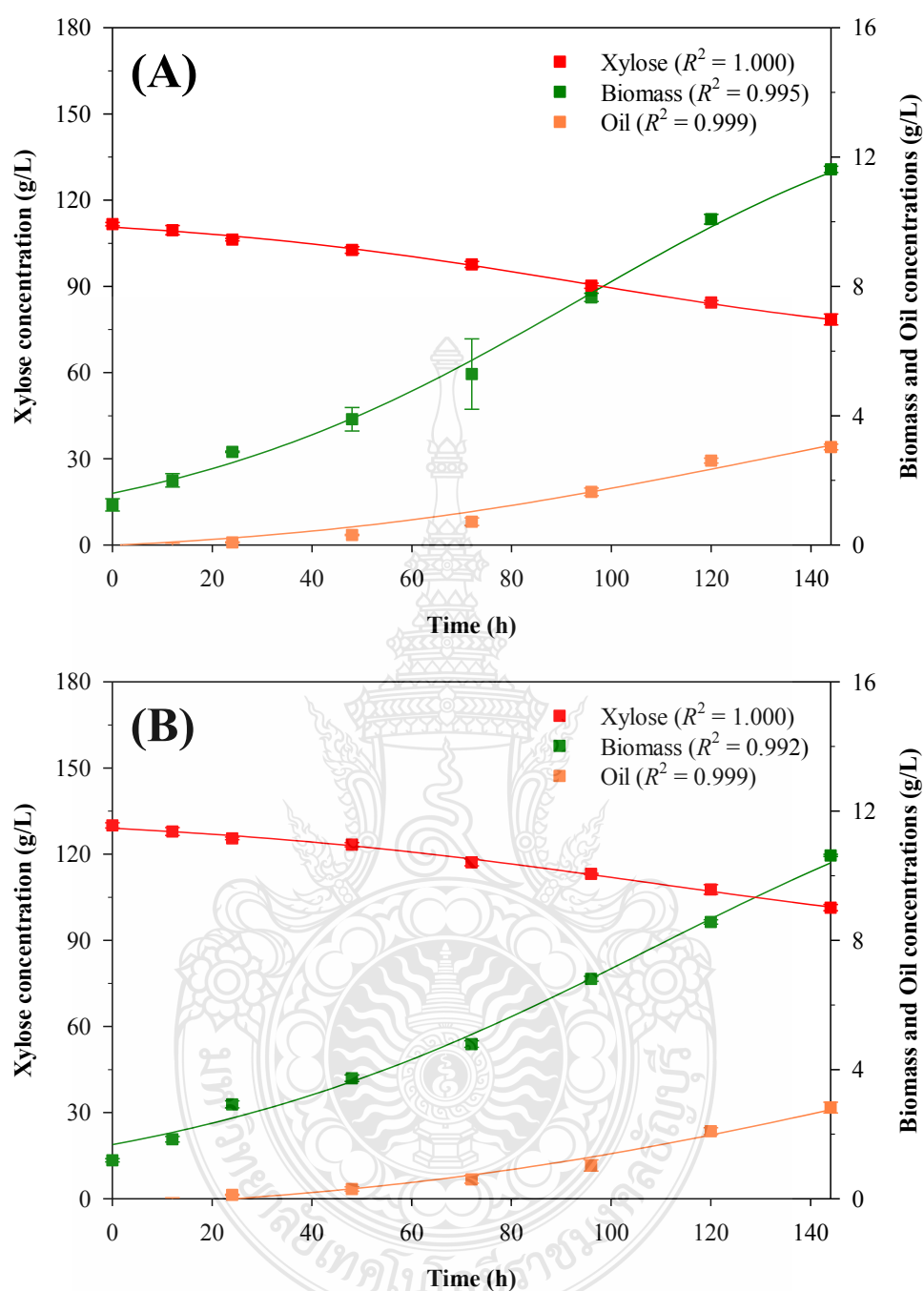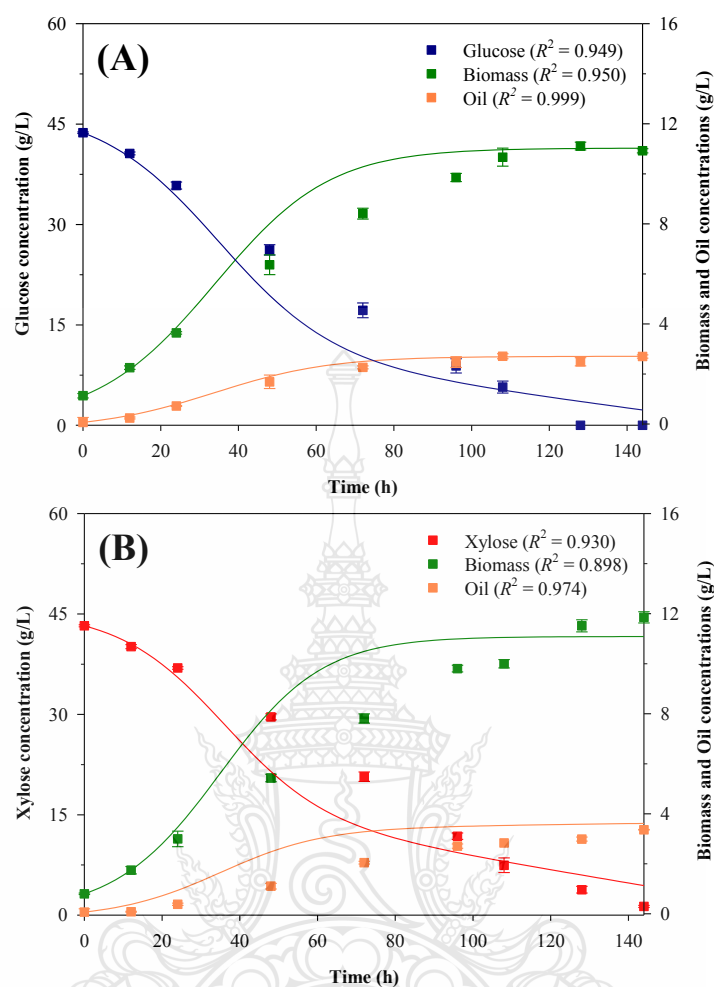
Figure 4.15 Experimental results (symbols) and model predictions (lines) of substrate
consumption, cell growth, and YO production profiles of *P. parantarctica*
CHC28 cultured at different glucose and xylose mixing ratios; (A) 1:0 and
(B) 0:1.
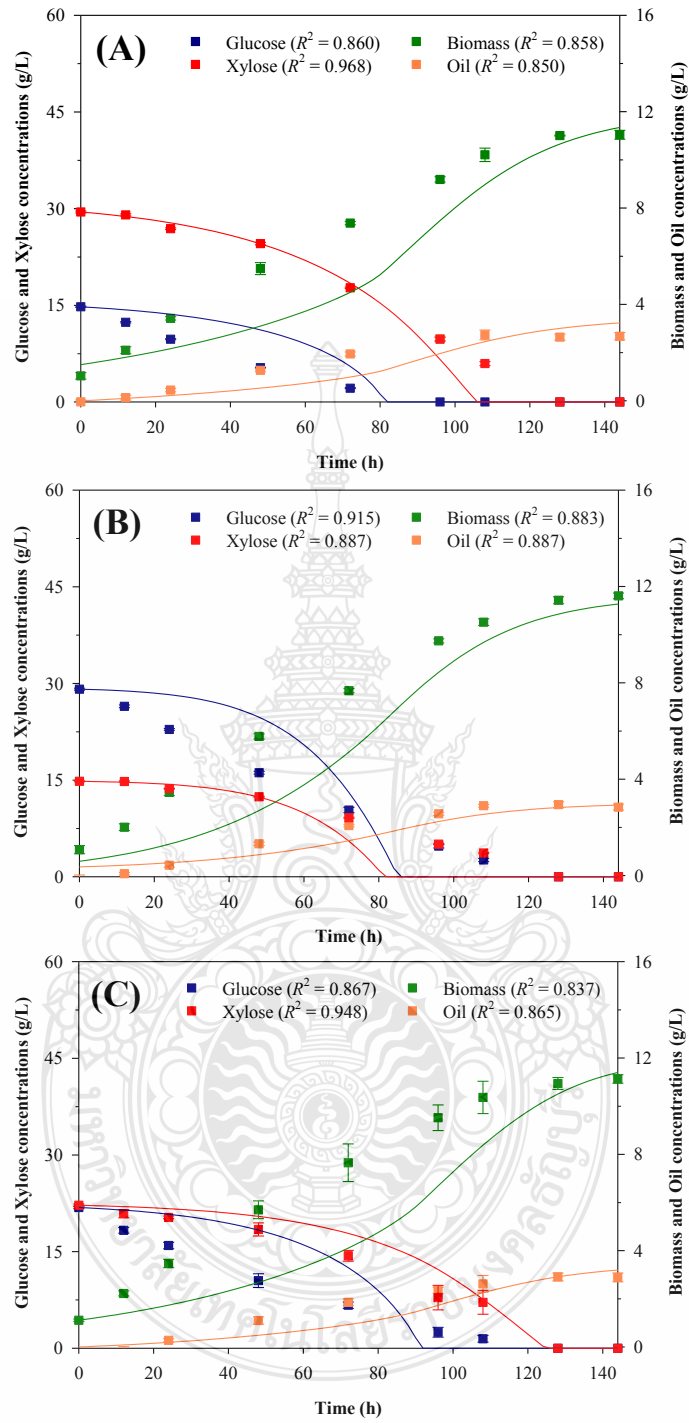
Figure 4.16 Experimental results (symbols) and model predictions (lines) of substrate consumption, cell growth, and YO production profiles of *P. parantarctica* CHC28 cultured at different glucose and xylose mixing ratios; (A) 1:2, (B) 1:1, and (C) 2:1.

4.8.3 Kinetics of YO production under organic acid supplementation

Simulation of the YO production profile under organic acid supplementation is presented in Figure 4.17 to 4.19. Almost all the experimental values were well-fitted with the modeled values, giving high R^2. The models of yeast growth, YO production, and substrate consumption when adding acetic acid at 1 and 5 g/L demonstrated that the R^2 values ranged from 0.913 to 0.975 and 0.910 to 0.989, respectively (Figure 4.17A and B). The yeast strain CHC28 did not grow and produce YO at a high acetic acid concentration (10 g/L), R^2 values ranged from 0.225 to 0.671 (Figure 4.17C). The developed kinetic models appropriately described the sigmoidal behavior under different microbial cultivation conditions. The experimental data at 10 g/L acetic acid did not follow sigmodal behavior, providing a low R^2 value. Furthermore, the R^2 values of yeast growth, YO production, and substrate consumption when adding citric and succinic acid (1 to 10 g/L) ranged from 0.950 to 0.994 and 0.930 to 0.986, respectively (Figure 4.18 and 4.19A to C).

The acid consumption profile was simulated by the Michaelis-Menten kinetic, as shown in Eq. (13). The R^2 values of acid consumption when adding acetic and citric acid at 1, 5, and 10 g/L were 0.787 and 0.726, 0.993 and 0.926, and 0.492 and 0.490, respectively (Figure 4.17 and 4.18A to C). The increase in succinic acid was an unexpected result in this study (Figure 4.19A to C). The experimental succinic acid value was not well-fitted by the acid consumption model, with lower R^2 value. Previous research has addressed succinic acid production by yeast strains including *Y. lipolytica*, *Saccharomyces cerevisiae*, *Pichia stipites*, and *Pichia kudriavzevii* [156-159]. However, succinic acid production by *P. parantarctica* CHC28 has never been reported.

For acetic acid addition, the $\mu_{max,xyl}$ of yeast CHC28 declined from 0.077 to 0.003 h^{-1} as acetic acid concentration increased. By contrast, the $\mu_{max,xyl}$ slightly changed when concentrations of citric and succinic acids increased (Table 4.10). Comparably, the X_{max}, $Y_{x/s,xyl}$, and $Y_{p/s,xyl}$ changed and altered the $\mu_{max,xyl}$ profiles. Acetic acid significantly influenced yeast growth more than citric and succinic acids, achieving maximum $Y_{p/s,xyl}$ at 0.10 with 1 g/L of acetic acid (Table 4.10).

The $m_{s,xyl}$ was lower under all acid supplementations indicating that xylose was slightly utilized for cell maintenance. Additionally, YO was generated as a growth-associated product since the α value was larger than the β value. The q_{Amax} related to acid consumption of yeast was 0.044 at 1 g/L of acetic acid (Table 4.10), while k_A represented the highest acid value utilized in extreme-saturated concentrations. The q_{Amax} value gradually decreased at high acid concentrations (>10 g/L) similar to YO production by *R. toruloides* AS 2.1389, indicating the inhibition effect of high acid concentrations on yeast cultivation [160].
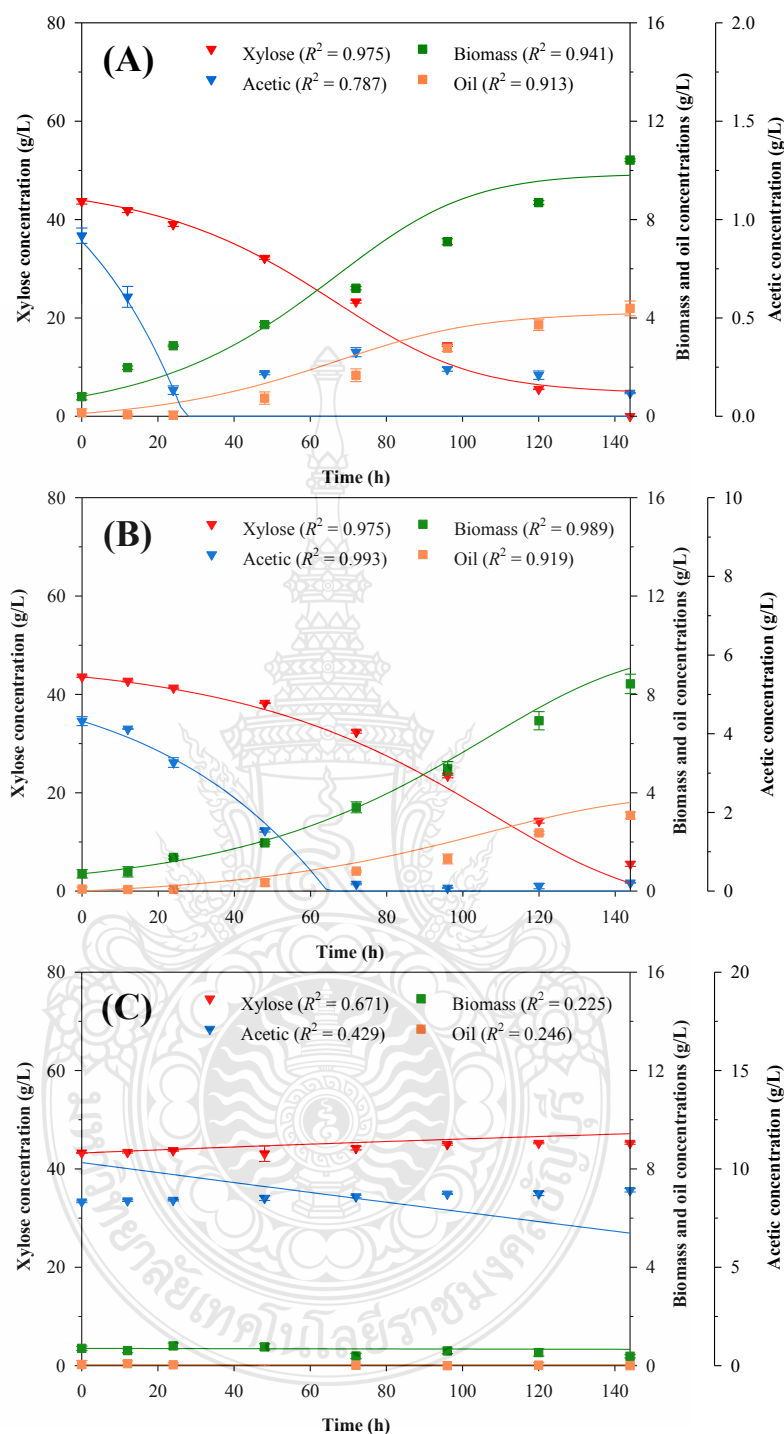
Figure 4.17 Experimental results (symbols) and model predictions (lines) of substrate consumption, cell growth, and YO production profiles of *P. parantarctica* CHC28 in X-OPM at different concentrations of acetic acid; (A) 1 g/L, (B) 5 g/L, and (C) 10 g/L.
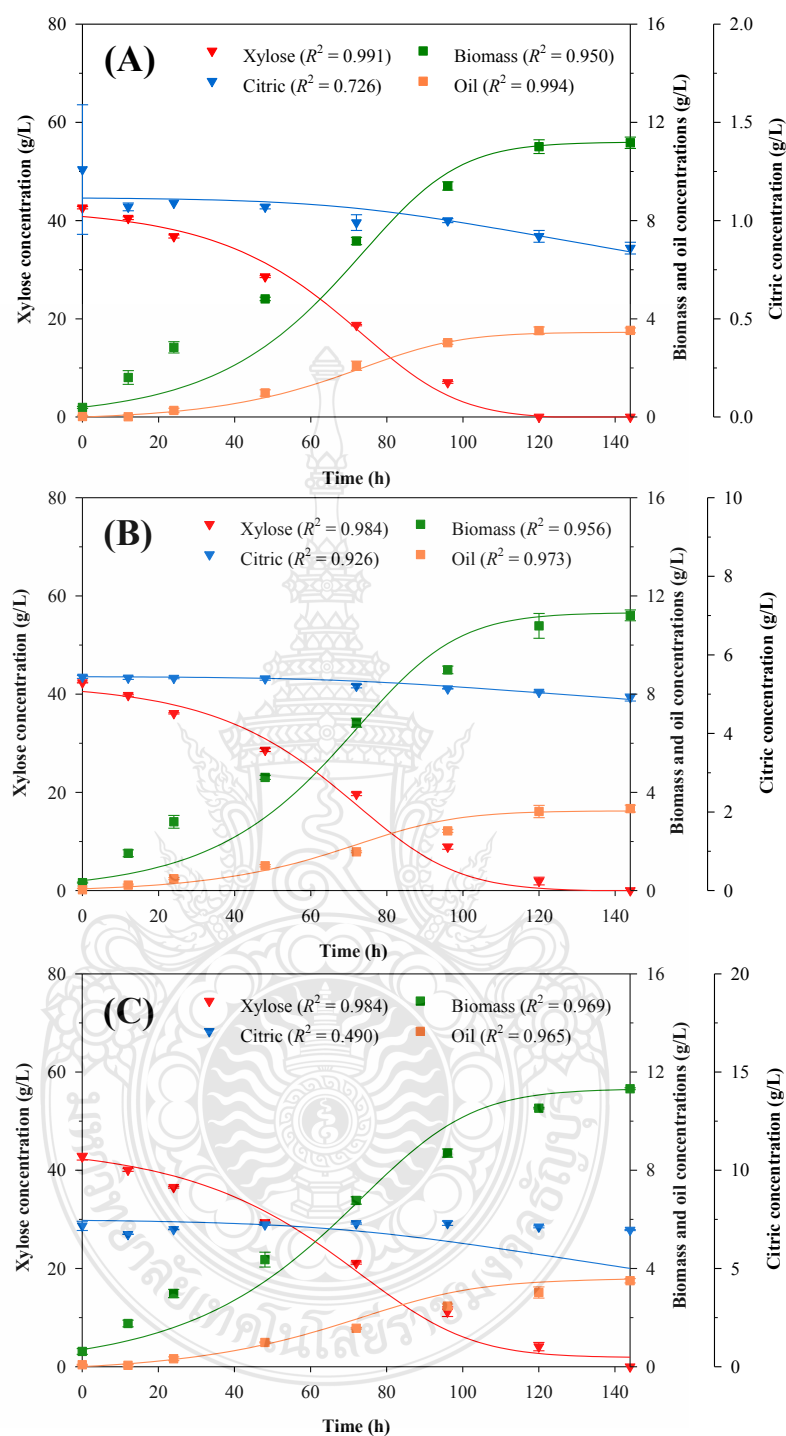
Figure 4.18 Experimental results (symbols) and model predictions (lines) of substrate consumption, cell growth, and YO production profiles of *P. parantarctica* CHC28 in X-OPM at different concentrations of citric acid; (A) 1 g/L, (B) 5 g/L, and (C) 10 g/L.
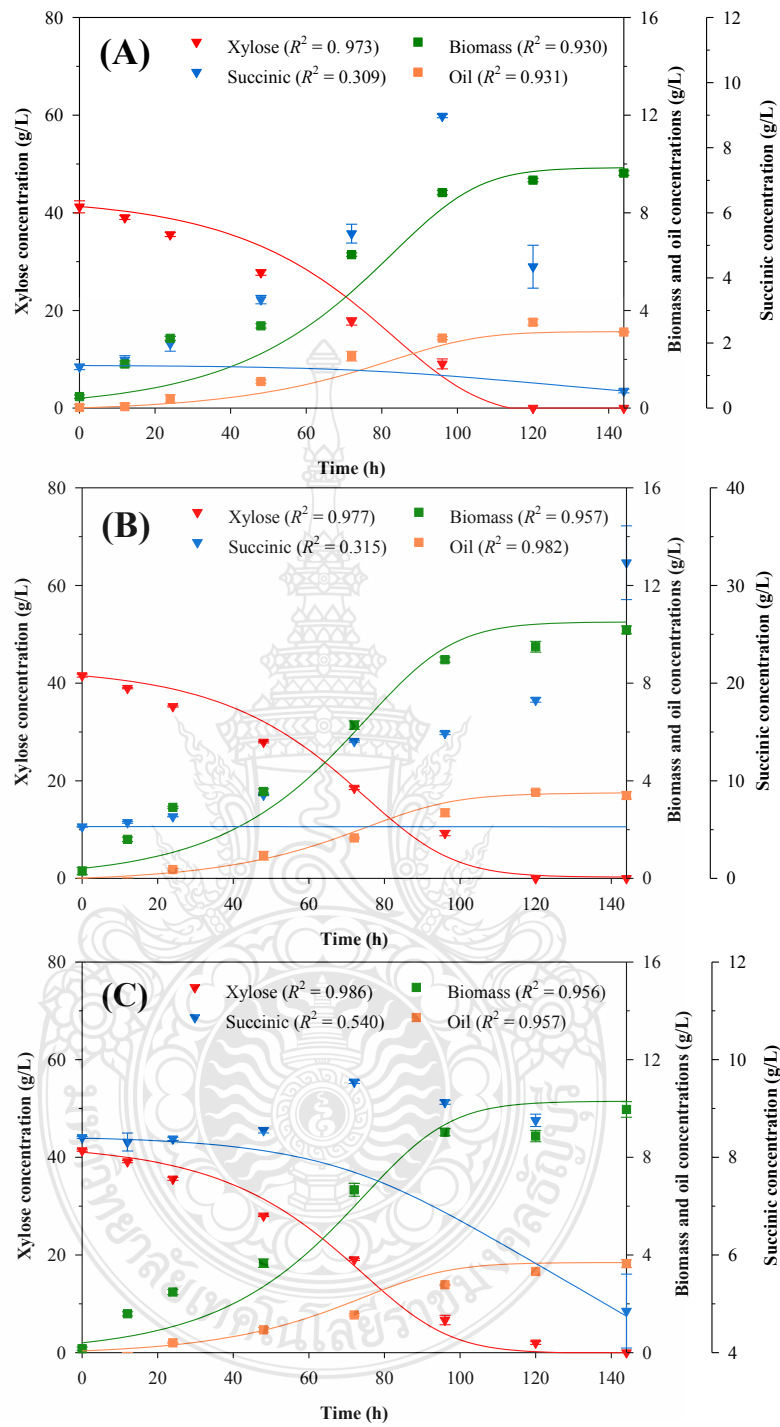
Figure 4.19 Experimental results (symbols) and model predictions (lines) of substrate consumption, cell growth, and YO production profiles of *P. parantarctica* CHC28 in X-OPM at different concentrations of succinic acid; (A) 1 g/L, (B) 5 g/L, and (C) 10 g/L.

Table 4.10 Model-estimated kinetic parameters of *P. parantarctica* CHC28 cultivation in different conditions.

Model	Parameter	Glu:Xyl ratio					Acetic acid (g/L)			Citric acid (g/L)			Succinic acid (g/L)		
		1:0	0:1	1:2	1:1	2:1	1	5	10	1	5	10	1	5	10
Cell growth	$\mu_{max,glu}$	0.071		0.080	0.071	0.060									
	$\mu_{max,xyl}$		0.080	0.020	0.035	0.049	0.077	0.062	0.003	0.096	0.091	0.090	0.113	0.112	0.112
	X_{max}	11.03	11.09	12.0	12.13	11.61	9.86	9.92	0.49	11.20	11.33	11.32	9.86	10.51	10.30
	r			0.48	0.57	0.32									
	$k_{i,glu}$	409		5	12	70									
	$k_{i,xyl}$		445	87	17	28	40	29	20	35	40	30	21	26	26
	NRMS	0.906	1.418	1.510	1.813	1.607	0.893	0.322	0.163	1.032	0.971	0.769	1.073	0.887	0.888
Substrate consumption	$Y_{x/s,glu}$	0.30		0.60	0.60	0.30									
	$Y_{x/s,xyl}$		0.37	0.33	0.54	0.88	0.24	0.21	0.01	0.26	0.27	0.26	0.23	0.25	0.24
	$m_{s,glu}$	0.007		0.001	0.001	0									
	$m_{s,xyl}$		0.009	0.001	0	0	0.001	0.004	0.002	0	0	0	0.004	0	0
	$NRMS_{glu}$	3.660		2.677	3.902	4.028									
	$NRMS_{xyl}$		4.067	2.280	2.069	2.427	2.461	2.402	1.141	1.620	2.168	2.066	2.860	2.624	2.026
YO production	α	0.265	0.324	0.328	0.310	0.240	0.423	0.431	0	0.319	0.291	0.317	0.331	0.338	0.366
	β	0	0	0	0	0	0	0	0	0	0	0	0	0	0
	$Y_{p/s,glu}$	0.08		0.20	0.19	0.07									
	$Y_{p/s,xyl}$		0.12	0.14	0.17	0.21	0.10	0.09	0	0.08	0.08	0.08	0.08	0.08	0.088
	NRMS	0.148	0.769	0.518	0.471	0.362	0.504	0.396	0.038	0.111	0.217	0.275	0.354	0.194	0.321
Acid consumption	q_{Amax}						0.044	0.062	0	0.003	0.002	0.001	0	0	0
	k_A						8.33	8.33	8.33	5.44	5.44	5.44	1.27	1.27	1.27
	n						0.67	0.82	0.44	1.07	1.05	0.80	0.66	0.66	0.81
	NRMS						0.184	0.152	1.420	0.059	0.056	0.967	3.512	11.62	1.470

4.8.4 Kinetics of YO production under batch and fed-batch cultivations of RSH-OPM

The substrate consumption, cell growth, and yeast oil (YO) production profiles of *P. parantarctica* CHC28 by RSH-OPM were elucidated under batch and fed-batch cultivation modes, as depicted in Figure 4.20 and 4.21. The experimental data were effectively modeled using the modified logistic equation for yeast growth, the Luedeking-Piret equation for YO production, and the substrate consumption rate equation (Eq. (2) to (12)). The experimental values were fitted to the model predictions using the curve fit function of Berkeley Madonna^{TM} software, resulting in a comprehensive representation of the dynamic processes.

The simulation of YO production profiles under RSH-OPM batch cultivation mode yielded high R^2 values, ranging from 0.903 to 0.994 (Figure 4.20), indicating a strong correlation between the model and the experimental data. R^2 is a crucial tool for deciding the relationship between the dependent variable and a group of explanatory variables by defining the regression sum of squares to the total sum of squares ratio, also known as the coefficient of determination [161]. The R^2 value is generally used in predictive modeling to evaluate how well regression models fit data or compare the efficacy of several models by matching model and experimental data [161]. Multiple fields of previous research used R^2 for comparison of the goodness of fit in mathematical modelings, such as the kinetics of hydrogen production by *Caldicellulosiruptor kronotskyensis* [162], the growth kinetics of spoilage bacteria in chilled chicken [163], optimization processes in wheat and soy dough mixtures by bacteria fermentation [164], optimization the jatropha seed drying [165], and improving nanomaterials for substance adsorption and desorption [166], etc. Additionally, the *NRMS* values ranged from 0.184 to 1.106 (Table 4.11), signifying the accuracy of the model in predicting the YO production dynamics. *NRMS* is a criterion suitable for a wider data range to evaluate the best-fit model. It represents the actual error between the calculated experimental data at all points by normalizing the root mean square from the data of q_{cal} and q_{exp} [107].

Both glucose and xylose exerted comparable effects on yeast growth, with $\mu_{max,glu}$ and $\mu_{max,xyl}$ estimated at 0.050 and 0.049 h^{-1}, respectively. Moreover, the biomass yield from glucose ($Y_{x/s,glu}$) and xylose ($Y_{x/s,xyl}$) exhibited

98

comparable values of 0.41 and 0.40, respectively. Likewise, the YO yield from glucose ($Y_{p/s,glu}$) and xylose ($Y_{p/s,xyl}$) were consistently observed at 0.16 for both substrates. Further, these results could be used to design the bioprocess of YO production by using mixing or a single substrate as a carbon source. Moreover, the inhibition constants, $k_{i,glu}$, and $k_{i,xyl}$, quantifying the inhibitory effect of glucose and xylose, were determined as 50.15 and 2.02, respectively (Table 4.11). The results also found that the value of $k_{i,glu}$ was higher than $k_{i,xyl}$, demonstrating that the growth inhibition by glucose was lower than xylose. The yeast could utilize glucose faster than xylose. In addition, the xylose was used after glucose was almost consumed. That xylose consumption was depressed through sugar-transporting enzyme allosteric competition or catabolic suppression under mixed sugar conditions [109].

These results demonstrated the successful application of the mathematical model in capturing the YO production dynamics under RSH-OPM batch cultivation, providing valuable insights into the substrate-dependent effects on yeast growth and YO synthesis. The mathematical models are beneficial for performing process simulations. They are also used to evaluate the best process conditions before conducting them at the pilot plant or industrial scale without having to carry out a significant number of experiments [167, 168]. Previous research has applied the mathematical model to optimize the methods of essential oils extraction using as antimicrobial agents in an industrial scale [168]. Nachtergaele [169] applied statistical and mathematical modeling for biorefinery processes from bio-based feedstock to estimate the production efficiency. Suggesting, the mathematical modeling is helpful to evaluate the bioprocess strategies for industrial processes.

The experimental and model prediction results for YO production of *P. parantarctica* CHC28 under fed-batch cultivation mode with different feedings of RSH-based medium and RSH were illustrated in Figure 4.21A and B. The simulations of yeast growth and YO production under fed-batch cultivation mode with RSH-based medium feeding (Figure 4.21A) in the 1st to 4th batch offered R^2 values ranging from 0.643 to 0.955 and 0.907 to 0.957, respectively, while the NRMS ranged from 0.130 to 0.498 and 0.114 to 0.188, respectively. Upon considering glucose and xylose consumptions, it was found that R^2 values presented were 0.905 to 0.962 and 0.904 to 0.941, respectively (Table 4.11).

In addition, during the fed-batch mode with RSH feeding from the 1st to 3rd batch, the R^2 values for yeast growth and YO production ranged from 0.628 to 0.904 and 0.873 to 0.942, respectively, with *NRMS* values at 0.377 to 0.721 and 0.113 to 0.448, respectively (Table 4.11). However, in the 4th batch of the aforementioned mode, low R^2 values were obtained for yeast growth (0.411) and YO production (0.192) (Table 4.11). This result may be attributed to the inherent decrease in yeast growth and YO production during the 4th batch, leading to a lack of a sigmoid curve in the data (Figure 4.21B) and causing an imperfect fit with the model equations. Nonetheless, the simulation of glucose and xylose consumption showed satisfactory modeling, with R^2 values ranging from 0.759 to 0.962 and NRMS values ranging from 0.047 to 1.675 for all feeding periods during the fed-batch operation (Table 4.11).

The trend of both $\mu_{max,glu}$ and $\mu_{max,xyl}$ gradually decreased with repeated cultivation using RSH-based medium and RSH. Particularly, the $\mu_{max,glu}$ and $\mu_{max,xyl}$ dropped more significantly with RSH feeding compared to RSH-based medium feeding. Furthermore, during the 4th batch of RSH feeding, the $\mu_{max,glu}$ and $\mu_{max,xyl}$ suddenly decreased to their lowest values (0.003 and 0.005 h^{-1}, respectively) (Table 4.11). It was suggested that under the RSH feeding mode, the other essential nutrients were less than in the RSH-based medium feeding mode and declined consistency, resulting the yeast growth was decreased. Correspondingly, the $k_{i,glu}$ and $k_{i,xyl}$ values were steadily lowered with each feeding (Table 4.11). The substrate inhibition coefficient (k_i) value indicates the cell growth behavior influenced by the substrate. A high k_i value signifies that the supplied substrate slightly inhibited yeast growth during cultivation. The k_i value gradually lowers if less sugar was utilized for growth and YO generation. The decreased k_i value demonstrated that the effect of substrate inhibition on yeast growth was increased.

The biomass yield obtained from glucose was higher than that from xylose, resulting in higher $Y_{x/s,glu}$ values than $Y_{x/s,xyl}$, as indicated by the *r* value. This demonstrates that glucose was utilized to produce more biomass than xylose, except for the 4th batch of RSH feeding. Furthermore, the $Y_{x/s,glu}$ and $Y_{x/s,xyl}$ values showed a slight reduction from the 1st to the 4th batch for RSH-based medium feedings (Table 4.11). Regarding YO production in the fed-batch mode with RHS-based

medium feeding, $Y_{p/s,glu}$ and $Y_{p/s,xyl}$ decreased slightly from 0.16 to 0.13. In contrast, $Y_{p/s,glu}$ and $Y_{p/s,xyl}$ exhibited a significant drop in the RHS feeding condition (Table 4.11). The result denoted that the yeast growth decreased with repeated cycles of RHS feeding mode without essential nutrients supplemented in the medium. In comparison to the RSH-based medium, the product yield parameter decreased considerably. According to this study, yeast may utilize the carbon source more effectively for oil synthesis in an RSH-based medium than in RSH feeding [84, 152].

The estimated values of $m_{s,glu}$ and $m_{s,xyl}$ were very low (Table 4.11), indicating that the RSH substrate was primarily utilized for growth and YO production rather than cell maintenance. The YO production of *P. parantarctica* CHC28 was identified as a growth-associated product, with the α value being higher than the β value in all cultivations (Table 4.11). This suggests that higher YO production was facilitated by increased yeast growth.
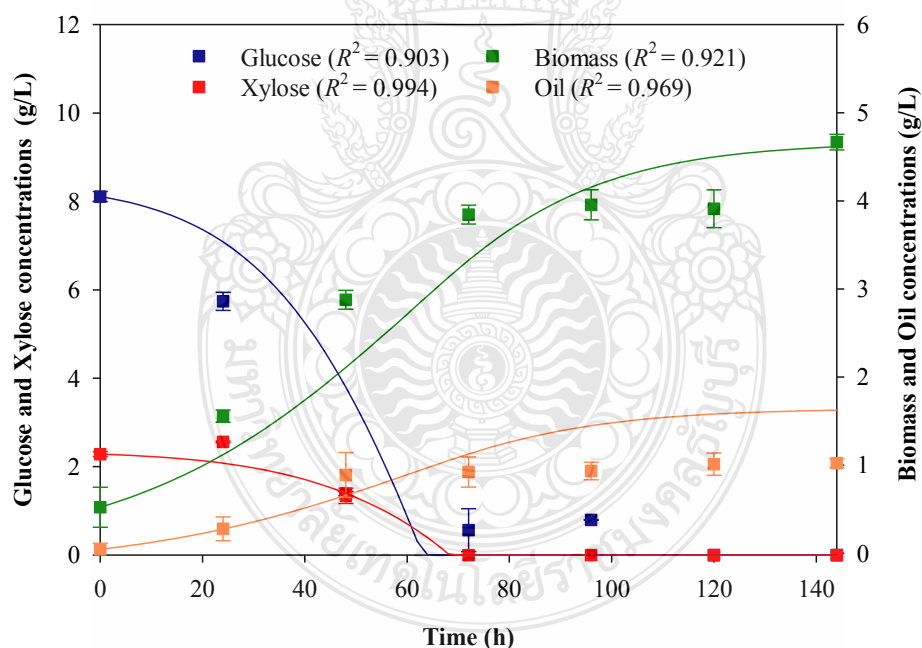
Figure 4.20 Experimental results (symbols) and model predictions (lines) of substrate consumption, cell growth, and YO production profiles of *P. parantarctica* CHC28 by batch cultivation mode in RSH-OPM.
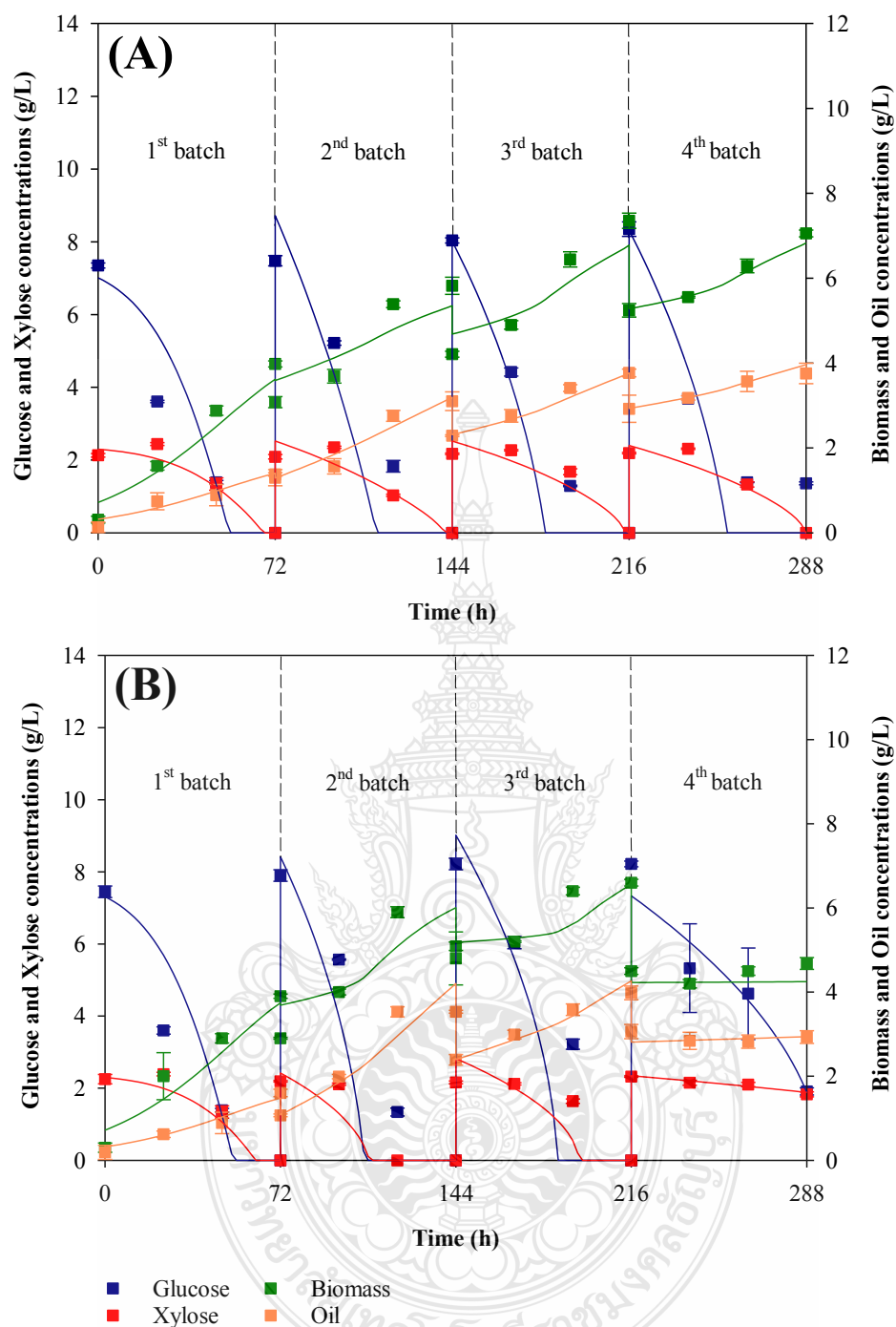
Figure 4.21 Experimental results (symbols) and model predictions (lines) of
substrate consumption, cell growth, and YO production profiles of
P. parantarctica CHC28 by fed-batch cultivation mode with
different feeding of (A) RSH-based medium and (B) RSH.

Table 4.11 Model-estimated kinetic parameters of *P. parantarctica* CHC28 cultivation in different cultivation with RSH.

Model	Parameter	Cultivation mode								
		Batch	Fed-batch mode with RSH-based medium				Fed-batch mode with RSH			
			1st batch	2nd batch	3rd batch	4th batch	1st batch	2nd batch	3rd batch	4th batch
Cell growth	$\mu_{max,glu}$	0.050	0.048	0.042	0.039	0.032	0.049	0.037	0.028	0.003
	$\mu_{max,xyl}$	0.049	0.045	0.041	0.039	0.031	0.047	0.036	0.029	0.005
	X_{max}	4.67	4.70	5.88	7.89	8.04	4.80	6.88	7.97	7.19
	r	0.75	0.75	0.66	0.65	0.63	0.74	0.73	0.58	0.53
	$k_{i,glu}$	50.15	50.15	7.60	3.00	2.90	50.15	2.30	1.00	0.47
	$k_{i,xyl}$	2.02	2.02	0.35	0.17	0.14	2.02	0.39	0.08	0.01
	R^2	0.921	0.914	0.643	0.752	0.955	0.904	0.628	0.634	0.411
	NRMS	0.453	0.338	0.498	0.465	0.130	0.377	0.721	0.417	0.287
Substrate consumption	$Y_{x/s,glu}$	0.41	0.43	0.42	0.47	0.38	0.42	0.26	0.13	0.02
	$Y_{x/s,xyl}$	0.40	0.42	0.41	0.45	0.37	0.41	0.25	0.12	0.02
	$m_{s,glu}$	0.001	0	0	0	0	0	0	0	0
	$m_{s,xyl}$	0.001	0	0.001	0.001	0.001	0	0.001	0.001	0
	R^2_{glu}	0.903	0.905	0.905	0.962	0.918	0.895	0.916	0.845	0.926
	R^2_{xyl}	0.994	0.941	0.904	0.904	0.931	0.934	0.849	0.759	0.932
	$NRMS_{glu}$	1.106	0.941	1.176	0.666	1.051	1.049	1.071	1.675	0.577
	$NRMS_{xyl}$	0.184	0.224	0.307	0.310	0.246	0.243	0.460	0.640	0.047
YO production	α	0.386	0.369	0.331	0.331	0.331	0.379	0.337	0.343	0.305
	β	0	0	0.004	0.002	0.001	0	0.007	0.003	0
	$Y_{p/s,glu}$	0.16	0.16	0.14	0.16	0.13	0.16	0.09	0.04	0
	$Y_{p/s,xyl}$	0.16	0.15	0.14	0.15	0.12	0.16	0.08	0.04	0
	R^2	0.969	0.907	0.935	0.957	0.922	0.938	0.873	0.942	0.192
	NRMS	0.386	0.132	0.188	0.117	0.114	0.113	0.448	0.173	0.128

4.9 Fatty acid profiles of *P. parantarctica* CHC28 under different cultivation

The fatty acid compositions of YO were produced under different conditions, illustrated as heat maps by the percent of peak area of GC-MS (Figure 4.22 and 4.23). All experimented cultural conditions showed a slight effect on the fatty acid compositions of YO. The main fatty acids were C:16 and C:18 fatty acids. The average of C:16 to C:18 fatty acids contained in YO of *P. parantarctica* CHC28 was 85.3% in all xylose concentrations. By contrast, when a co-carbon source was used, the average value of C:16 to C:18 fatty acids decreased slightly to 72.3%. When acetic, citric, and succinic acids were supplemented in yeast cultivation, average values of C:16 to C:18 fatty acids were enhanced by 87.8, 89.0, and 84.8%, respectively. Considerately, the YO product of *P. parantarctica* derived from RSH-based carbon source cultivations presented C:16 and C:18 fatty acids as the main composition also with xylose-based carbon source cultivations by fatty acids of C:16 and C:18 ranged from 88.2 to 94.6%. Likewise, several yeast strains including *Y. lipolytica*, *Cyberlindnera saturnus*, *R. toruloides*, *Cutaneotrichosporon curvatum*, and *Lipomyces lipofer* presented C:16 and C:18 as the main fatty acids at up to 87% [170], while *Apiotrichum brassicae* and *P. kudriavzevii* accumulated C:16 and C:18 fatty acids at more than 80% [171]. The yeast *Rhodosporidium babjevae* UCDFST 04-877 contained the highest C18:1 at 62.92% [172]. Maisonneuve *et al*. reported on the fatty acid profiles of vegetable oils. They found that C:16 and C:18 were the main fatty acids in soybean oil, palm oil, and sunflower oil at 95.3, 98.4, and 100%, respectively [173]. These results were similar to the YO of *P. parantarctica* CHC28 in this study.

BPU foam formation from soybean oil has been reported. The results indicated that soybean-derived polyols could be used to substitute petroleum oil-derived polyols and synthesize flexible PU foams [174]. The fatty acid profile of CHC28 was similar to vegetable oil and could be converted into polyols as the substrate for making BPU foam [175-178]. Polyol formation reactions take place at the unsaturated double bond positions of long chain fatty acids. This epoxidizes the functional groups by opening the oxirane ring that then reacts with diisocyanates to produce PUs [11, 179]. Therefore, YO could be used as the substrate for BPU foam formation, similar to vegetable oils.
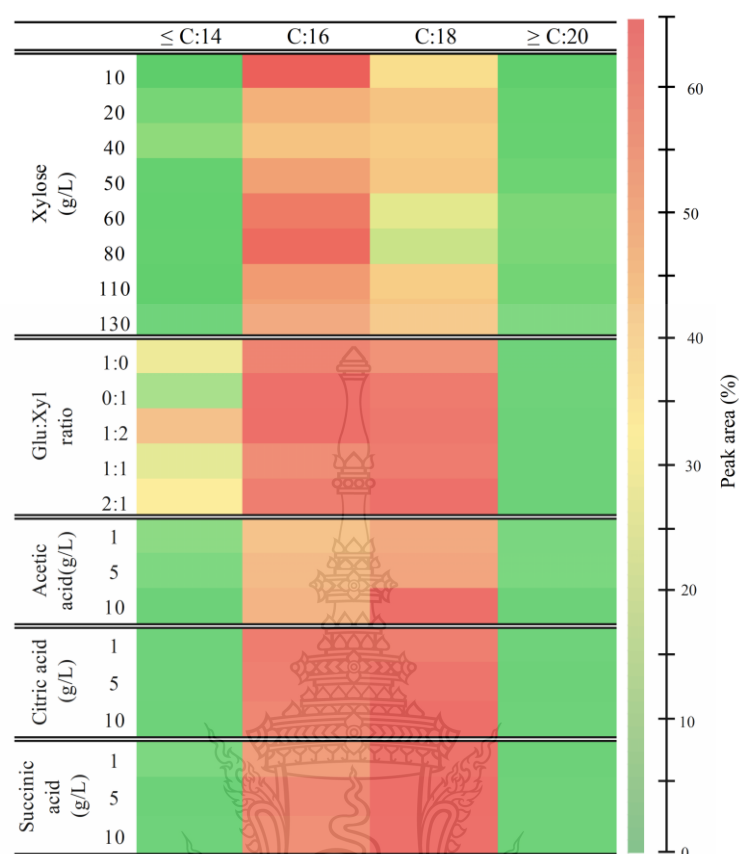
Figure 4.22 Heat maps showing fatty acid compositions of *P. parantarctica* CHC28 cultivation in different conditions.
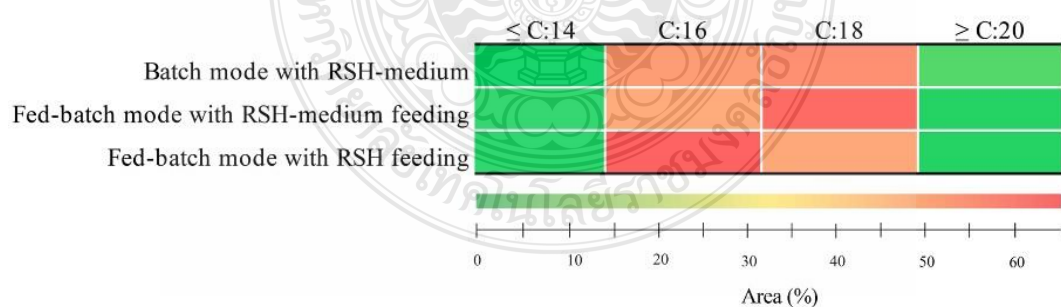
Figure 4.23 Heat maps showing fatty acid compositions of *P. parantarctica* CHC28 cultivation in different cultivation modes under RSH-OPM.

4.10 Structure of BPU foams

In this study, YO was first transformed to the polyol form before utilization to produce BPU foam polymer by the reaction of YO polyol (–OH group) and isocyanate (–NCO group) [180]. The polymer was formed as YO polyols, with excess isocyanate (toluene di-isocyanate) to complete the polymerization process. The formation of PU required a ratio between the NCO and OH groups (called the NCO index) of over 1.1 [7, 181]. The feasibility of polymer production was tested by preparing rigid and semi-rigid BPU foams according to previous reports with slight adaptations [35]. Rigid and semi-rigid BPU foams and scanning electron microscopy (SEM) analyses are shown in Figure 4.24 to 4.25. The structure of BPU foams produced from xyl-based and RSH-based YO of *P. parantarctica* CHC28 were similar (Figure 4.24A, B and 4.25A, B). Results indicated that the surface of rigid BPU foam was smooth with a few holes, while the semi-rigid BPU foam presented many non-uniform holes (Figure 4.24C, D and 4.25C, D). The holes were formed due to the release of CO_2 by the reaction between water and di-isocyanate during BPU foam preparation [182]. Previous research reported the application of YO produced from *Cryptococcus curvatus* as a bio-based polyol PU precursor [12], while YO generated by *R. toruloides* ATCC 10788 has been used for both rigid and semi-rigid BPU foam formation [182]. The bio-oil was transformed into polyols and generated characteristics of both rigid and semi-rigid BPU foams depending on the preparation process. The physical and chemical properties of BPU foams could also be modified by adjusting the natural raw materials, catalyst, surfactant, and blowing agents [183]. BPU foam has excellent thermal insulating properties, low density and thermal conductivity, and is usually used as a heat-insulating material in refrigerator chambers and construction [184]. Previous research reported that using bio-oil instead of fossil polyol at up to 80% improved heat insulation properties [183, 185, 186].
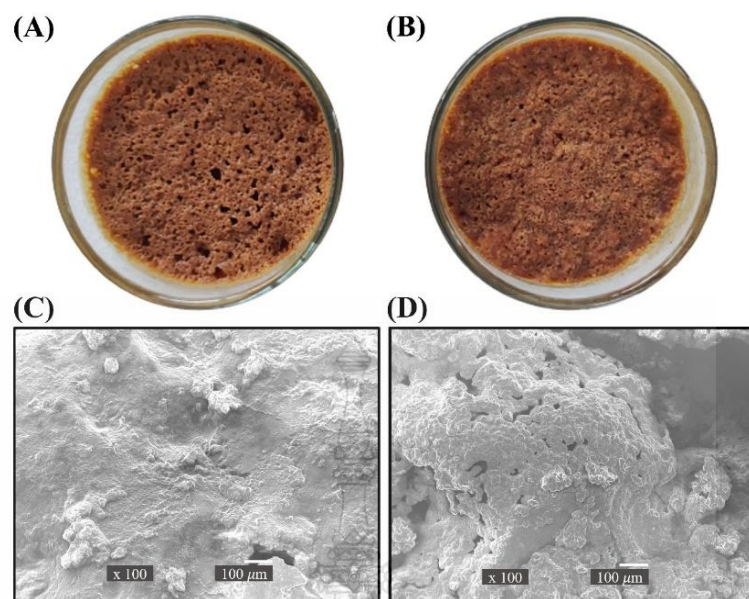
Figure 4.24 (A) Rigid BPU and (B) semi-rigid BPU foams prepared from xyl-based YO. SEM images of (C) rigid BPU and (D) semi-rigid BPU foams.
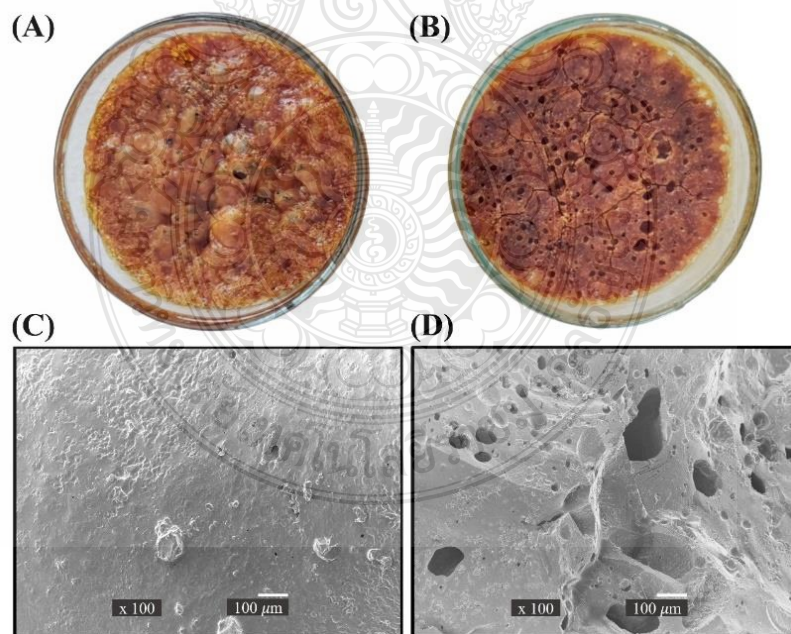
Figure 4.25 (A) Rigid BPU and (B) semi-rigid BPU foams prepared from RSH-based YO. SEM images of (C) rigid BPU and (D) semi-rigid BPU foams.

4.11 Density and water absorption properties of BPU foams

The density of rigid and semi-rigid BPU was investigated according to ASTM D729. The results showed that rigid BPUs produced from xyl-based and RSH-based YO did not exhibit significant differences in density (p-value > .05). However, the density of the semi-rigid BPU produced from xylose-based YO was significantly greater than that made from RSH-based YO (p-value ≤ .05) (Table 4.12). It is possible to obtain various monomers from the fatty acids in crude oil materials used in BPU synthesis from polyols derived from xylose-based yeast oil (YO). The xylose-based YO yielded a higher proportion of C18 fatty acids compared to C16 by 8.6%. Conversely, the proportion of C18 was slightly higher than C16 by only 2.4% (Figure heatmap). Due to the differences in oil derivatives, such as composition types, distribution of fatty acids, number of distributed fatty acids, hydroxyl sites, and unsaturation within the fatty acid tri-ester chains of polyols, these factors influence the properties of the resulting polyurethane (PU) [187]. Previous research reported that PU derived from soybean oil decreased density when formulated with polyols possessing lower hydroxyl numbers, requiring a lower reactivity of isocyanates than formulations with polyols featuring higher hydroxyl numbers [188]. Additionally, the properties of PU, including rigidity, cross-linking density, mechanical strength, and dimensional structure, were influenced by factors like the type of additives used, the cross-linking of urethane polymers, and the techniques employed for PU foaming [189]. The application of PU is generally classified according to density. Low-density PU (0.5-1.5 g/cm^3) is used as corrosion barriers and body sound absorption in the automotive industry [7].

The water absorption of BPUs produced from xyl-based YO was significantly higher than RSH-based YO (p-value ≤ .05) (Table 4.12). This variation in water absorption could be attributed to differences in cell structure arising from variations in raw material composition and foaming techniques, ultimately impacting the cell permeability [190]. The water absorption is influenced by the distribution of foam cells, with higher water absorption linked to more open cell structures. In contrast, lower values of open cells are associated with decreased water absorption [190]. Członka et al. have reported that PU foams synthesized from linseed oils in lower-density foam reduced the water absorption [191]. Water absorption by BPU softened the material as an advantage for medical

applications [7]. Results demonstrated that both types of BPU formed in this study could be considered for specific industries. However, the properties and production process of BPU need further comprehensive investigation before considering industrial-scale application.

Table 4.12 Density and water absorption properties of BPU.

Conditions	Density (g/cm^3)	Water absorption (%), 24 h
Standard PU	1.12-1.24	0.1-0.6
Rigid BPU		
Xyl-based YO	0.95 ± 0.10^a	30.4 ± 5.8^a
RSH-based YO	0.95 ± 0.07^a	23.3 ± 2.1^b
Semi-rigid BPU		
Xyl-based YO	0.93 ± 0.07^a	31.4 ± 3.9^a
RSH-based YO	0.86 ± 0.02^b	24.2 ± 1.0^b

*Different superscripts presented a significant difference in the same column at p-value $\leq .05$.

4.12 The FTIR infrared spectra of BPU

The FTIR spectrums of Xyl-based YO and RSH-based YO, both rigid BPU and semi-rigid BPU foams, were presented in Figure 4.26 and 4.27A to C. Figure 4.26 and 4.27A presented the FTIR chromatogram of Xyl-based YO and RSH-based YO. The result showed that the bands at approximately 2853 and 2923 cm^{-1}were assigned to stretching vibrations of CH$_3$ and CH$_2$ aliphatic chains of both YO, respectively. This result was similar to the band of castor, soybean, sunflower, and corn oil [192-194]. FTIR presented two functional groups of absorption bands at 1465 and 1734 to 1710 cm^{-1} arising from carbonyl $-C=O$, and that $C-C$ stretching vibration at 1076 cm^{-1} signaled by Xyl-based YO similar to plant essential oils [195]. In contrast, $C-O$ at 1169 cm^{-1} shown in RSH-based YO due to the ant-symmetric and asymmetric axial stretching (Figure 4.26 and 4.27A), which is close to Jatropha, soybean, sunflower oil [192]. In addition, the band at 1465 cm^{-1} corresponded to the double bonds deformation of alkene CH$_2$ groups [194], showing in both Xyl and RSH-based YO structures (Figure 4.26 and 4.27A). The sharp band at 754 and 752 cm^{-1} of both YO were assigned to $-$CH out-of-

plane bending [193, 196]. The FTIR spectrum of rigid and semi-rigid BPU foam was used to confirm the presence of urethane linkages (Figure 4.26 and 4.27B, C). The band at approximately 3292 and 3268 cm^{-1} of rigid BPU foams and semi-rigid BPU foams at 3304 and 3280 cm^{-1} were assigned to the characteristic −NH stretching vibration region [197]. The bands at approximately 2852 and 2921 cm^{-1}were assigned to CH$_2$ and CH$_3$ stretching vibrations in all BPU foam (Figure 4.26 and 4.27B, C). For both semi-rigid BPUs, the 1707 and 1740 cm^{-1} band was presented as the urethane stretching vibration (C=O, non-H-bonded) (Figure 4.26 and 4.27C). In addition, the band at approximately 1640 cm^{-1} corresponded to the urethane stretching vibration (C=O, H-bonded) of all BPU foams (Figure 4.26 and 4.27B, C). It had been reported that the band at 1640 cm^{-1} was typical of bidentate urea that interacted through hydrogen bonds with the surrounding molecules, indicating a hard domain ordering [197]. The presence of a band at approximately 1086 to 1088 cm^{-1} and 1060 to 1075 cm^{-1} was attributed to the N–CO–O urethane bond (Figure 4.26 and 4.27B, C). The band at 875 to 720 cm^{-1} and 873 to 686 cm^{-1} (Figure 4.26 and 4.27B) includes 876 to 669 cm^{-1} and 877 to 682 cm^{-1} (Figure 4.26 and 4.27C) assigned to the axial deformation vibrations that are typical of the angular deformation outside the plane of the C-H bond structured in the aromatic ring [182, 198, 199].
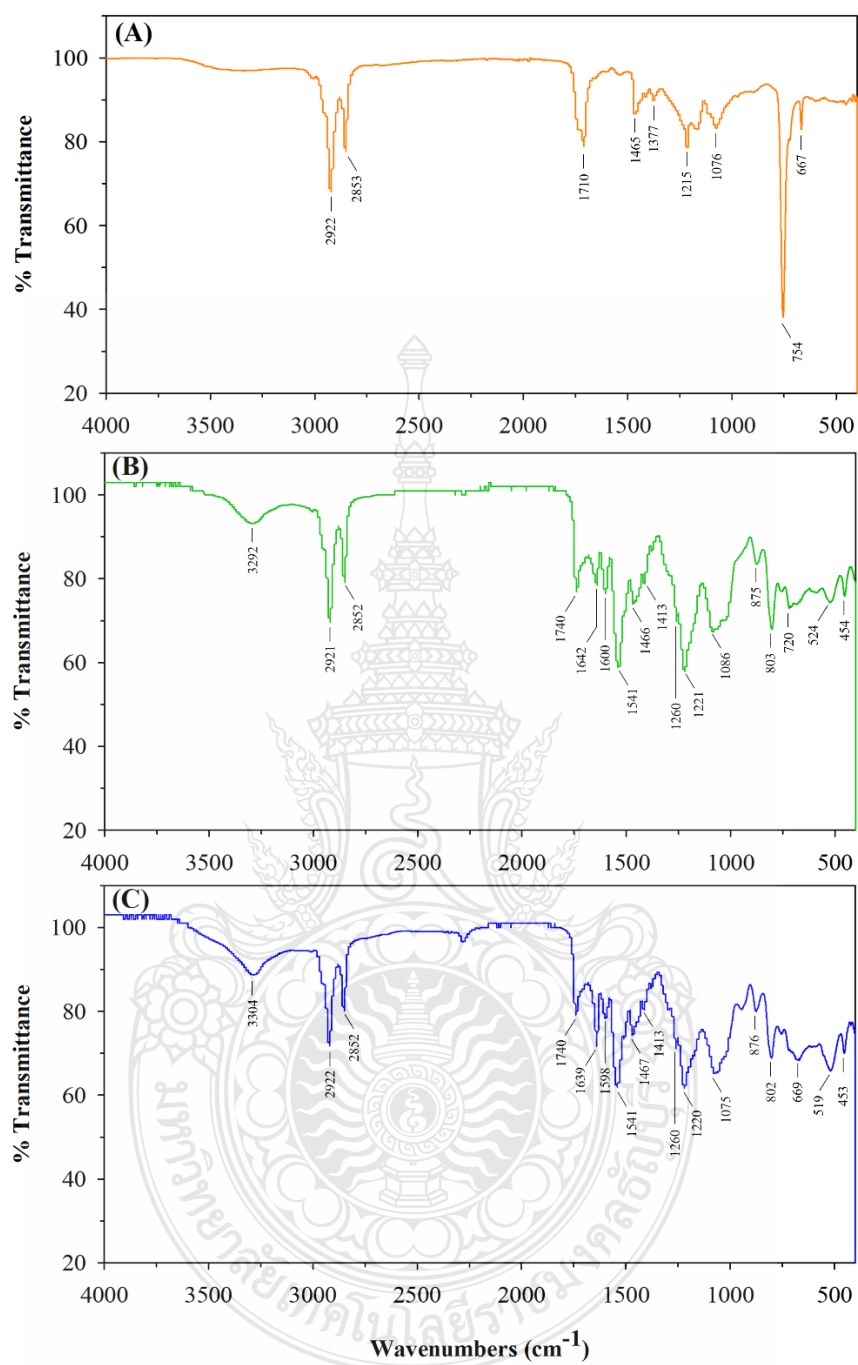
Figure 4.26 FTIR spectra of (A) Xyl-based YO, (B) rigid BPU, and (C) semi-rigid BPU.
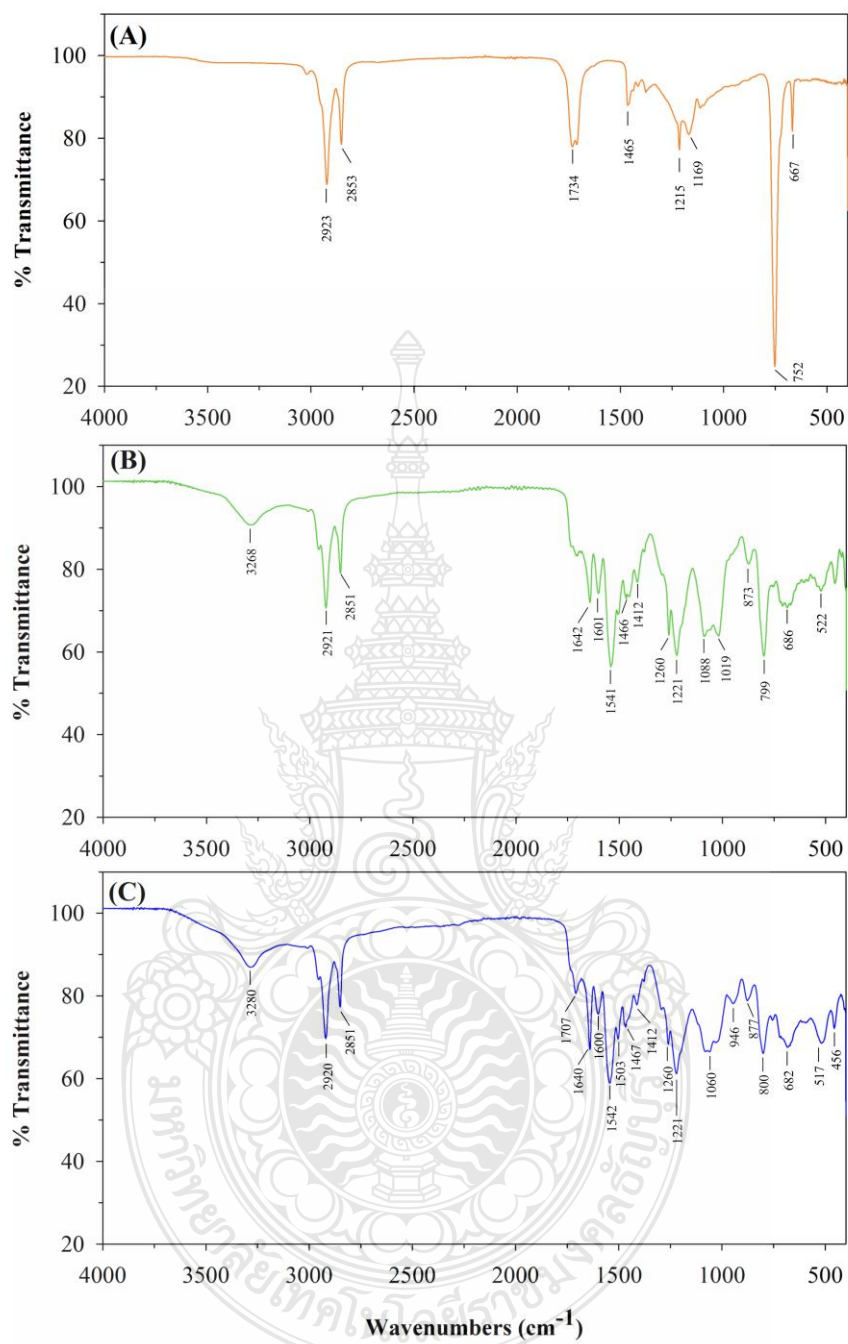
Figure 4.27 FTIR spectra of (A) RSH-based YO, (B) rigid BPU, and (C) semi-rigid BPU.

CHAPTER 5
CONCLUSIONS

This study focused on the selection of efficient yeast strains for xylose-based oil production. The results identified *P. parantarctica* CHC28 as the most effective yeast strain for yielding YO from xylose. The highest biomass and YO were achieved at 12.91 ± 0.08 and 3.20 ± 0.12 g/L, respectively, with intracellular oil accumulation reaching 24.8 ± 0.75%. Investigating the influence of initial xylose concentrations on YO production revealed optimal conditions at 40 g/L xylose, resulting in 3.36 ± 0.01 g/L YO and an oil content of 28.4 ± 0.5%. Remarkably, xylose-based YO formation increased by 24.4% under these conditions compared to glucose-based cultivation. However, co-cultivation using glucose-xylose as carbon sources negatively impacted YO formation compared to single-carbon sources. The different glucose-to-xylose ratios did not significantly affect biomass and YO production in *P. parantarctica* cultivation. Adding 1 g/L acetic acid, YO production from xylose was enhanced to 4.39 ± 0.30 g/L, higher than the unsupplemented condition by 30.7%. Notably, C:16 and C:18 FAs constituted the predominant FAs in *P. parantarctica* CHC28-derived YO, accounting for over 84.8% in the xylose-based medium.

Consequently, RSH was applied as the primary substrate for producing YO by *P. parantarctica* CHC28 cultivation, focusing on optimizing cultural conditions and YO production. The results exhibited the optimal parameters for YO production from RSH, including 10 g/L RSH, 0.5 g/L $(NH_4)_2SO_4$, and 9 g/L KH_2PO_4. Under these optimal conditions, the biomass and YO reached 4.67 ± 0.09 and 1.02 ± 0.05 g/L, respectively. A high cell-density (HCD) cultivation strategy using fed-batch processes with various feeding approaches was employed to enhance YO production efficiency further. The outcome demonstrated that utilizing an RSH-based medium for feeding significantly improved substrate utilization efficiency for yeast growth and YO production. Remarkably, the highest biomass and YO production of 7.36 ± 0.18 and 3.77 ± 0.09 g/L were achieved after 216 h of cultivation. In addition, the FA composition of YO produced

with different RSH feeding modes exhibited similarity. The FA profile predominantly comprised C:16 and C:18 FAs, constituting over 88.2%.

The mathematical modeling effectively simulated the YO production profile by the Berkeley Madonna^{TM} program. The kinetics of yeast growth and YO production were modeled, yielding a best fit with R^2 values up to 1 for the modified Logistic and Luedeking-Piret equations. The substrate and acid consumption rate equations explained yeast cultivation under co-carbon and acid supplementation, showing R^2 values up to 0.968 and 0.993, respectively.

Subsequently, the successful conversion of xyl-based and RSH-based YOs into rigid and semi-rigid BPU foams was achieved. BPU foam properties incorporated density and water absorption were evaluated using ASTM D729 and ASTM D570 analysis. The observed density and water absorption of BPU foams ranged from 0.86 to 0.95 g/cm³ and 23.3% to 31.4%, respectively. FTIR analysis was conducted to investigate the chemical structure of both YO and BPUs, presenting a different chemical spectrum between the two materials. This result demonstrated that the chemical structure of YO was successfully transformed into BPU.

In summary, the RSH could be enhanced in value by serving as a substrate for YO production, subsequently converted into BPU foams. The yielded YO had potential as an alternative feedstock for biodegradable polymers. However, confirming the BPU structure compared to commercial polymers requires NMR analysis of the chemical structure of the synthesized BPU. Moreover, the feasibility of the YO and BPU production processes requires comprehensive enhancement before contemplating industrial-scale application.

List of Bibliography

[1]   X.-y. LI, Q.-f. LI, Y.-h. ZHAO, M.-q. KANG, and J.-w. WANG, "Utilization of carbon dioxide in polyurethane," *Journal of Fuel Chemistry and Technology,* vol. 50, no. 2, pp. 195-209, 2022.

[2]   B. E. Rittmann, "Opportunities for renewable bioenergy using microorganisms," *Biotechnol Bioeng,* vol. 100, no. 2, pp. 203-12, 2008.

[3]   B. K. Uprety, W. Chaiwong, C. Ewelike, and S. K. Rakshit, "Biodiesel production using heterogeneous catalysts including wood ash and the importance of enhancing byproduct glycerol purity," *Energy Conversion and Management,* vol. 115, pp. 191-199, 2016.

[4]   R. Chinthapalli, P. Skoczinski, M. Carus, W. Baltus, D. D. Guzman, H. Käb, A. Raschka, and J. Ravenstijn, "Biobased building blocks and polymers—global capacities, production and trends, 2018–2023," *Industrial Biotechnology,* vol. 15, no. 4, pp. 237-241, 2019.

[5]   A. Pellis, M. Malinconico, A. Guarneri, and L. Gardossi, "Renewable polymers and plastics: Performance beyond the green," *New Biotechnology,* vol. 60, pp. 146-158, 2021.

[6]   European-bioplastics. Bioplastic market data 2019 [Online] Available: https://www. european-bioplastics.org/wp-content/uploads/2019/11/Report_Bioplastics-Market-Data_2019_short_version.pdf

[7]   M. Szycher, *Handbook of Polyurethanes.* Florida: Taylor & Francis, 2013.

[8]   Y. Deng, R. Dewil, L. Appels, R. Ansart, J. Baeyens, and Q. Kang, "Reviewing the thermo-chemical recycling of waste polyurethane foam," *Journal of Environmental Management,* vol. 278, no. Pt 1, p. 111527, 2021.

[9]   H. Pawlik and A. Prociak, "Influence of palm oil-based polyol on the properties of flexible polyurethane foams," *Journal of Polymers and the Environment,* vol. 20, no. 2, pp. 438-445, 2012.

[10]   X. Kong, G. Liu, H. Qi, and J. M. Curtis, "Preparation and characterization of high-solid polyurethane coating systems based on vegetable oil derived polyols," *Progress in organic coatings,* vol. 76, no. 9, pp. 1151-1160, 2013.

[11] R. Chen, C. Zhang, and M. R. Kessler, "Polyols and polyurethanes prepared from epoxidized soybean oil ring-opened by polyhydroxy fatty acids with varying OH numbers," *Journal of Applied Polymer Science,* vol. 132, no. 1, 2015.

[12] M. Samavi and S. Rakshit, "Utilization of microbial oil from poplar wood hemicellulose prehydrolysate for the production of polyol using chemo-enzymatic epoxidation," *Biotechnology and bioprocess engineering,* vol. 25, pp. 327-335, 2020.

[13] G. Vicente, L. F. Bautistaa, R. Rodríguez, F. J. Gutiérrez, I. Sádabaa, R. M. Ruiz-Vázquez, S. Torres-Martínez, and V. Garre, "Biodiesel production from biomass of an oleaginous fungus," *Biochemical Engineering Journal,* vol. 48, no. 1, pp. 22-27, 2009.

[14] X. Meng, J. Yang, X. Xu, L. Zhang, Q. Nie, and M. Xian, "Biodiesel production from oleaginous microorganisms," *Renewable Energy,* vol. 34, no. 1, pp. 1-5, 2009.

[15] L. Matsakas, N. Bonturi, E. A. Miranda, U. Rova, and P. Christakopoulos, "High concentrations of dried sorghum stalks as a biomass feedstock for single cell oil production by *Rhodosporidium toruloides*," *Biotechnol Biofuels,* vol. 8, no. 1, p. 6, 2015.

[16] L. Qin, L. Liu, A.-P. Zeng, and D. Wei, "From low-cost substrates to single cell oils synthesized by oleaginous yeasts," *Bioresource technology,* vol. 245, pp. 1507-1519, 2017.

[17] M. Spagnuolo, A. Yaguchi, and M. Blenner, "Oleaginous yeast for biofuel and oleochemical production," *Current Opinion in Biotechnology,* vol. 57, pp. 73-81, 2019.

[18] A. Areesirisuk, C. Chiu, T. Yen, C. Liu, and J. Guo, "A novel oleaginous yeast strain with high lipid productivity and its application to alternative biodiesel production," *Applied biochemistry and microbiology,* vol. 51, pp. 411-418, 2015.

[19]   J. L. Adrio, "Oleaginous yeasts: promising platforms for the production of oleochemicals and biofuels," *Biotechnology and bioengineering,* vol. 114, no. 9, pp. 1915-1920, 2017.

[20]   C. Rakkitkanphun, J. Teeka, D. Kaewpa, and A. Areesirisuk, "Purification of biodiesel-derived crude glycerol by acidification to be used as a carbon source for microbial oil production by oleaginous yeast *Pseudozyma parantarctica* CHC28," *Biomass Conversion and Biorefinery,* pp. 1-11, 2021.

[21]   A. O. Ayeni, O. A. Adeeyo, O. M. Oresegun, and T. E. Oladimeji, "Compositional analysis of lignocellulosic materials: Evaluation of an economically viable method suitable for woody and non-woody biomass," *American Journal of Engineering Research (AJER),* vol. 4, no. 4, pp. 14-19, 2015.

[22]   N. Sorek, T. H. Yeats, H. Szemenyei, H. Youngs, and C. R. Somerville, "The implications of lignocellulosic biomass chemical composition for the production of advanced biofuels," *Bioscience,* vol. 64, no. 3, pp. 192-201, 2014.

[23]   J.-E. Lee, P. V. Vadlani, and D. Min, "Sustainable production of microbial lipids from lignocellulosic biomass using oleaginous yeast cultures," *Journal of Sustainable Bioenergy Systems,* vol. 7, no. 1, pp. 36-50, 2017.

[24]   V. Menon and M. Rao, "Trends in bioconversion of lignocellulose: biofuels, platform chemicals & biorefinery concept," *Progress in energy and combustion science,* vol. 38, no. 4, pp. 522-550, 2012.

[25]   T. Yoshida, H. Nonaka, and Y. Matsumura, "Hydrothermal treatment of cellulose as a pretreatment for ethanol fermentation: Cellulose hydrolysis experiments," *Journal of the Japan Institute of Energy,* vol. 84, no. 7, pp. 544-548, 2005.

[26]   J. Brandenburg, J. Blomqvist, V. Shapaval, A. Kohler, S. Sampels, M. Sandgren, and V. Passoth, "Oleaginous yeasts respond differently to carbon sources present in lignocellulose hydrolysate," *Biotechnology for Biofuels,* vol. 14, no. 1, pp. 1-12, 2021.

List of Bibliography (Continued)

[27]   Z. Chen and C. Wan, "Effects of salts contained in lignocellulose-derived sugar streams on microbial lipid production," *Applied biochemistry and biotechnology,* vol. 183, no. 4, pp. 1362-1374, 2017.

[28]   M. Chmielarz, J. Blomqvist, S. Sampels, M. Sandgren, and V. Passoth, "Microbial lipid production from crude glycerol and hemicellulosic hydrolysate with oleaginous yeasts," *Biotechnology for Biofuels,* vol. 14, no. 1, pp. 1-11, 2021.

[29]   C. S. Osorio-González, K. Hegde, P. Ferreira, S. K. Brar, A. Kermanshahipour, C. R. Soccol, and A. Avalos-Ramírez, "Lipid production in *Rhodosporidium toruloides* using C-6 and C-5 wood hydrolysate: A comparative study," *Biomass and Bioenergy,* vol. 130, p. 105355, 2019.

[30]   S. Khan, R. Siddique, W. Sajjad, G. Nabi, K. M. Hayat, P. Duan, and L. Yao, "Biodiesel production from algae to overcome the energy crisis," *HAYATI Journal of Biosciences,* vol. 24, no. 4, pp. 163-167, 2017.

[31]   B.-F. Lin, J.-H. Huang, and D.-Y. Huang, "Experimental study of the effects of vegetable oil methyl ester on DI diesel engine performance characteristics and pollutant emissions," *fuel,* vol. 88, no. 9, pp. 1779-1785, 2009.

[32]   M. Ayoub and A. Z. Abdullah, "Critical review on the current scenario and significance of crude glycerol resulting from biodiesel industry towards more sustainable renewable energy industry," *Renewable and Sustainable Energy Reviews,* vol. 16, no. 5, pp. 2671-2686, 2012.

[33]   B. Imre and B. Pukánszky, "Compatibilization in bio-based and biodegradable polymer blends," *European Polymer Journal,* vol. 49, no. 6, pp. 1215-1233, 2013.

[34]   M. Szycher, *Szycher's handbook of polyurethanes*. CRC press, 1999.

[35]   S. S. Narine, X. Kong, L. Bouzidi, and P. Sporns, "Physical properties of polyurethanes produced from polyols from seed oils: II. Foams," *Journal of the American Oil Chemists' Society,* vol. 84, no. 1, pp. 65-72, 2007.

[36]   N. Saifuddin, O. Chun Wen, L. Wei Zhan, and K. Xin Ning, "Palm oil based polyols for polyurethane foams application," in *Proceedings of International Conference on Advances in Renewable Energy Technologies*, 2010, pp. 6-7.

[37] K. M. Zia, H. N. Bhatti, and I. A. Bhatti, "Methods for polyurethane and polyurethane composites, recycling and recovery: A review," *Reactive and functional polymers,* vol. 67, no. 8, pp. 675-692, 2007.

[38] N. V. Gama, A. Ferreira, and A. Barros-Timmons, "Polyurethane foams: Past, present, and future," *Materials,* vol. 11, no. 10, p. 1841, 2018.

[39] M. Ionescu, *Chemistry and technology of polyols for polyurethanes*. iSmithers Rapra Publishing, 2005.

[40] K. Ashida, "Polyurethane and Related Foams: Chemistry and Technology, Chap. 4," ed: Taylor & Francis Group, LLC, 2007.

[41] X. Wang, P. Zhang, Z. Huang, W. Xing, L. Song, and Y. Hu, "Effect of aluminum diethylphosphinate on the thermal stability and flame retardancy of flexible polyurethane foams," *Fire Safety Journal,* vol. 106, pp. 72-79, 2019.

[42] G. Tang, L. Zhou, P. Zhang, Z. Han, D. Chen, X. Liu, and Z. Zhou, "Effect of aluminum diethylphosphinate on flame retardant and thermal properties of rigid polyurethane foam composites," *Journal of Thermal Analysis and Calorimetry,* vol. 140, pp. 625-636, 2020.

[43] B. S. Kim, J. Choi, Y. S. Park, Y. Qian, and S. E. Shim, "Semi-rigid polyurethane foam and polymethylsilsesquioxane aerogel composite for thermal insulation and sound absorption," *Macromolecular Research,* vol. 30, no. 4, pp. 245-253, 2022.

[44] P. Felizardo, M. J. N. Correia, I. Raposo, J. F. Mendes, R. Berkemeier, and J. M. Bordado, "Production of biodiesel from waste frying oils," *Waste management,* vol. 26, no. 5, pp. 487-494, 2006.

[45] M. G. Kulkarni and A. K. Dalai, "Waste cooking oil an economical source for biodiesel: a review," *Industrial & engineering chemistry research,* vol. 45, no. 9, pp. 2901-2913, 2006.

[46] P. Sahoo and L. Das, "Process optimization for biodiesel production from Jatropha, Karanja and Polanga oils," *fuel,* vol. 88, no. 9, pp. 1588-1594, 2009.

[47] M. E. Di Pietro, A. Mannu, and A. Mele, "NMR determination of free fatty acids in vegetable oils," *Processes,* vol. 8, no. 4, p. 410, 2020.

[48] M. J.-L. Tschan, E. Brulé, P. Haquette, and C. M. Thomas, "Synthesis of biodegradable polymers from renewable resources," *Polymer Chemistry,* vol. 3, no. 4, pp. 836-851, 2012.

[49] A. Areesirisuk, C.-H. Chiu, T.-B. Yen, C.-H. Liu, and J.-H. Guo, "A novel oleaginous yeast strain with high lipid productivity and its application to alternative biodiesel production," *Applied biochemistry and microbiology,* vol. 51, no. 4, pp. 411-418, 2015.

[50] S. Bellou, I.-E. Triantaphyllidou, P. Mizerakis, and G. Aggelis, "High lipid accumulation in *Yarrowia lipolytica* cultivated under double limitation of nitrogen and magnesium," *Journal of Biotechnology,* vol. 234, pp. 116-126, 2016.

[51] T. W. Jeffries, "Engineering yeasts for xylose metabolism," *Current opinion in biotechnology,* vol. 17, no. 3, pp. 320-326, 2006.

[52] R. Robles-Iglesias, C. Naveira-Pazos, C. Fernández-Blanco, M. C. Veiga, and C. Kennes, "Factors affecting the optimisation and scale-up of lipid accumulation in oleaginous yeasts for sustainable biofuels production," *Renewable and Sustainable Energy Reviews,* vol. 171, p. 113043, 2023.

[53] F. Shahidi, *Bailey's Industrial Oil and Fat Products, Industrial and Nonedible Products from Oils and Fats*. John Wiley & Sons, 2005.

[54] M. Ngamsirisomsakul, A. Reungsang, and M. B. Kongkeitkajorn, "Assessing oleaginous yeasts for their potentials on microbial lipid production from sugarcane bagasse and the effects of physical changes on lipid production," *Bioresource Technology Reports,* vol. 14, p. 100650, 2021.

[55] R. Poontawee, W. Lorliam, P. Polburee, and S. Limtong, "Oleaginous yeasts: Biodiversity and cultivation," *Fungal Biology Reviews,* vol. 44, p. 100295, 2023.

[56] J. Liu, M. Yuan, J.-N. Liu, and X.-F. Huang, "Bioconversion of mixed volatile fatty acids into microbial lipids by *Cryptococcus curvatus* ATCC 20509," *Bioresource technology,* vol. 241, pp. 645-651, 2017.

List of Bibliography (Continued)

[57] S. Parsons, F. Abeln, M. C. McManus, and C. J. Chuck, "Techno-economic analysis (TEA) of microbial oil production from waste resources as part of a biorefinery concept: assessment at multiple scales under uncertainty," *Journal of Chemical Technology & Biotechnology,* vol. 94, no. 3, pp. 701-711, 2019.

[58] Y. Li, Z. K. Zhao, and F. Bai, "High-density cultivation of oleaginous yeast *Rhodosporidium toruloides* Y4 in fed-batch culture," *Enzyme and Microbial Technology,* vol. 41, no. 3, pp. 312-317, 2007.

[59] Y. Wang, S. Zhang, Z. Zhu, H. Shen, X. Lin, X. Jin, X. Jiao, and Z. K. Zhao, "Systems analysis of phosphate-limitation-induced lipid accumulation by the oleaginous yeast *Rhodosporidium toruloides*," *Biotechnology for Biofuels,* vol. 11, pp. 1-15, 2018.

[60] S. Wu, C. Hu, G. Jin, X. Zhao, and Z. K. Zhao, "Phosphate-limitation mediated lipid production by *Rhodosporidium toruloides*," *Bioresource technology,* vol. 101, no. 15, pp. 6124-6129, 2010.

[61] I. Kolouchová, O. Maťátková, K. Sigler, J. Masák, and T. Řezanka, "Lipid accumulation by oleaginous and non-oleaginous yeast strains in nitrogen and phosphate limitation," *Folia Microbiologica,* vol. 61, pp. 431-438, 2016.

[62] F. R. Amin, F. R. Amin, H. Khalid, H. Zhang, S. U. Rahman, R. Zhang, G. Liu, and C. Chen, "Pretreatment methods of lignocellulosic biomass for anaerobic digestion," *AMB Express,* vol. 7, pp. 1-12, 2017.

[63] J. Strakowska, L. Błaszczyk, and J. Chełkowski, "The significance of cellulolytic enzymes produced by *Trichoderma* in opportunistic lifestyle of this fungus," *Journal of Basic Microbiology,* vol. 54, no. S1, pp. S2-S13, 2014.

[64] F. Bilo, S. Pandini, L. Sartore, L. E. Depero, G. Gargiulo, A. Bonassi, S. Federici, and E. Bontempi, "A sustainable bioplastic obtained from rice straw," *Journal of cleaner production,* vol. 200, pp. 357-368, 2018.

List of Bibliography (Continued)

[65] A. Domínguez, F. J. Deive, L. Pastrana, M. L. Rúa, M. A. Longo, and M. A. Sanroman, "Thermostable lipolytic enzymes production in batch and continuous cultures of *Thermus thermophilus* HB27," *Bioprocess and biosystems engineering,* vol. 33, no. 3, pp. 347-354, 2010.

[66] H. Kawaguchi, T. Hasunuma, C. Ogino, and A. Kondo, "Bioprocessing of bio-based chemicals produced from lignocellulosic feedstocks," *Current opinion in biotechnology,* vol. 42, pp. 30-39, 2016.

[67] N. Lecksiwilai, S. H. Gheewala, M. Sagisaka, and K. Yamaguchi, "Net Energy Ratio and Life cycle greenhouse gases (GHG) assessment of bio-dimethyl ether (DME) produced from various agricultural residues in Thailand," *Journal of cleaner production,* vol. 134, pp. 523-531, 2016.

[68] N. Syaftika and Y. Matsumura, "Comparative study of hydrothermal pretreatment for rice straw and its corresponding mixture of cellulose, xylan, and lignin," *Bioresource technology,* vol. 255, pp. 1-6, 2018.

[69] A. Verardi, A. Blasi, T. Marino, A. Molino, and V. Calabrò, "Effect of steam-pretreatment combined with hydrogen peroxide on lignocellulosic agricultural wastes for bioethanol production: analysis of derived sugars and other by-products," *Journal of energy chemistry,* vol. 27, no. 2, pp. 535-543, 2018.

[70] H. Zhang, Y. Xu, and S. Yu, "Co-production of functional xylooligosaccharides and fermentable sugars from corncob with effective acetic acid prehydrolysis," *Bioresource Technology,* vol. 234, pp. 343-349, 2017.

[71] H. Chen, X. Zhao, and D. Liu, "Relative significance of the negative impacts of hemicelluloses on enzymatic cellulose hydrolysis is dependent on lignin content: evidence from substrate structural features and protein adsorption," *ACS Sustainable Chemistry & Engineering,* vol. 4, no. 12, pp. 6668-6679, 2016.

[72] S. Rashid, M. Ishak, K. Rahman, and K. Ismail, "Ethanol Production from Alkaline-treated Rice Straw via Separate Hydrolysis and Fermentation (SHF) using *K. marxianus* UniMAP 1-1," in *IOP Conference Series: Earth and Environmental Science*, 2021, vol. 765, no. 1: IOP Publishing, p. 012052.

List of Bibliography (Continued)

[73] A. Valles, M. Capilla, F. Álvarez-Hornos, M. García-Puchol, P. San-Valero, and C. Gabaldón, "Optimization of alkali pretreatment to enhance rice straw conversion to butanol," *Biomass and Bioenergy,* vol. 150, p. 106131, 2021.

[74] J. R. Almeida, T. Modig, A. Petersson, B. Hähn-Hägerdal, G. Lidén, and M. F. Gorwa-Grauslund, "Increased tolerance and conversion of inhibitors in lignocellulosic hydrolysates by *Saccharomyces cerevisiae,*" *Journal of Chemical Technology & Biotechnology: International Research in Process, Environmental & Clean Technology,* vol. 82, no. 4, pp. 340-349, 2007.

[75] C. Hu, X. Zhao, J. Zhao, S. Wu, and Z. K. Zhao, "Effects of biomass hydrolysis by-products on oleaginous yeast *Rhodosporidium toruloides,*" *Bioresource technology,* vol. 100, no. 20, pp. 4843-4847, 2009.

[76] B. Diwan and P. Gupta, "Conversion of rice straw to caprylic acid-rich microbial oils by oleaginous yeast isolates," *Biomass Conversion and Biorefinery,* pp. 1-14, 2020.

[77] H. T. Doan, P. T. M. Nguyen, T. T. Tran, T. K. Nguyen, M. D. Tran, and D. B. Nguyen, "Optimizing lime pretreatment of rice straw for biolipid production using oleaginous microorganisms," *Chemosphere,* vol. 269, p. 129390, 2021.

[78] G. W. Park, H. N. Chang, K. Jung, C. Seo, Y. Kim, J. H. Choi, H. C. Woo, and I. Hwang, "Production of microbial lipid by *Cryptococcus curvatus* on rice straw hydrolysates," *Process Biochemistry,* vol. 56, pp. 147-153, 2017.

[79] M. D. Cunha Abreu Xavier and T. T. Franco, "Obtaining hemicellulosic hydrolysate from sugarcane bagasse for microbial oil production by *Lipomyces starkeyi,*" *Biotechnology Letters,* vol. 43, pp. 967-979, 2021.

[80] M. Zhao, W. Zhou, Y. Wang, J. Wang, J. Zhang, and Z. Gong, "Combination of simultaneous saccharification and fermentation of corn stover with consolidated bioprocessing of cassava starch enhances lipid production by the amylolytic oleaginous yeast *Lipomyces starkeyi,*" *Bioresource Technology,* vol. 364, p. 128096, 2022.

List of Bibliography (Continued)

[81] R. Saini, K. Hegde, C. S. Osorio-Gonzalez, S. K. Brar, and P. Vezina, "Evaluating the potential of *Rhodosporidium toruloides*-1588 for high lipid production using undetoxified wood hydrolysate as a carbon source," *Energies,* vol. 13, no. 22, p. 5960, 2020.

[82] R. Saini, C. S. Osorio-Gonzalez, K. Hegde, S. K. Brar, and P. Vezina, "A co-fermentation strategy with wood hydrolysate and crude glycerol to enhance the lipid accumulation in *Rhodosporidium toruloides*-1588," *Bioresource Technology,* vol. 364, p. 127821, 2022.

[83] S. Papanikolaou, M. Galiotou-Panayotou, I. Chevalot, M. Komaitis, I. Marc, and G. Aggelis, "Influence of glucose and saturated free-fatty acid mixtures on citric acid and lipid production by *Yarrowia lipolytica*," *Current Microbiology,* vol. 52, pp. 134-142, 2006.

[84] G. Singh, S. Sinha, K. K. Kumar, N. A. Gaur, K. Bandyopadhyay, and D. Paul, "High density cultivation of oleaginous yeast isolates in 'mandi' waste for enhanced lipid production using sugarcane molasses as feed," *fuel,* vol. 276, p. 118073, 2020.

[85] F. Abeln and C. J. Chuck, "Achieving a high-density oleaginous yeast culture: Comparison of four processing strategies using *Metschnikowia pulcherrima*," *Biotechnology and Bioengineering,* vol. 116, no. 12, pp. 3200-3214, 2019.

[86] P. R. Pawar, A. M. Lali, and G. Prakash, "Integration of continuous-high cell density-fed-batch fermentation for *Aurantiochytrium limacinum* for simultaneous high biomass, lipids and docosahexaenoic acid production," *Bioresource Technology,* vol. 325, p. 124636, 2021.

[87] T. V. D. Rodrigues, E. C. Teixeira, L. P. Macedo, G. M. Dos Santos, C. A. V. Burkert, and J. F. de Medeiros Burkert, "Agroindustrial byproduct-based media in the production of microbial oil rich in oleic acid and carotenoids," *Bioprocess and Biosystems Engineering,* vol. 45, no. 4, pp. 721-732, 2022.

[88] M. Á. Villegas-Méndez, A. Papadaki, C. Pateraki, N. Balagurusamy, J. Montañez, A. A. Koutinas, and L. Morales-Oyervides, "Fed-batch bioprocess development for astaxanthin production by *Xanthophyllomyces dendrorhous* based on the utilization of Prosopis sp. pods extract," *Biochemical Engineering Journal,* vol. 166, p. 107844, 2021.

[89] M. Á. Villegas-Méndez, J. Montañez, J. C. Contreras-Esquivel, I. Salmerón, A. A. Koutinas, and L. Morales-Oyervides, "Scale-up and fed-batch cultivation strategy for the enhanced co-production of microbial lipids and carotenoids using renewable waste feedstock," *Journal of Environmental Management,* vol. 339, p. 117866, 2023.

[90] E. E. Karamerou and C. Webb, "Cultivation modes for microbial oil production using oleaginous yeasts–a review," *Biochemical Engineering Journal,* vol. 151, p. 107322, 2019.

[91] S. Papanikolaou and G. Aggelis, "Lipid production by *Yarrowia lipolytica* growing on industrial glycerol in a single-stage continuous culture," *Bioresource technology,* vol. 82, no. 1, pp. 43-49, 2002.

[92] H. Shen, Z. Gong, X. Yang, G. Jin, F. Bai, and Z. K. Zhao, "Kinetics of continuous cultivation of the oleaginous yeast *Rhodosporidium toruloides*," *Journal of biotechnology,* vol. 168, no. 1, pp. 85-89, 2013.

[93] N. Bonturi, A. Crucello, A. J. C. Viana, and E. A. Miranda, "Microbial oil production in sugarcane bagasse hemicellulosic hydrolysate without nutrient supplementation by a *Rhodosporidium toruloides* adapted strain," *Process Biochemistry,* vol. 57, pp. 16-25, 2017.

[94] T. Chaiyaso and A. Manowattana, "Enhancement of carotenoids and lipids production by oleaginous red yeast *Sporidiobolus pararoseus* KM281507," *Preparative Biochemistry and Biotechnology,* vol. 48, no. 1, pp. 13-23, 2018.

[95] R. L. Amza, P. Kahar, A. B. Juanssilfero, N. Miyamoto, H. Otsuka, C. Kihira, C. Ogino, and A. Kondo, "High cell density cultivation of *Lipomyces starkeyi* for achieving highly efficient lipid production from sugar under low C/N ratio," *Biochemical Engineering Journal,* vol. 149, p. 107236, 2019.

[96] B. K. Uprety, J. V. Reddy, S. S. Dalli, and S. K. Rakshit, "Utilization of microbial oil obtained from crude glycerol for the production of polyol and its subsequent conversion to polyurethane foams," *Bioresource technology,* vol. 235, pp. 309-315, 2017.

[97] Z. Miao, X. Tian, W. Liang, Y. He, and G. Wang, "Bioconversion of corncob hydrolysate into microbial lipid by an oleaginous yeast *Rhodotorula taiwanensis* AM2352 for biodiesel production," *Renewable Energy,* vol. 161, pp. 91-97, 2020.

[98] Y. Lugani, J. Singh, and B. S. Sooch, "Scale-up process for xylose reductase production using rice straw hydrolysate," *Biomass Conversion and Biorefinery,* pp. 1-12, 2021.

[99] C. Hu, S. Wu, Q. Wang, G. Jin, H. Shen, and Z. K. Zhao, "Simultaneous utilization of glucose and xylose for lipid production by *Trichosporon cutaneum*," *Biotechnology for Biofuels,* vol. 4, no. 1, pp. 1-8, 2011.

[100] J. Feng, J.-S. Zhang, W. Jia, Y. Yang, F. Liu, and C.-C. Lin, "An unstructured kinetic model for the improvement of triterpenes production by *Ganoderma lucidum* G0119 based on nitrogen source effect," *Biotechnology and bioprocess engineering,* vol. 19, pp. 727-732, 2014.

[101] T. Chaleewong, P. Khunnonkwao, C. Puchongkawarin, and K. Jantama, "Kinetic modeling of succinate production from glucose and xylose by metabolically engineered *Escherichia coli* KJ12201," *Biochemical Engineering Journal,* vol. 185, p. 108487, 2022.

[102] C. Birgen, O. T. Berglihn, H. A. Preisig, and A. Wentzel, "Kinetic study of butanol production from mixtures of glucose and xylose and investigation of different pre-growth strategies," *Biochemical engineering journal,* vol. 147, pp. 110-117, 2019.

List of Bibliography (Continued)

[103] J. Marudkla, W.-C. Lee, S. Wannawilai, Y. Chisti, and S. Sirisansaneeyakul, "Model of acetic acid-affected growth and poly(3-hydroxybutyrate) production by *Cupriavidus necator* DSM 545," *Journal of Biotechnology,* vol. 268, pp. 12-20, 2018.

[104] S. Wannawilai, Y. Chisti, and S. Sirisansaneeyakul, "A model of furfural-inhibited growth and xylitol production by *Candida magnoliae* TISTR 5663," *Food and Bioproducts Processing,* vol. 105, pp. 129-140, 2017.

[105] C. Rakkitkanphun, J. Teeka, D. Kaewpa, and A. Areesirisuk, "Purification of biodiesel-derived crude glycerol by acidification to be used as a carbon source for microbial oil production by oleaginous yeast *Pseudozyma parantarctica* CHC28," *Biomass Conversion and Biorefinery,* 2021.

[106] K. V. Kumar, "Pseudo-second order models for the adsorption of safranin onto activated carbon: comparison of linear and non-linear regression methods," *J Hazard Mater,* vol. 142, no. 1-2, pp. 564-7, 2007.

[107] X. Yang and B. Al-Duri, "Kinetic modeling of liquid-phase adsorption of reactive dyes on activated carbon," *Journal of Colloid and Interface Science,* vol. 287, no. 1, pp. 25-34, 2005.

[108] E. Bligh and W. Dyer, "A rapid method of total lipid extraction and purification," *Canadian Journal of Biochemistry and Physiology,* vol. 37, no. 8, pp. 911-917, 1959.

[109] A. B. Juanssilfero, P. Kahar, R. L. Amza, N. Miyamoto, H. Otsuka, H. Matsumoto, C. Kihira, A. Thontowi, Yopi, C. Ogino, B. Prasetya, and A. Kondo, "Effect of inoculum size on single-cell oil production from glucose and xylose using oleaginous yeast *Lipomyces starkeyi*," *Journal of bioscience and bioengineering,* vol. 125, no. 6, pp. 695-702, 2018.

[110] D. Lamers, N. V. Biezen, D. Martens, L. Peters, E. V. D. Zilver, N. J. Dreumel, R. H. Wijffels, and C. Lokman, "Selection of oleaginous yeasts for fatty acid production," *BMC biotechnology,* vol. 16, no. 1, pp. 1-10, 2016.

List of Bibliography (Continued)

[111] L. Qvirist, F. Mierke, R. Vazquez Juarez, and T. Andlid, "Screening of xylose utilizing and high lipid producing yeast strains as a potential candidate for industrial application," *BMC microbiology,* vol. 22, no. 1, pp. 1-14, 2022.

[112] A. Tanimur, M. Takashima, T. Sugita, R. Endoh, M. Ohkuma, S. Kishino, J. Ogawa, and J. Shima, "Lipid production through simultaneous utilization of glucose, xylose, and l-arabinose by *Pseudozyma hubeiensis*: a comparative screening study," *AMB Express,* vol. 6, pp. 1-9, 2016.

[113] D. Berikten, E. Z. Hoşgün, A. Gökdal Otuzbiroğlu, B. Bozan, and M. Kıvanç, "Lipid Production from Crude Glycerol by Newly Isolated Oleaginous Yeasts: Strain Selection, Molecular Identification and Fatty Acid Analysis," *Waste and Biomass Valorization,* pp. 1-10, 2021.

[114] S. Chaturvedi, R. Tiwari, A. Bhattacharya, L. Nain, and S. K. Khare, "Production of single cell oil by using cassava peel substrate from oleaginous yeast *Rhodotorula glutinis*," *Biocatalysis and Agricultural Biotechnology,* vol. 21, p. 101308, 2019.

[115] S. Sagia, A. Sharma, S. Singh, S. Chaturvedi, P. K. S. Nain, and L. Nain, "Single cell oil production by a novel yeast *Trichosporon mycotoxinivorans* for complete and ecofriendly valorization of paddy straw," *Electronic Journal of Biotechnology,* vol. 44, pp. 60-68, 2020.

[116] S. Siwina and R. Leesing, "Bioconversion of durian (*Durio zibethinus* Murr.) peel hydrolysate into biodiesel by newly isolated oleaginous yeast *Rhodotorula mucilaginosa* KKUSY14," *Renewable Energy,* vol. 163, pp. 237-245, 2021.

[117] Z. E. Duman-Özdamar, V. A. Martins dos Santos, J. Hugenholtz, and M. Suarez-Diez, "Tailoring and optimizing fatty acid production by oleaginous yeasts through the systematic exploration of their physiological fitness," *Microbial Cell Factories,* vol. 21, no. 1, pp. 1-13, 2022.

List of Bibliography (Continued)

[118] N. M. Vieira, R. C. V. D. Santos, V. K. D. C. Germano, R. Z. Ventorim, E. L. M. D. Almeida, F. A. D. Silveira, J. I. R. Júnior, and W. B. D. Silveira, "Isolation of a new *Papiliotrema laurentii* strain that displays capacity to achieve high lipid content from xylose," *3 Biotech,* vol. 10, no. 9, pp. 1-14, 2020.

[119] S. Fakas, S. Papanikolaou, A. Batsos, M. Galiotou-Panayotou, A. Mallouchos, and G. Aggelis, "Evaluating renewable carbon sources as substrates for single cell oil production by *Cunninghamella echinulata* and *Mortierella isabellina*," *Biomass and bioenergy,* vol. 33, no. 4, pp. 573-580, 2009.

[120] C. T. Evans and C. Ratledge, "Induction of xylulose-5-phosphate phosphoketolase in a variety of yeasts grown ond-xylose: the key to efficient xylose metabolism," *Archives of microbiology,* vol. 139, no. 1, pp. 48-52, 1984.

[121] C. A. Henard, E. F. Freed, and M. T. Guarnieri, "Phosphoketolase pathway engineering for carbon-efficient biocatalysis," *Current Opinion in Biotechnology,* vol. 36, pp. 183-188, 2015.

[122] X. Lu, Y. Liu, Y. Yang, S. Wang, Q. Wang, X. Wang, Z. Yan, J. Cheng, C. Liu, X. Yang, H. Luo, S. Yang, J. Gou, L. Ye, L. Lu, Z. Zhang, Y. Guo, Y. Nie, J. Lin, S. Li, C. Tian, T. Cai, B. Zhuo, H. Ma, and H. Jiang, "Constructing a synthetic pathway for acetyl-coenzyme A from one-carbon through enzyme design," *Nature communications,* vol. 10, no. 1, pp. 1-10, 2019.

[123] T. L. Taylor, "Phosphotransacetylase and xylulose 5-phosphate/fructose 6-phosphate phosphoketolase: Two eukaryotic partners of acetate kinase," Clemson University, 2015.

[124] S. S. Jagtap and C. V. Rao, "Microbial conversion of xylose into useful bioproducts," *Applied microbiology and biotechnology,* vol. 102, no. 21, pp. 9015-9036, 2018.

[125] S. Papanikolaou and G. Aggelis, "Lipids of oleaginous yeasts. Part I: Biochemistry of single cell oil production," *European Journal of Lipid Science and Technology,* vol. 113, no. 8, pp. 1031-1051, 2011.

[126] X. Yu, Y. Zheng, X. Xiong, and S. Chen, "Co-utilization of glucose, xylose and cellobiose by the oleaginous yeast *Cryptococcus curvatus*," *biomass and bioenergy,* vol. 71, pp. 340-349, 2014.

[127] C. Ratledge, "Biochemistry, stoichiometry, substrates and economics in: Single Cell Oil,(Ed.) RS Moreton," ed: Longman Scientific & Technical, Longman House Burnt Mill, Harlow and Essex, 1988.

[128] A. B. Juanssilfero, E. Agustriana, Ahmad, N. Izzati, U. Perwitasari, Fahrurrozi, A. B. N. Putra, P. Lisdiyanti, and Yopi, "Lipid production by oleaginous yeast *Lipomyces starkeyi* InaCC Y604 in the presence of furfural and 5-hydroxymethylfurfural as the inhibitory chemical compounds," in *AIP Conference Proceedings*, 2023, vol. 2606, no. 1: AIP Publishing.

[129] A. K. Yadav, A. Kuila, and V. K. Garlapati, "Biodiesel Production from Brassica juncea Using Oleaginous Yeast," *Applied Biochemistry and Biotechnology,* vol. 194, no. 9, pp. 4066-4080, 2022.

[130] Z. Liu, F. Natalizio, G. Dragone, and S. I. Mussatto, "Maximizing the simultaneous production of lipids and carotenoids by *Rhodosporidium toruloides* from wheat straw hydrolysate and perspectives for large-scale implementation," *Bioresource Technology,* vol. 340, p. 125598, 2021.

[131] X.-F. Huang, J.-N. Liu, L.-J. Lu, K.-M. Peng, G.-X. Yang, and J. Liu, "Culture strategies for lipid production using acetic acid as sole carbon source by *Rhodosporidium toruloides*," *Bioresource technology,* vol. 206, pp. 141-149, 2016.

[132] X.-f. Huang, Y. Shen, H.-j. Luo, J.-n. Liu, and J. Liu, "Enhancement of extracellular lipid production by oleaginous yeast through preculture and sequencing batch culture strategy with acetic acid," *Bioresource technology,* vol. 247, pp. 395-401, 2018.

[133] Y. Zheng, Z. Chi, B. K. Ahring, and S. Chen, "Oleaginous yeast *Cryptococcus curvatus* for biofuel production: ammonia's effect," *biomass and bioenergy,* vol. 37, pp. 114-121, 2012.

List of Bibliography (Continued)

[134] D. Voet and J. G. Voet, *Biochemistry*. John Wiley & Sons, 2010.

[135] C. Chen, X. Deng, W. Kong, M. F. Qaseem, S. Zhao, Y. Li, and A. Wu, "Rice straws with different cell wall components differ on abilities of saccharification," *Frontiers in Bioengineering and Biotechnology,* vol. 8, p. 624314, 2021.

[136] J. C. García Domínguez, M. J. Díaz Blanco, M. T. García Domínguez, M. J. Feria Infante, D. Gómez Lozano, and F. López Baldovín, "Search for optimum conditions of wheat straw hemicelluloses cold alkaline extraction process," 2013.

[137] G. Kaur, M. S. Taggar, A. Kalia, M. Krishania, and A. Singh, "Fungal Secretomes of *Aspergillus terreus* Repertoires Cultivated on Native and acid/alkali Treated Paddy Straw for Cellulase and Xylanase Production," *BioEnergy Research,* pp. 1-15, 2023.

[138] L. Canilha, V. T. O. Santos, G. J. M. Rocha, J. B. A. E. Silva, M. Giulietti, S. S. Silva, M. G. A. Felipe, A. Ferraz, A. M. F. Milagres, and W. Carvalho, "A study on the pretreatment of a sugarcane bagasse sample with dilute sulfuric acid," *Journal of Industrial Microbiology and Biotechnology,* vol. 38, no. 9, pp. 1467-75, 2011.

[139] J. C. López-Linares, E. Ruiz, I. Romero, E. Castro, and P. Manzanares, "Xylitol production from exhausted olive pomace by *Candida boidinii*," *Applied Sciences,* vol. 10, no. 19, p. 6966, 2020.

[140] R. A. de Oliveira, C. E. V. Rossell, J. Venus, S. C. Rabelo, and R. Maciel Filho, "Detoxification of sugarcane-derived hemicellulosic hydrolysate using a lactic acid producing strain," *Journal of biotechnology,* vol. 278, pp. 56-63, 2018.

[141] Y. Sun, X. Li, L. Wu, Y. Li, F. Li, Z. Xiu, and Y. Tong, "The advanced performance of microbial consortium for simultaneous utilization of glucose and xylose to produce lactic acid directly from dilute sulfuric acid pretreated corn stover," *Biotechnology for Biofuels,* vol. 14, no. 1, pp. 1-12, 2021.

[142] P. E. Plaza, M. Coca, S. Lucas Yagüe, M. Fernández-Delgado, J. C. López-Linares, and M. T. García-Cubero, "Exploring the use of high solid loadings in enzymatic hydrolysis to improve biobutanol production from brewers' spent grains," *The Canadian Journal of Chemical Engineering,* vol. 99, no. 12, pp. 2607-2618, 2021.

[143] L. Canilha, W. Carvalho, M. d. G. de Almeida Felipe, J. B. de Almeida e Silva, and M. Giulietti, "Ethanol production from sugarcane bagasse hydrolysate using *Pichia stipitis*," *Applied Biochemistry and Biotechnology,* vol. 161, pp. 84-92, 2010.

[144] X. Wang, Y. Wang, Q. He, Y. Liu, M. Zhao, Y. Liu, W. Zhou, and Z. Gong, "Highly efficient fed-batch modes for enzymatic hydrolysis and microbial lipogenesis from alkaline organosolv pretreated corn stover for biodiesel production," *Renewable Energy,* vol. 197, pp. 1133-1143, 2022.

[145] Z. Gao, Y. Ma, Q. Wang, M. Zhang, J. Wang, and Y. Liu, "Effect of crude glycerol impurities on lipid preparation by *Rhodosporidium toruloides* yeast 32489," *Bioresource technology,* vol. 218, pp. 373-379, 2016.

[146] B. Cheirsilp, R. Intasit, and Y. Louhasakul, "Biovalorization of whole old oil palm trunk as low-cost nutrient sources for biomass and lipid production by oleaginous yeasts through batch and fed-batch fermentation," *Biomass Conversion and Biorefinery,* pp. 1-10, 2022.

[147] P. J. Slininger, B. S. Dien, C. P. Kurtzman, B. R. Moser, E. L. Bakota, S. R. Thompson, P. J. O'Bryan, M. A. Cotta, V. Balan, M. Jin, L. D. C. Sousa, and B. E. Dale, "Comparative lipid production by oleaginous yeasts in hydrolyzates of lignocellulosic biomass and process strategy for high titers," *Biotechnol Bioeng,* vol. 113, no. 8, pp. 1676-90, 2016.

[148] Y.-H. Chang, K.-S. Chang, C.-L. Hsu, L.-T. Chuang, C.-Y. Chen, F.-Y. Huang, and H.-D. Jang, "A comparative study on batch and fed-batch cultures of oleaginous yeast *Cryptococcus* sp. in glucose-based media and corncob hydrolysate for microbial oil production," *Fuel,* vol. 105, pp. 711-717, 2013.

[149] Q. Fei, M. O'Brien, R. Nelson, X. Chen, A. Lowell, and N. Dowe, "Enhanced lipid production by *Rhodosporidium toruloides* using different fed-batch feeding strategies with lignocellulosic hydrolysate as the sole carbon source," *Biotechnol Biofuels,* vol. 9, p. 130, 2016.

[150] Z. Gong, X. Wang, W. Yuan, Y. Wang, W. Zhou, G. Wang, and Y. Liu, "Fed-batch enzymatic hydrolysis of alkaline organosolv-pretreated corn stover facilitating high concentrations and yields of fermentable sugars for microbial lipid production," *Biotechnol Biofuels,* vol. 13, p. 13, 2020.

[151] M. A. Villegas-Mendez, J. Montanez, J. C. Contreras-Esquivel, I. Salmeron, A. A. Koutinas, and L. Morales-Oyervides, "Scale-up and fed-batch cultivation strategy for the enhanced co-production of microbial lipids and carotenoids using renewable waste feedstock," *J Environ Manage,* vol. 339, p. 117866, 2023.

[152] J. Chen, X. Zhang, S. Yan, R. D. Tyagi, and P. Drogui, "Lipid production from fed-batch fermentation of crude glycerol directed by the kinetic study of batch fermentations," *fuel,* vol. 209, pp. 1-9, 2017.

[153] V. Béligon, L. Poughon, G. Christophe, A. Lebert, C. Larroche, and P. Fontanille, "Validation of a predictive model for fed-batch and continuous lipids production processes from acetic acid using the oleaginous yeast *Cryptococcus curvatus*," *Biochemical Engineering Journal,* vol. 111, pp. 117-128, 2016.

[154] B. BK, S. N. Mudliar, V. Bokade, and S. Debnath, "Effect of furfural, acetic acid and 5-hydroxymethylfurfural on yeast growth and xylitol fermentation using *Pichia stipitis* NCIM 3497," *Biomass Conversion and Biorefinery,* pp. 1-15, 2022.

[155] D. Farias, R. R. de Andrade, and F. Maugeri-Filho, "Kinetic modeling of ethanol production by *Scheffersomyces stipitis* from xylose," *Applied biochemistry and biotechnology,* vol. 172, pp. 361-379, 2014.

[156] V. Narisetty, A. A. Prabhu, R. R. Bommareddy, R. Cox, D. Agrawal, A. Misra, M. A. Haider, A. Bhatnagar, A. Pandey, and V. Kumar, "Development of Hypertolerant Strain of Yarrowia lipolytica Accumulating Succinic Acid Using High Levels of Acetate," *ACS Sustainable Chemistry & Engineering,* vol. 10, no. 33, pp. 10858-10869, 2022.

[157] V. S. Nishida, A. L. Woiciechowski, K. K. Valladares-Diestra, L. A. Z. Torres, L. P. D. S. Vandenberghe, A. Z. Filho, and C. R. Soccol, "Bioethanol and succinic acid co-production from imidazole-pretreated soybean hulls," *Industrial crops and products,* vol. 172, p. 114060, 2021.

[158] K. L. Ong, C. Li, X. Li, Y. Zhang, J. Xu, and C. S. K. Lin, "Co-fermentation of glucose and xylose from sugarcane bagasse into succinic acid by *Yarrowia lipolytica*," *Biochemical Engineering Journal,* vol. 148, pp. 108-115, 2019.

[159] Y. Xi, T. Zhan, H. Xu, J. Chen, C. Bi, F. Fan, and X. Zhang, "Characterization of JEN family carboxylate transporters from the acid-tolerant yeast *Pichia kudriavzevii* and their applications in succinic acid production," *Microbial Biotechnology,* vol. 14, no. 3, pp. 1130-1147, 2021.

[160] X. F. Huang, J. N. Liu, L. J. Lu, K. M. Peng, G. X. Yang, and J. Liu, "Culture strategies for lipid production using acetic acid as sole carbon source by *Rhodosporidium toruloides*," *Bioresour Technol,* vol. 206, pp. 141-149, 2016.

[161] R. Sapra, "Using R2 with caution," *Current Medicine Research and Practice,* vol. 4, no. 3, pp. 130-134, 2014.

[162] T. Vongkampang, K. Sreenivas, J. Engvall, C. Grey, and E. W. van Niel, "Characterization of simultaneous uptake of xylose and glucose in *Caldicellulosiruptor kronotskyensis* for optimal hydrogen production," *Biotechnology for Biofuels,* vol. 14, pp. 1-11, 2021.

[163] X. Mai, W. Wang, X. Zhang, D. Wang, F. Liu, and Z. Sun, "Mathematical Modeling of the Effects of Temperature and Modified Atmosphere Packaging on the Growth Kinetics of *Pseudomonas Lundensis* and *Shewanella Putrefaciens* in Chilled Chicken," *Foods,* vol. 11, no. 18, p. 2824, 2022.

[164] E.-H. Dulf, D. C. Vodnar, A. Danku, A. G. Martău, B.-E. Teleky, F. V. Dulf, M. F. Ramadan, and O. Crisan, "Mathematical Modeling and Optimization of *Lactobacillus* Species Single and Co-Culture Fermentation Processes in Wheat and Soy Dough Mixtures," *Frontiers in Bioengineering and Biotechnology,* vol. 10, p. 888827, 2022.

[165] Y. G. Keneni, A. T. Hvoslef-Eide, and J. M. Marchetti, "Mathematical modelling of the drying kinetics of *Jatropha curcas* L. seeds," *Industrial crops and products,* vol. 132, pp. 12-20, 2019.

[166] A. E. D. Mahmoud, "Graphene-based nanomaterials for the removal of organic pollutants: Insights into linear versus nonlinear mathematical models," *Journal of Environmental Management,* vol. 270, p. 110911, 2020.

[167] A. Martinho, H. A. Matos, R. Gani, B. Sarup, and W. Youngreen, "Modelling and simulation of vegetable oil processes," *Food and Bioproducts Processing,* vol. 86, no. 2, pp. 87-95, 2008.

[168] F. Reyes-Jurado, A. Franco-Vega, N. Ramírez-Corona, E. Palou, and A. López-Malo, "Essential oils: antimicrobial activities, extraction methods, and their modeling," *Food Engineering Reviews,* vol. 7, pp. 275-297, 2015.

[169] P. Nachtergaele, "Converting a challenge into an opportunity: optimization of fatty acid production from variable feedstocks via process modelling," PhD PhD Thesis, Faculty of Bioscience Engineering, Ghent University, Ghent, Belgium, 2021. [Online]. Available: http://hdl.handle.net/1854/LU-8718860

[170] M. Llamas, M. Dourou, C. González-Fernández, G. Aggelis, and E. Tomás-Pejó, "Screening of oleaginous yeasts for lipid production using volatile fatty acids as substrate," *Biomass and bioenergy,* vol. 138, p. 105553, 2020.

[171] S. Bettencourt, C. Miranda, T. A. Pozdniakova, P. Sampaio, R. Franco-Duarte, and C. Pais, "Single cell oil production by oleaginous yeasts grown in synthetic and waste-derived volatile fatty acids," *Microorganisms,* vol. 8, no. 11, p. 1809, 2020.

[172] I. R. Sitepu, R. Sestric, L. Ignatia, D. Levin, J. B. German, L. A. Gillies, L. A. G. Almada, and K. L. Boundy-Mills, "Manipulation of culture conditions alters lipid content and fatty acid profiles of a wide variety of known and new oleaginous yeast species," *Bioresource technology,* vol. 144, pp. 360-369, 2013.

[173] L. Maisonneuve, G. Chollet, E. Grau, and H. Cramail, "Vegetable oils: a source of polyols for polyurethane materials," *OCL Oilseeds and fats crops and lipids,* vol. 23, no. 5, p. D508 (10 pages), 2016.

[174] L. Zhang, H. K. Jeon, J. Malsam, R. Herrington, and C. W. Macosko, "Substituting soybean oil-based polyol into polyurethane flexible foams," *Polymer,* vol. 48, no. 22, pp. 6656-6667, 2007.

[175] A. E. Coman, J. Peyrton, G. Hubca, A. Sarbu, A. R. Gabor, C. A. Nicolae, T. V. Iordache, and L. Averous, "Synthesis and characterization of renewable polyurethane foams using different biobased polyols from olive oil," *European Polymer Journal,* vol. 149, p. 110363, 2021.

[176] M. Kirpluks, D. Kalnbunde, H. Benes, and U. Cabulis, "Natural oil based highly functional polyols as feedstock for rigid polyurethane foam thermal insulation," *Industrial crops and products,* vol. 122, pp. 627-636, 2018.

[177] J. H. Lee, S. H. Kim, and K. W. Oh, "Bio-based polyurethane foams with castor oil based multifunctional polyols for improved compressive properties," *Polymers,* vol. 13, no. 4, p. 576, 2021.

[178] K. Uram, A. Prociak, and M. Kurańska, "Influence of the chemical structure of rapeseed oil-based polyols on selected properties of polyurethane foams," *Polimery,* vol. 65, no. 10, pp. 698-707, 2020.

[179] M. Desroches, M. Escouvois, R. Auvergne, S. Caillol, and B. Boutevin, "From vegetable oils to polyurethanes: synthetic routes to polyols and main industrial products," *Polymer reviews,* vol. 52, no. 1, pp. 38-79, 2012.

[180] M. L. Pinto, "Formulation, preparation, and characterization of polyurethane foams," *J Chem Educ,* vol. 87, pp. 212-215, 2010.

[181] M. Szycher, "Polyurethanes," *Szycher's handbook of Polyurethanes,* 1999.

[182] B. K. Uprety, J. V. Reddy, S. S. Dalli, and S. K. Rakshit, "Utilization of microbial oil obtained from crude glycerol for the production of polyol and its subsequent conversion to polyurethane foams," *Bioresour Technol,* vol. 235, pp. 309-315, 2017.

[183] N. Marcovich, M. Kurańska, A. Prociak, E. Malewska, and K. Kulpa, "Open cell semi-rigid polyurethane foams synthesized using palm oil-based bio-polyol," *Industrial crops and products,* vol. 102, pp. 88-96, 2017.

[184] V. B. Veronese, R. K. Menger, M. M. d. C. Forte, and C. L. Petzhold, "Rigid polyurethane foam based on modified vegetable oil," *Journal of Applied Polymer Science,* vol. 120, no. 1, pp. 530-537, 2011.

[185] M. Z. Arniza, S. S. Hoong, Z. Idris, S. K. Yeong, H. A. Hassan, A. K. Din, and Y. M. Choo, "Synthesis of Transesterified Palm Olein-Based Polyol and Rigid Polyurethanes from this Polyol," *J Am Oil Chem Soc,* vol. 92, no. 2, pp. 243-255, 2015.

[186] M. Kurańska, P. Aleksander, K. Mikelis, and C. Ugis, "Porous polyurethane composites based on bio-components," *Composites Science and Technology,* vol. 75, pp. 70-76, 2013.

[187] E. Sharmin, F. Zafar, and S. Ahmad, "Seed Oil Based Polyurethanes: An Insight," *Polyurethane,* 2012.

[188] H. Fan, A. Tekeei, G. J. Suppes, and F. H. Hsieh, "Rigid polyurethane foams made from high viscosity soy-polyols," *Journal of Applied Polymer Science,* vol. 127, no. 3, pp. 1623-1629, 2013.

[189] H. Janik, M. Sienkiewicz, and J. Kucinska-Lipka, *Handbook of thermoset plastics: 9. Polyurethanes*. Elsevier Inc. Chapters, 2013.

[190] A. Kairytė and S. Vėjelis, "Evaluation of forming mixture composition impact on properties of water blown rigid polyurethane (PUR) foam from rapeseed oil polyol," *Industrial crops and products,* vol. 66, pp. 210-215, 2015.

[191] S. Członka, M. F. Bertino, J. Kośny, A. Strąkowska, M. Masłowski, and K. Strzelec, "Linseed oil as a natural modifier of rigid polyurethane foams," *Industrial crops and products,* vol. 115, pp. 40-51, 2018.

[192] N. K. Attia, S. A. El-Mekkawi, O. A. Elardy, and E. A. Abdelkader, "Chemical and rheological assessment of produced biolubricants from different vegetable oils," *Fuel,* vol. 271, 2020.

[193] A. Rohman and R. Ariani, "Authentication of Nigella sativa seed oil in binary and ternary mixtures with corn oil and soybean oil using FTIR spectroscopy coupled with partial least square," *Scientific World Journal,* vol. 2013, p. 740142, 2013.

[194] C. S. Carriço, T. Fraga, and V. M. D. Pasa, "Production and characterization of polyurethane foams from a simple mixture of castor oil, crude glycerol and untreated lignin as bio-based polyols," *European Polymer Journal,* vol. 85, pp. 53-61, 2016.

[195] M.-I. Morar, F. Fetea, A. M. Rotar, M. Nagy, and C. Semeniuc, "Characterization of essential oils extracted from different aromatic plants by FTIR spectroscopy," *Bulletin of University of Agricultural Sciences and Veterinary Medicine Cluj-Napoca. Food Science and Technology,* vol. 74, pp. 37-38, 2017.

[196] M. E. S. C. M. Mirghani, Y.B., "A new method for determining gossypol in cottonseed oil by FTIR spectroscopy," *Journal of the American Oil Chemists' Society,* vol. 80, no. 7, pp. 625-628, 2003.

[197] P. Cinelli, I. Anguillesi, and A. Lazzeri, "Green synthesis of flexible polyurethane foams from liquefied lignin," *European Polymer Journal,* vol. 49, no. 6, pp. 1174-1184, 2013.

[198] X. Kong, Narine, Suresh S., "Physical properties of polyurethane plastic sheets produced from polyols from canola oil," *Biomacromolecules,* vol. 8, pp. 2203-2209, 2007.

[199] R. D. V. V. Lopes, N. P. D. Loureiro, A. P. T. Pezzin, A. C. M. Gomes, I. S. Resck, and M. J. A. Sales, "Synthesis of polyols and polyurethanes from vegetable oils–kinetic and characterization," *Journal of Polymer Research,* vol. 20, no. 9, 2013.

Biography

Name - Surname	Miss Thidarat Samranrit
Date of Birth	June 13, 1997
Address	87/2, M. 5, Latyao, Latyao, Nakhonsawan, 60150
Education	Mater of Science (Applied Biology Program) (2020-2023)
Telephone Number	091-725-9661
Email address	t.samranrit@gmail.com